Stabilization of a Steady State in Time-delay Oscillators Coupled by Delay Connections

Stabilization of a Steady State in Time-delay Oscillators Coupled by Delay Connections

Luan Ba Le

Department of Electrical and Information Systems
Graduate School of Engineering
Osaka Prefecture University

January 2014

Contents

Chapter 1

Introduction

1.1 Background

1.1.1 Oscillations in autonomous systems

Oscillations are well known as important phenomena in nature and artificial systems [1]. They can be classified into forced oscillations and unforced oscillations (i.e., self-excited oscillations). The self-excited oscillations occur in nonlinear autonomous systems, in which external energy is constantly provided and their nonlinearity maintains their oscillations. Nonlinear autonomous systems with self-excited oscillations are called *oscillators* throughout this thesis. The oscillations, such as the periodic firing of pacemaker cells [2, 3], the rhythm of pendulum clocks, the rhythm of metronomes, and the cyclic motions of heat engines [1], are beneficial to performances of their various systems. Other oscillations, such as the wind-driven vibrations of bridges [4, 5], the oscillations in direct current (DC) micro-grids [6], and the vibrations of cutting machines [7, 8], harm the stability and degrade the performance of their various systems.

In applications, it is imperative to avoid or suppress the harmful oscillations. In order to do this, the influence of the system parameters on the harmful oscillations must be investigated, and then the parameters must be chosen in such a way that the oscillations do not occur. Although this method is practical in many cases, changing the parameters can be very costly. This is because avoiding harmful oscillations may require major changes in the system, and the system may even need to be abandoned due to practical restrictions. An alternative is to suppress harmful oscillations with feedback control; this is more practical, since it does not require major changes in the system. In the field of control engineering, many schemes have been proposed for suppressing oscillations with feedback. In the field of nonlinear science, there is a significant control scheme for suppressing oscillations: Hövel and Scholl [9] applied a delayed feedback control (DFC) method, which had been proposed by Pyragas [10][1], to the suppression of oscillations (see Table 1.1). Their

[1] The original DFC method introduced by Pyragas [10] stabilizes unstable periodic orbits embedded in a chaotic attractor.

scheme stabilizes an unstable steady state embedded within a system of oscillators, without direct knowledge of the steady state position. Thus, the DFC method has been useful for experimental situations, and it has been extended to various situations: Ahlborn and Parlitz proposed a multiple DFC method [11]; and Konishi and Hara proposed a queue-based DFC method [12] (see Table 1.1). The multiple DFC method uses two or more different and independent delayed feedback signals. Its advantage is that stabilization can be induced even for long delay times. The queue-based DFC method uses a first-in-first-out (FIFO) queue for a delayed feedback signal. Its primary advantage is that it is easy to implement the delayed signal using inexpensive and simple electronic devices.

1.1.2 Coupled oscillators

Connections between oscillators were first studied in 1665 by Huygens, who noticed that pendulum clocks in the same room were synchronized [13]. In daily life, we can observe this phenomenon, for example, in the flash of fireflies [14], the firing of pacemaker cells [2], and the chirping of crickets [15]. The dynamics of these phenomena can be described by coupled oscillators. In the field of nonlinear science, researchers have found many interesting phenomena relating to coupled oscillators, but if they are harmful in practice, for instance, the oscillations in DC micro-grids [6], they must be suppressed.

Amplitude death, the stabilization of a steady state that is induced by a static connection[2], is a strong candidate for suppressing the oscillations in coupled oscillators. Yamaguchi and Shimizu [16] and Aronson *et al.* [17] observed this phenomenon in paired and networked oscillators, respectively (see Table 1.1). Unfortunately, a static connection cannot induce amplitude death for coupled *similar* oscillators. This is a crucial limitation of the use of amplitude death in practice. Reddy *et al.* showed that amplitude death can be induced in coupled similar oscillators [18], if the connections between the oscillators have a transmission delay (see Table 1.1). Moreover, Konishi *et al.* extended the multiple DFC method to a multiple delay connection which induces stabilization of coupled similar oscillators [19] (see Table 1.1). The advantage of this connection compared with a single delay connection is that amplitude death occurs even with long delays.

1.1.3 Motivation

Time delays inevitably exist in many dynamical systems [20,21], such as biological systems [21–24], traffic systems [25], and supply chain systems [26], since neither finite speeds of signal propagation nor finite speeds of processing signals can be avoided. Such delays can be neglected when they are short. However, long delays cannot be neglected, because they may induce self-excited oscillations in nonlinear autonomous systems, such as metal-cutting tools [7, 8], contact rotating systems

[2]A static connection is the simplest type of diffusive connection.

Table 1.1: Previous studies on stabilization of oscillators

	Static connection	**Delay connection**	**Multiple delay connection**	**Queue-based delay connection**
One oscillator	**N/A**	Hövel & Scholl, Phys. Rev. E., 2005 [9]	Ahlborn & Parlitz, Phys. Rev. Lett., 2004 [11]	Konishi & Hara, Dynam. Cont. Dis. B, 2011 [12]
Two oscillators	Aronson *et al.*, Physica D, 1990 [17]	Reddy *et al.*, Phys. Rev. Lett., 1998 [18]	Konishi *et al.*, Phys. Rev. E, 2010 [19]	Konishi, **Le** *et al.*, Euro. Phys. J. B, 2012 [39] (**Chapter 5**)
Three oscillators	Yamaguchi & Shimizu, Physica D, 1984 [16]			
Network oscillators				

[27], and oil-well drill-string systems [28]. Nonlinear autonomous systems with self-excited oscillations that are induced by delays are called *time-delay oscillators*. Some oscillations in time-delay oscillators are harmful for the performance of the system, and it is desirable to suppress these. Stability analyses and the control of time-delay oscillators have gained increasing attention from a theoretical viewpoint as well as for practical applications [29–31]; however, these are not easy tasks, since, due to the time delays, the dimension of oscillators is infinite.

Let us recall that the previous studies listed in Table 1.1 deal only with the stabilization of *non-time-delay* oscillators. However, we have seen above that the stabilization of *time-delay* oscillators is an important subject. The main purpose of this thesis is to apply the previous studies listed in Table 1.1 to the stabilization of *time-delay* oscillators (see Table 1.2). To begin with, we investigate amplitude death in systems of two or three time-delay oscillators, in which each oscillator has a different delay, and that are coupled by a static connection [32,33]. Our analytical results are verified by circuit experiments. It was reported that a single time-delay oscillator can be stabilized by the DFC method [34]. This result was applied to a pair of time-delay oscillators coupled by a delay connection [35]. In this thesis, this is extended to time-delay oscillator networks; the most important feature of our extension is that robust control theory is employed to simplify the stability analysis [36]. Furthermore, we apply the multiple DFC method to the stabilization of a single time-delay oscillator [37] and extend it to the stabilization of a pair of time-delay oscillators coupled by a multiple delay connection [38]. Finally, we apply the queue-based DFC method to the stabilization of non-time-delay oscillator networks with a queue-based delay connection [39] (see Table 1.1).

1.2 Outline

Chapter 2 investigates the dynamical behavior of both two and three time-delay oscillators coupled by a static connection, and finds that amplitude death occurs when their delay times are nonidentical [32, 33]. A cluster treatment of the characteristic root paradigm is used to rigorously delineate the stability region. Stability

Table 1.2: Our studies on stabilization of time-delay oscillators

<table>
<tr><th></th><th>Static connection</th><th>Delay connection</th><th>Multiple delay connection</th><th>Queue-based delay connection</th></tr>
<tr><td>One oscillator</td><td>N/A</td><td>Namajunas et al., Phys. Lett. A, 1995 [34]</td><td>Le et al., Nonlinear Dyn., 2012 [37] (Chapter 4)</td><td></td></tr>
<tr><td>Two oscillators</td><td>Le et al., Proc. of NOLTA, 2010 [32] (Chapter 2)</td><td>Konishi et al., Phys. Rev. E, 2008 [35]</td><td>Le et al., Proc. of NDES, 2012 [38](Chapter 4)</td><td></td></tr>
<tr><td>Three oscillators</td><td>Le et al., Proc. of IUTAM, 2011 [33] (Chapter 2)</td><td rowspan="2">Le et al., Phys. Rev. E, 2013 [36] (Chapter 3)</td><td rowspan="2"></td><td rowspan="2"></td></tr>
<tr><td>Network oscillators</td><td></td></tr>
</table>

analysis reveals that amplitude death still occurs when the delays are arbitrarily long. These theoretical results are then experimentally verified with electronic circuits.

Chapter 3 deals with amplitude death in networks of identical time-delay oscillators coupled by a delay connection [36]. Stability analysis allows us to derive a systematic procedure to design the connection (i.e., coupling strength and connection delay) for induction of amplitude death. The main advantage of this procedure is that the connection is guaranteed to induce amplitude death even if the oscillators have long time delays. Our analytical results are verified by numerical examples.

Chapter 4 demonstrates that an unstable fixed point of a single time-delay oscillator can be stabilized by the multiple DFC method [37]. This method has an advantage in that the stabilization occurs for any long delays in a feedback line, providing the relationship is maintained between these delays and the delay time in the oscillators. A systematic procedure is provided for designing the feedback gain and the multiple delays. These analytical results are experimentally verified with electronic circuits. Moreover, we also extend this control scheme to amplitude death in a pair of time-delay oscillators coupled by a multiple delay connection [38], which also allows us to obtain amplitude death even for long delays. The analysis, a design procedure, and circuit experiments are provided.

Chapter 5 proposes a queue-based delay connection which can be implemented by low-cost and simple delay devices [39]. This connection induces amplitude death in non-time-delay oscillator networks, and the stability of amplitude death is analyzed by a semi-discretization technique. The analytical results are checked with numerical simulations.

Chapter 6 summarizes our results.

Chapter 2

Stabilization of time-delay nonlinear oscillators coupled by a static connection

2.1 Introduction

Amplitude death, a diffusive connection-induced stabilization of unstable fixed points in coupled oscillators, has been the subject of extensive investigation for the past 15 years [16,17]. Aronson *et al.* analytically investigated the death phenomenon for two coupled nonlinear oscillators [17]. They reported that death never occurs when the coupled oscillators are identical. Reddy, Sen, and Johnston showed that a time-delayed coupling effect, which exists due to the finite speed of data propagation, is able to induce amplitude death even in identical coupled oscillators [18]. Their report has considerably intrigued those working in the field of nonlinear physics [40]. Atay showed that distributed time-delay connections facilitate amplitude death [41]. Konishi *et al.* reported that multiple delay [42] and time-varying delay [43] connections can also facilitate amplitude death in coupled oscillators.

In order to use amplitude death in practical situations, a mutual connection that induces death must be designed. However, one inevitably confronts two problems in such a design. The first is how to select the type of mutual interactions and how to determine the coupling parameters. The second one is how to deal with high-dimensional oscillators. Konishi *et al.* provided a solution for the above problems [35] and, in particular, focused on the amplitude death in a pair of time-delayed chaotic oscillators [20] coupled by three types of mutual interactions: static connections, dynamic connections, and delayed connections.

Since time-delay systems have been widely used to model undesirable nonlinear phenomena, such as chatter and chaos in metal-cutting tools [7, 8], the stabilization of time-delay systems has been an important issue for engineering applications. The previous paper [35] concluded that amplitude death can occur with dynamic and delayed connections, but cannot with static ones. Although, due to their complicated structure, dynamic and delayed connections are not easy to implement in

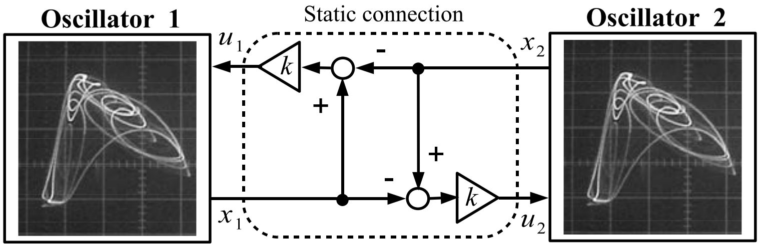

Figure 2.1: Block diagram of a pair of oscillators (2.1) coupled by a connection (2.2).

experimental situations, static connections have a simple structure. Therefore, static connections are the best solution from a cost standpoint.

The present chapter theoretically and analytically considers the stability of a pair of nonidentical time-delayed oscillators coupled by a static connection. It is difficult to use the traditional procedure for stability analysis to derive the boundaries of the amplitude death, since its characteristic equation includes a cross-talk term between the nonidentical delays. To overcome this difficulty, the present chapter applies to the characteristic equation the methodology proposed by Sipahi and Olgac [44]. This methodology allows us to derive directly, without trial-and-error testing, boundary curves for the amplitude death which are useful for the design of delay times. Furthermore, our theoretical results are verified with electronic circuit experiments.

2.2 Stability analysis

2.2.1 Two time-delay nonlinear oscillators

Let us consider a pair of nonidentical scalar time-delayed chaotic oscillators (see Fig. 2.1) [35]:

$$\begin{cases} \dot{x}_1 &= f(x_{1\tau_1}) - \alpha x_1 + u_1 \\ \dot{x}_2 &= f(x_{2\tau_2}) - \alpha x_2 + u_2 \end{cases}, \tag{2.1}$$

where $x_{1,2} \in \mathbb{R}$ and $u_{1,2} \in \mathbb{R}$ are the system states and coupling signals, respectively. $x_{1\tau_1,2\tau_2} := x_{1,2}(t-\tau_{1,2})$ are the delayed states; $\tau_{1,2} \geq 0$ are the delay times and $\alpha > 0$ is a parameter. Furthermore, $f : \mathbb{R} \to \mathbb{R}$ represents a nonlinear function, and the symbol $\mathbb{R}$ denotes the set of real numbers. These oscillators are coupled by the static connection described as

$$u_{1,2} = k(x_{1,2} - x_{2,1}), \tag{2.2}$$

where $k \in \mathbb{R}$ is the coupling strength.

Each individual oscillator without coupling (i.e., $u_{1,2} \equiv 0$) has the fixed points

$$x^* : 0 = f(x^*) - \alpha x^*. \tag{2.3}$$

Throughout this study, it is assumed that there is one unstable fixed point. The location of the fixed point x^* never changes even with coupling; in other words, the static connection changes only the stability of the point. The characteristic equation of the linearized system at the fixed point x^* can be rewritten as

$$a_0(\lambda) + a_1(\lambda)e^{-\lambda\tau_1} + a_2(\lambda)e^{-\lambda\tau_2} + a_3 e^{-\lambda(\tau_1+\tau_2)} = 0, \tag{2.4}$$

where

$$\begin{aligned} a_0(\lambda) &:= s^2 + 2(\alpha - k)\lambda + (\alpha - k)^2 - k^2, && (2.5)\\ a_1(\lambda) &= a_2(\lambda) := -\beta\lambda - \beta(\alpha - k), && (2.6)\\ a_3 &:= \beta^2, && (2.7)\\ \beta &:= \{\mathrm{d}f(x)/\mathrm{d}x\}_{x=x^*}. && (2.8) \end{aligned}$$

The nonlinear function f is given by

$$f(x) = \begin{cases} 0 & \text{if } x \le -4/3 \\ -1.8x - 2.4 & \text{if } -4/3 < x \le -0.8 \\ 1.2x & \text{if } -0.8 < x \le 0.8 \\ -1.8x + 2.4 & \text{if } 0.8 < x \le 4/3 \\ 0 & \text{if } x > 4/3 \end{cases}, \tag{2.9}$$

as a typical case study [45]. The three fixed points of an individual oscillator located at the intersection of $f(x)$ and αx are $x^* = \pm 6/7$ and 0. The slopes of $f(x)$ at x^* can be estimated as $\beta(\pm 6/7) = -1.8$ and $\beta(0) = 1.2$. The parameters are fixed at $\alpha = 1$ and $k = -2$. Additionally, in the absence of delay (i.e., $\tau_1 = \tau_2 = 0$), the characteristic equation (2.4) in the absence of delays has two roots, -6.79 and -2.80, so the number of unstable roots is zero.

The cluster treatment of characteristic roots (CTCR) paradigm is capable of deriving the boundary curves of a stability region in (τ_1, τ_2) space [44]. To simplify the stability analysis, we only identify the roots lying on the imaginary axis: $\lambda = j\lambda_{\mathrm{Im}}$, where the symbol j is denoted as $j = \sqrt{-1}$. The stability posture in (τ_1, τ_2) space is shown in Fig. 2.2, where the region of amplitude death is denoted by Ω. Every point on the boundary curves correspond to the purely imaginary root. The number of unstable roots in several regions are also indicated.

Figures 2.3(a) and 2.3(b) illustrate the time-series data of the two nonidentical oscillators for the following two parameter sets: (A) $\tau_1 = 4.4$, $\tau_2 = 6.8$; (B) $\tau_1 = 3.4$, $\tau_2 = 6.8$. These sets are indicated in Fig. 2.2. For the parameter set (A), the two identical oscillators without coupling behave chaotically until $t = 500$, and they become periodic after coupling. On the other hand, for the parameter set (B), before coupling, the two individual oscillators have chaotic motion. After coupling, the states $x_{1,2}(t)$ converge on $x^*_{1,2}$. When there is a wide-scale region of amplitude death, as shown in Fig. 2.4, it seems that one may choose (τ_1, τ_2) arbitrarily large and still obtain amplitude death, providing they are within the indicated area (see the dotted lines in Fig. 2.4), $\tau_{1,2} = 2\tau_{2,1} + \xi$, $0 \le \xi \le 2$. A static connection can induce death over a region Ω that has a wide range of delay-times. However, we do not yet have proof of this.

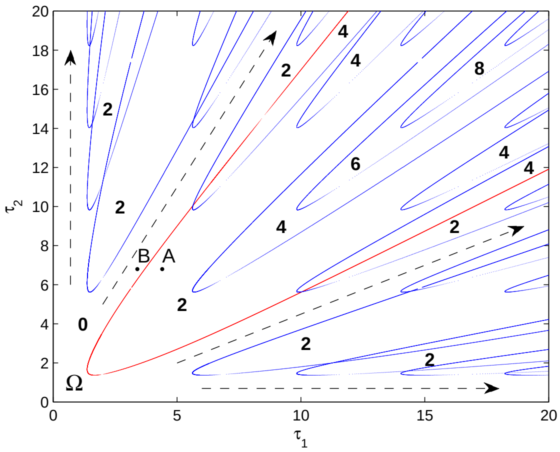

Figure 2.2: Region of amplitude death Ω and the boundary curves of stability.

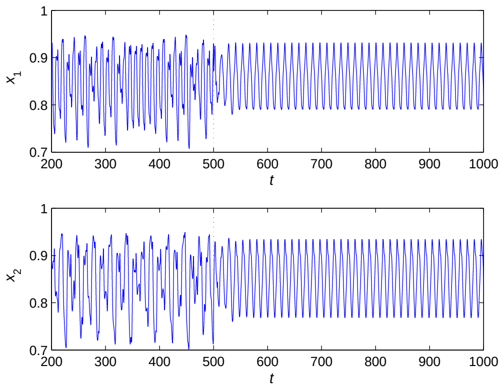

(a) (A) $\tau_1 = 4.4$, $\tau_2 = 6.8$.

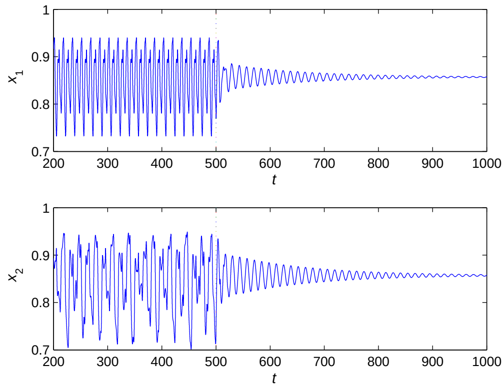

(b) (B) $\tau_1 = 3.4$, $\tau_2 = 6.8$.

Figure 2.3: Time series data $x_{1,2}(t)$ of coupled oscillators (numerical simulation)

2.2.2 Three time-delay nonlinear oscillators

Let us extend our results to three oscillators. For three time-delayed oscillators, the characteristic equation includes cross-talk terms for three time delays. It is difficult to deal with the cross-talk terms; therefore, the standard procedure for analyzing the characteristic equation [18, 35, 41, 43, 46–48] is useless. To overcome this difficulty, this section employs two novel methodologies: advanced clustering with frequency sweeping (ACSF) [49] and cluster treatment of characteristic roots (CTCR) [44]. The combination of the ACSF and CTCR methods is a powerful tool that allows us to analyze the stability of the steady state and to obtain the stability boundary curves in parameter space.

Consider the three time-delayed nonlinear oscillators,

$$\dot{x}_i = f(x_{\tau_i}) - \alpha x_i + u_i,\ (i = 1, 2, 3),$$

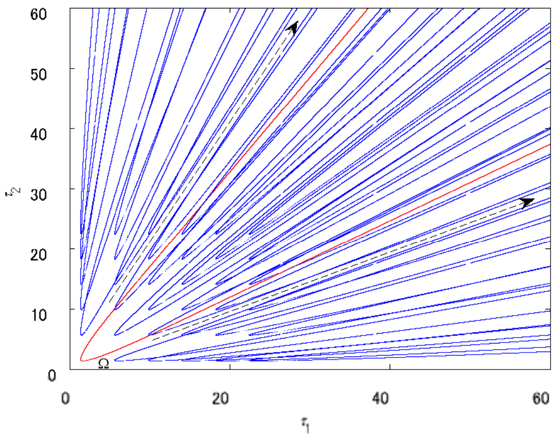

Figure 2.4: Wide-scale region of amplitude death and the boundary curves of stability.

where $x_i \in \mathbb{R}$ and $u_i \in \mathbb{R}$ denote the system state and coupling signal, respectively. When $x_{\tau_i} := x_i(t - \tau_i)$ is the delayed state, $\tau_i \geq 0$ is the delay time and $\alpha = 1$ is a parameter, the nonlinear function is

$$f(x) = \begin{cases} 0.95x + 1.4 & \text{if } x \leq 1.7 \\ -1.6x + 5.75 & \text{if } 1.7 < x \leq 4.3 \\ -1.15 & \text{if } x > 4.3 \end{cases}.$$

The oscillators are coupled by a static connection, with a coupling strength $k \in \mathbb{R}$:

$$u_{1,2,3} = \frac{1}{2}k(x_{2,1,1} + x_{3,3,2} - 2x_{1,2,3}).$$

Without coupling, each individual oscillator (i.e., $u_{1,2,3} \equiv 0$) has an unstable fixed point $x^* : 0 = f(x^*) - \alpha x^*$. The location of the fixed point x^* never changes even with coupling; understandably, the static connection changes only its stability. The combination of the ACSF and CTCR methods allow us to obtain the boundary curves in three-dimensional (τ_1, τ_2, k) space with $\tau_3 = 6$, as shown in Fig. 2.5(a). The cross-section surface of the three-dimensional curves at $k = 2$ is illustrated in Fig. 2.5(b), where the region of amplitude death is denoted by Ω. Every point on the curves corresponds to the purely imaginary root of the characteristic equation. The numbers of unstable roots are stated in several of the regions. Figure 2.6 shows the time-series data of the oscillators at points (A) and (B) in Fig. 2.5(b); they are, respectively, outside and inside the region of amplitude death. At point (A), as shown in Fig. 2.6(a), the state variables of the three oscillators, $[x_1(t), x_2(t), x_3(t)]$, do not converge on the steady state after coupling at $t = 500$. In contrast, the stabilization is induced at point (B) inside the region of amplitude death as shown in Fig. 2.6(b). These time-series data agree with our boundary curves.

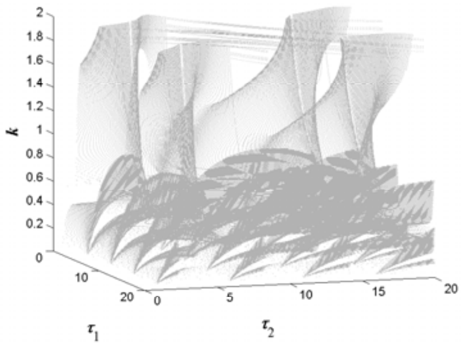

(a) (τ_1, τ_2, k) space with $\tau_3 = 6$

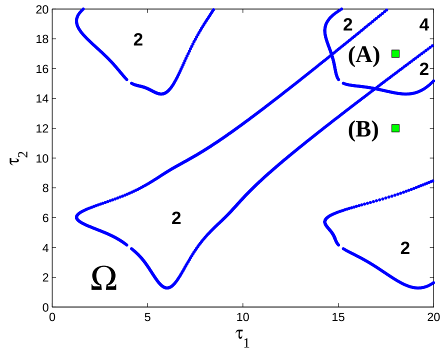

(b) (τ_1, τ_2) space with $\tau_3 = 6$ and $k = 2$

Figure 2.5: Stability boundary curves for the steady state.

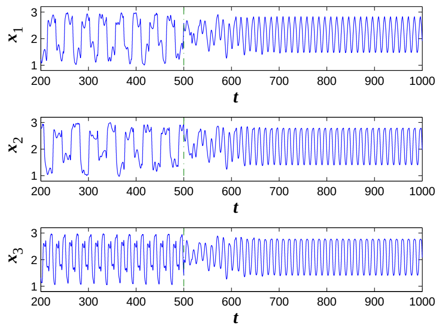

(a) $\tau_1 = 18, \tau_2 = 17, \tau_3 = 6, k = 2$ (A)

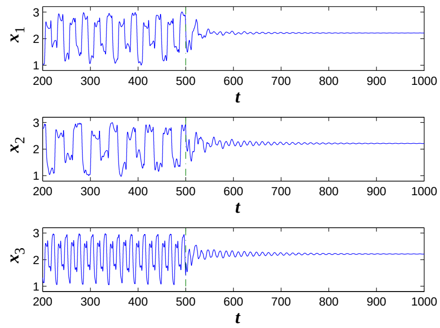

(b) $\tau_1 = 18, \tau_2 = 12, \tau_3 = 6, k = 2$ (B)

Figure 2.6: Time-series data $x_{1,2,3}(t)$ before and after coupling.

2.3 Electronic circuit experiments

The two chaotic oscillators coupled by the static connection are sketched in Fig. 2.7. The delay units employ the bucket brigade delay line MN3011 (Panasonic) to generate the delayed signal [35] and the nonlinear function is implemented by three op-amps and two diodes.

Here, x_i denotes the voltage of the i-th oscillator. The boxes labeled $-\tau_i$ and f are the time-delay unit and the nonlinear function unit, respectively. These oscillators are governed by

$$\begin{cases} C_n\dot{x}_1(t) &= \dfrac{1}{R_n}\left\{f(x_1(t-\tau_1)) - x_1(t)\right\} + u_1(t) \\ C_n\dot{x}_2(t) &= \dfrac{1}{R_n}\left\{f(x_2(t-\tau_2)) - x_2(t)\right\} + u_2(t) \end{cases}, \tag{2.10}$$

where R_n, C_n are a resistor and capacitor, respectively. The coupling terms $u_{1,2}(t)$

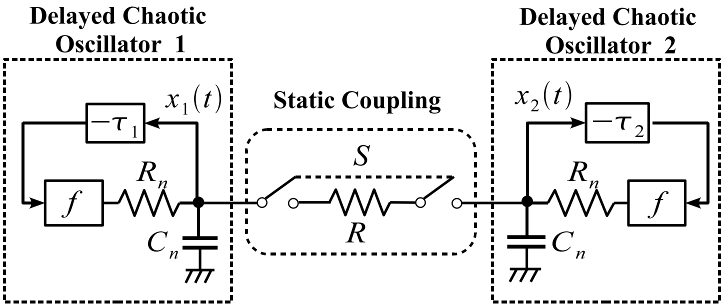

Figure 2.7: Two time-delay chaotic oscillators coupled by a static connection.

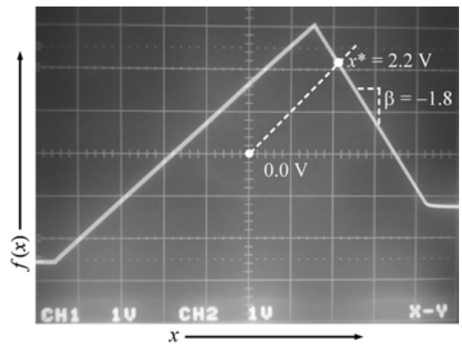

Figure 2.8: Nonlinear function $f(x)$. Horizontal axis: x (1V/div); vertical axis: $f(x)$ (1V/div).

are the currents from the connection circuit to the oscillators. The static connection is described by

$$u_{1,2}(t) = -\frac{1}{R}\left\{x_{1,2}(t) - x_{2,1}(t)\right\}. \tag{2.11}$$

It is sufficient to treat the above circuits as dimensionless oscillators (2.1) in the following relations:

$$\begin{aligned}
&\tilde{t} := \frac{t}{R_n C_n},\ \tilde{\tau}_{1,2} := \frac{\tau_{1,2}}{R_n C_n},\\
&\dot{x}_{1,2} := \frac{\mathrm{d}x_{1,2}(\tilde{t})}{\mathrm{d}\tilde{t}},\ x_{1,2} := x_{1,2}(\tilde{t}),\ x_{1,2\tau} := x_{1,2}(\tilde{t} - \tilde{\tau}_{1,2}),\\
&u_{1,2} := u_{1,2}(\tilde{t}),\ k := -\frac{R_n}{R}.
\end{aligned}$$

These relations show that the circuit equation (2.10) is identical to equation (2.1) with $\alpha = 1$. The input–output characteristic of the nonlinear function unit is shown in Fig. 2.8. From the characteristic, the fixed point $x^* = 2.2$ V and the slope $\beta(x^*) = -1.8$ are approximately estimated. The circuit parameters and the coupling

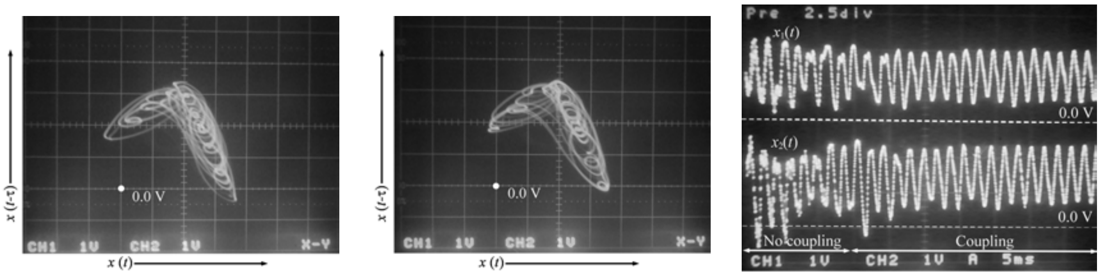

(a) (b) (c)

Figure 2.9: Experimental verification with parameter set (A): (a) chaotic behavior of oscillator 1; (b) chaotic behavior of oscillator 2 (horizontal axis: $x(t-\tau)$ (0.5V/div), vertical axis: $x(t)$ (0.5V/div)); (c) time series data $x_{1,2}(t)$ (V) just before and after coupling.

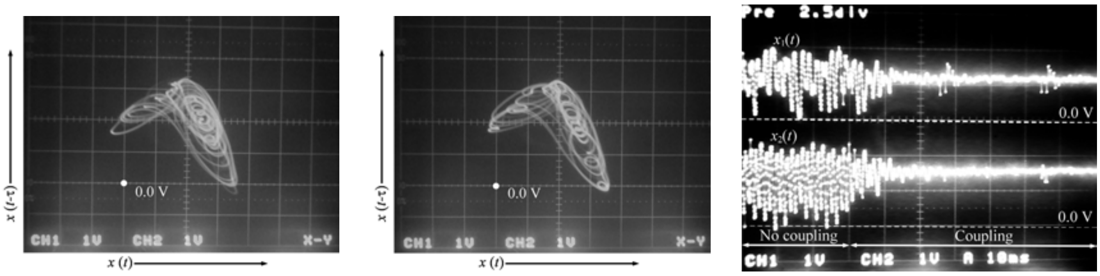

(a) (b) (c)

Figure 2.10: Experimental verification with parameter set (B): (a) chaotic behavior of oscillator 1; (b) chaotic behavior of oscillator 2 (horizontal axis: $x(t-\tau)$ (0.5V/div), vertical axis: $x(t)$ (0.5V/div)); (c) time series data $x_{1,2}(t)$ (V) just before and after coupling.

resistor are fixed at $R_n = 1.0$ kΩ, $C_n = 1.0$ μF, and $R = 0.5$ kΩ. We consider two parameter sets: (A) $\tau_1 = 4.4$ ms, $\tau_2 = 6.8$ ms; (B) $\tau_1 = 3.4$ ms, $\tau_2 = 6.8$ ms. In dimensionless oscillators (2.1), $\tilde{\tau}_{1,2}$ for the two parameter sets correspond to (A) $\tilde{\tau}_1 = 4.4$, $\tilde{\tau}_2 = 6.8$; (B) $\tilde{\tau}_1 = 3.4$, $\tilde{\tau}_2 = 6.8$, which are indicated as the points A and B in Fig. 2.2. Figures 2.9(a) and 2.9(b) show that with parameter set (A), the individual oscillators exhibit chaotic behavior. When the switch S shown in Fig. 2.7 is closed, the two individual circuits are connected by the coupling resistor. After S is closed, the chaotic behavior changes to a periodic motion, but amplitude death is not observed, as shown in Fig. 2.9(c). With parameter set (B), the individual oscillators exhibit chaotic behavior (see Figs. 2.10(a) and 2.10(b)). The oscillators behave chaotically until S is closed. As shown in Fig. 2.10(c), the states $x_{1,2}(t)$ gradually converge on $x^*_{1,2}$: amplitude death occurs, after S is closed. This experimental study confirms that the region of amplitude death estimated by analytical insight in the preceding section agrees well with the electronic circuit experiments.

2.4 Conclusion

The present chapter investigated amplitude death induced by a static connection between two nonidentical time-delayed chaotic oscillators. The precise shape derived by the CTCR paradigm for the region of amplitude death leads to the conclusion that even relatively long delay times can induce amplitude death. This is important, because systems with large delay times are frequently encountered in various applications. Moreover, our analytical results were experimentally confirmed by real electronic oscillators. The stability boundary curves in the parameter space were derived by using a combination of the ACSF and CTCR methods.

Chapter 3

Stabilization of time-delay nonlinear oscillators coupled by a delay connection

3.1 Introduction

There has been some interest in coupled nonlinear oscillators from the viewpoints of both academia [50, 51] and engineering applications [52–55]. A diffusive-connection-induced stabilization of unstable steady states in coupled oscillators, which is often referred to as amplitude death, has been investigated for over two decades [16, 17]. Although this phenomenon never occurs in coupled identical oscillators [17, 56], a *time-delayed* connection can induce it [18]. Such time-delay-induced death has received considerable attention from analytical [19, 43, 46, 57–65] and experimental [66, 67] points of view.

It is generally known, when engineering nonlinear systems, that time delays induce self-excited oscillations, such as are seen in metal-cutting processes [7, 8] and contact rotating systems [27]. These oscillations are generally considered to be harmful in engineering applications. When self-excited oscillations occur in a number of identical time-delayed nonlinear systems, the phenomenon of amplitude death has a great deal of potential as a candidate for suppressing such oscillations [1]. Most previous studies on amplitude death, however, have dealt with the stabilization of oscillators without time delays. Recently, amplitude death in a pair of time-delayed oscillators coupled by a delayed connection was analytically investigated, and the analytical results were experimentally confirmed by electronic circuits [35]. Furthermore, Höfener, Sethia, and Gross investigated the stability of large networks consisting of time-delayed oscillators coupled by a delayed connection [69].

The present chapter proposes a systematic procedure for designing the connection parameters. This procedure has the following two advantages: the designed connection parameters are valid for any network topology, and the procedure is valid for any

[1] The relevant concept, using the connection control method to suppress harmful oscillations in flexible structures (e.g., multistory buildings), was first proposed in the field of civil engineering [68].

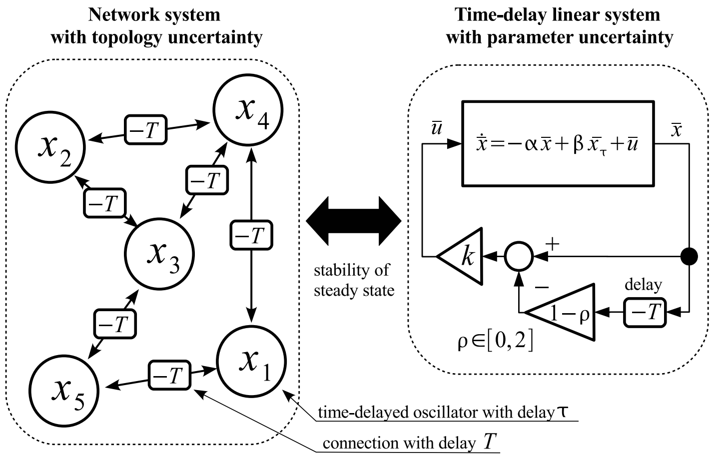

Figure 3.1: Illustration of a network system consisting of delayed oscillators (3.1) coupled by a delay connection (3.2) with topology uncertainty and a time-delay linear system with parameter uncertainty. The stability of the steady state (3.4) in the network is equivalent to that of the linear system.

length of delay in the oscillators. This procedure is based on the following facts: the stability of time-delayed oscillators coupled by a delayed connection with topology uncertainty can be reduced to that of a time-delay linear system with parameter uncertainty; an uncertain linear system can be analyzed by using robust control theory [70, 71]. These analytical results are verified by numerical simulations.

3.2 Problem statement

Consider a network system consisting of scalar nonlinear time-delayed oscillators

$$\dot{x}_n = -\alpha x_n + f(x_{n,\tau}) + u_n, \tag{3.1}$$

where $x_n \in \mathbb{R}$ and $u_n \in \mathbb{R}$ are the state variable and the coupling signal of oscillator n, respectively; $f : \mathbb{R} \to \mathbb{R}$ denotes a nonlinear function; and $x_{n,\tau} := x_n(t-\tau)$ is the delayed variable with oscillator delay $\tau \geq 0$. Here $\alpha > 0$ is a parameter. As illustrated in Fig. 3.1, each oscillator is coupled by a delayed connection,

$$u_n = k\left\{x_n - \frac{1}{d_n}\left(\sum_{m=1}^{N} c_{nm} x_{m,T}\right)\right\}, \tag{3.2}$$

where $k \in \mathbb{R}$ is the coupling strength. This is a kind of diffusive connection. $N \geq 2$ denotes the total number of oscillators, and $T \geq 0$ is the connection delay. The network topology is governed by c_{nm}: if oscillator n is connected to oscillator m, then $c_{nm} = c_{mn} = 1$, otherwise $c_{nm} = c_{mn} = 0$. The self-delayed signals $x_{n,T} := x_n(t-T)$ are not allowed to be injected, that is $c_{nn} = 0$. The number of oscillators that are connected to oscillator n, called the degree of oscillator n, is written as $d_n = \sum_{m=1}^{N} c_{nm}$. Suppose that there is no isolated oscillator, that is, $d_n > 0$. Each oscillator (3.1) without coupling (i.e., $k = 0$) has the fixed point

$$x^* : 0 = -\alpha x^* + f(x^*). \tag{3.3}$$

A steady state of oscillators (3.1) coupled by a delayed connection (3.2) is described by

$$[x_1 \cdots x_N]^T = [x^* \cdots x^*]^T. \tag{3.4}$$

The fixed point x^* is assumed to be unstable throughout this study. Note that a delayed connection (3.2) can change the stability of x^*, but it cannot change its location. The diffusive-connection-induced stabilization of a steady state (3.4) is often referred to as amplitude death. Note that this network system ($N \geq 2$) is an extension of the delay-coupled time-delayed oscillators ($N = 2$) proposed in a previous study [35].

3.3 Stability analysis

In order to analyze the linear stability of the steady state, we have to consider the dynamics of the linearized oscillators and connection,

$$\dot{\delta x}_n = -\alpha \delta x_n + \beta \delta x_{n,\tau} + \delta u_n, \tag{3.5}$$

$$\delta u_n = k \left\{ \delta x_n - \frac{1}{d_n} \left(\sum_{m=1}^{N} c_{nm} \delta x_{m,T} \right) \right\}, \tag{3.6}$$

where $\delta x_n \in \mathbb{R}$ denotes the variation of oscillator n around the fixed point x^*, that is, $\delta x_n := x_n - x^*$. Here $\beta := \{\mathrm{d}f(x)/\mathrm{d}x\}_{x=x^*}$ is the derivative of $f(x)$ at $x = x^*$. The linearized dynamics around the steady state are governed by

$$\dot{\delta \boldsymbol{x}} = (k-\alpha)\delta \boldsymbol{x} + \beta \delta \boldsymbol{x}_\tau - k\boldsymbol{C}\delta \boldsymbol{x}_T, \tag{3.7}$$

where $\delta \boldsymbol{x} := [\delta x_1 \cdots \delta x_N]^T$. The delayed variations are denoted by $\delta \boldsymbol{x}_\tau := \delta \boldsymbol{x}(t-\tau)$ and $\delta \boldsymbol{x}_T := \delta \boldsymbol{x}(t-T)$. The elements of $\boldsymbol{C}$ are given by $\{\boldsymbol{C}\}_{nm} = c_{nm}/d_n$ for $n \neq m$ and $\{\boldsymbol{C}\}_{nn} = 0$.

The characteristic equation of the linear system (3.7) is described by

$$\det \left[(s-k+\alpha)\boldsymbol{I}_N - \beta \boldsymbol{I}_N e^{-s\tau} + k\boldsymbol{C}e^{-sT} \right] = 0, \tag{3.8}$$

where s is a complex number. This linear system is stable if and only if all the roots s of Eq. (3.8) are in the open left-half complex plane. Hence, we shall focus on the location of the roots s in the complex plane.Note that $\boldsymbol{H} := \boldsymbol{I}_N - \boldsymbol{C}$ is similar to a real symmetric matrix $\tilde{\boldsymbol{H}} := \boldsymbol{I}_N - \boldsymbol{D}^{-1/2}\boldsymbol{A}\boldsymbol{D}^{-1/2}$, where $\boldsymbol{D} := \mathrm{diag}\{d_1, \ldots, d_n\}$ and $\boldsymbol{A} := \boldsymbol{D}\boldsymbol{C}$ [2]. Thus, $\boldsymbol{H}$ and $\tilde{\boldsymbol{H}}$ have the same real eigenvalues ρ_q $(q = 1, \ldots, N)$. It is generally known that a real symmetric matrix is similar to the diagonal matrix whose diagonal elements are its real eigenvalues. As a consequence, $\boldsymbol{H}$ is similar to this diagonal matrix, and can be diagonalized as

$$\boldsymbol{P}^{-1}\boldsymbol{H}\boldsymbol{P} = \mathrm{diag}(\rho_1, \ldots, \rho_N),$$

where $\boldsymbol{P}$ is a diagonal transformation matrix. It should be noted that the eigenvalues of $\tilde{\boldsymbol{H}}$, which are equivalent to those of $\boldsymbol{H}$, are within the range $\rho_q \in [0, 2]$ for any network topology (see Lemma 1.7 in [72] and reference [58] for details):

$$0 = \rho_1 \leq \rho_2 \leq \cdots \leq \rho_N \leq 2. \tag{3.9}$$

This fact allows us to simplify the characteristic equation (3.8):

$$\begin{aligned} g(s) &= \det\left[\boldsymbol{P}^{-1}\left\{(s - k + \alpha - \beta e^{-s\tau})\,\boldsymbol{I}_N + k\boldsymbol{C}e^{-sT}\right\}\boldsymbol{P}\right] \\ &= \det\left[\left(s - k + \alpha - \beta e^{-s\tau} + ke^{-sT}\right)\boldsymbol{I}_N - ke^{-sT}\boldsymbol{P}^{-1}\boldsymbol{H}\boldsymbol{P}\right] \\ &= \det\left[\left(s - k + \alpha - \beta e^{-s\tau} + ke^{-sT}\right)\boldsymbol{I}_N - ke^{-sT}\mathrm{diag}(\rho_1, \ldots, \rho_N)\right] \\ &= 0. \end{aligned} \tag{3.10}$$

As $g(s)$ is a determinant of the diagonal matrix, it can be expressed as a product of the characteristic equations of scalar systems,

$$g(s) := \prod_{q=1}^{N} \bar{g}(s, \rho_q) = 0, \tag{3.11}$$

where the quasi-polynomial $\bar{g}(s, \rho)$ is given by

$$\bar{g}(s, \rho) := s + \alpha - k\left\{1 - (1 - \rho)e^{-sT}\right\} - \beta e^{-s\tau}. \tag{3.12}$$

It is obvious that the steady state is stable for any network topology if all the roots s of $\bar{g}(s, \rho) = 0$ are in the open left-half complex plane for all $\rho \in [0, 2]$. It must be emphasized that $\bar{g}(s, \rho)$,defined by Eq. (3.12), is equivalent to the characteristic quasi-polynomial of a time-delay linear system with parameter uncertainty (see Fig. 3.1),

$$\begin{aligned} \dot{\bar{x}} &= -\alpha\bar{x} + \beta\bar{x}_\tau + \bar{u}, \\ \bar{u} &= k\left\{\bar{x} - (1 - \rho)\bar{x}_T\right\}, \end{aligned} \tag{3.13}$$

[2]From $\{\boldsymbol{A}\}_{nm} = \{\boldsymbol{D}\boldsymbol{C}\}_{nm} = c_{nm}$, we see that $\tilde{\boldsymbol{H}}$ is a real symmetric matrix. Further, it is obvious that $\boldsymbol{H}$ is similar to $\tilde{\boldsymbol{H}}$ because $\boldsymbol{H} = \boldsymbol{D}^{-1/2}\tilde{\boldsymbol{H}}\boldsymbol{D}^{1/2}$ holds.

where $\bar{x} \in \mathbb{R}$ is the state variable and $\rho \in [0, 2]$ can be treated as an uncertain parameter. We see that the stability of the steady state in the network with oscillators (3.1) and connection (3.2) with topology uncertainty is equivalent to that of the linear system (3.13) with parameter uncertainty. The next section proposes a procedure to design the delayed connection parameters, k and T, such that all of the roots of $\bar{g}(s, \rho) = 0$ are in the open left-half complex plane for all $\rho \in [0, 2]$.

3.4 Design of connection

In the previous study [35], it was shown that, if $\alpha < \beta$ holds, amplitude death never occurs at the steady state in a pair of oscillators (i.e., $N = 2$) [3]. Now we extend this property to a network system with oscillators (3.1) and connection (3.2).

Lemma 1. *Amplitude death never occurs at steady state (3.4) in a network system consisting of oscillators (3.1) coupled by connection (3.2) if $\alpha < \beta$ holds.*

Proof. Consider the stability of $\bar{g}(s, 0)$. This quasi-polynomial at $s = 0$ is $\bar{g}(0, 0) = \alpha - \beta$ and, for real positive s, $\bar{g}(s, 0) \to +\infty$ as $s \to +\infty$. This implies that, if $\alpha < \beta$ (i.e., $\bar{g}(0, 0) < 0$) holds, $\bar{g}(s, 0) = 0$ has at least one real positive root. Since $\rho_1 = 0$ is always true due to Eq. (3.9), the characteristic equation $g(s) = 0$ includes $\bar{g}(s, 0) = 0$. Thus, the stability of $\bar{g}(s, 0)$ is a necessary condition for that of $g(s) = 0$. As a result, it is sufficient that $\alpha < \beta$ for $g(s)$ to be unstable. □

The fixed point x^* of oscillators (3.1) without coupling (i.e., $k = 0$) is stable for any $\tau \geq 0$ if $|\beta| < \alpha$ holds (see Sec. 5.2 in Ref. [73]). From this condition and Lemma 1, the present study has to consider oscillators (3.1) satisfying

$$\beta < -\alpha < 0. \tag{3.14}$$

This assumption indicates that x^* is unstable, and thus amplitude death may occur at the steady state. Our main goal is to provide a systematic procedure for designing the coupling strength k and the connection delay T such that the steady state in a network system is stable for any topology $\boldsymbol{C}$ and for any oscillator delay $\tau \geq 0$. The eigenvalue $\rho \in [0, 2]$, which is the uncertain parameter of $\bar{g}(s, \rho)$, depends on the network topology $\boldsymbol{C}$; therefore, if the family of quasi-polynomials,

$$\Omega := \{\bar{g}(s, \rho) \mid \rho \in [0, 2]\}, \tag{3.15}$$

is stable, the stability of the steady state is guaranteed regardless of the network topology. Since all the coefficients of $\bar{g}(s, \rho)$ are affine functions of ρ (see Eq. (3.12)), the family Ω can be rewritten as a convex combination of the two quasi-polynomials, $\bar{g}(s, 0)$ and $\bar{g}(s, 2)$, in the coefficient space,

$$\Omega := \{(1 - \mu)\bar{g}(s, 0) + \mu\bar{g}(s, 2) \mid \mu \in [0, 1]\}, \tag{3.16}$$

[3]This fact implies that, in a pair of delayed oscillators, the odd-number property remains even for amplitude death.

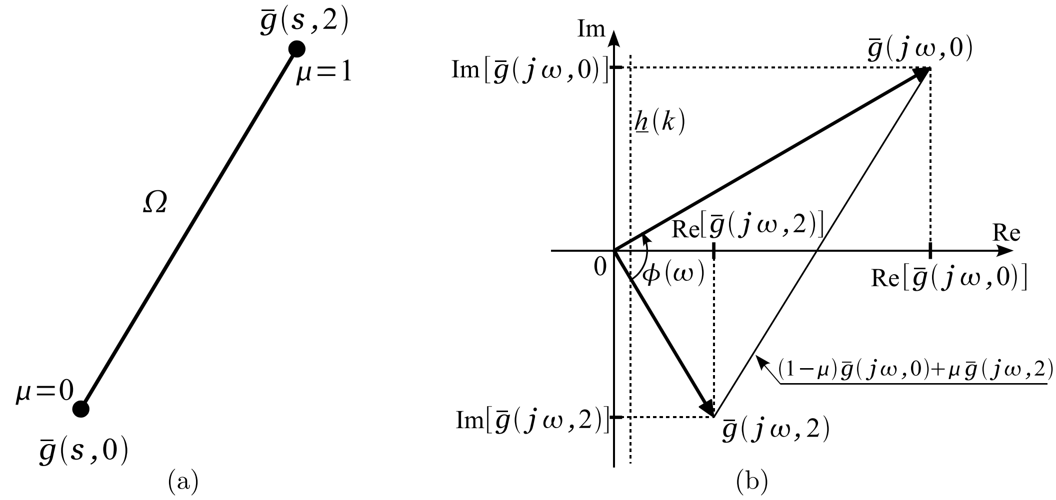

Figure 3.2: Sketches of segment Ω and vectors $\bar{g}(j\omega,0)$ and $\bar{g}(j\omega,2)$: (a) Ω with vertices $\bar{g}(s,0)$ and $\bar{g}(s,2)$ in the coefficient space; and (b) vectors $\bar{g}(j\omega,0)$ and $\bar{g}(j\omega,2)$ on the complex plane.

where the one parameter is given by $\mu := \rho/2$. As a result, $\bar{g}(s,\rho)$ for $\rho \in [0,2]$ defined by Eq. (3.15), which is equivalent to the one-parameter family $\bar{g}(s,2\mu)$ for $\mu \in [0,1]$ defined by Eq. (3.16), forms a segment with vertices $\bar{g}(s,0)$ and $\bar{g}(s,2)$ in the coefficient space as illustrated in Fig. 3.2(a). One may conclude that we must to check the stability of the entire segment to guarantee the stability of Ω. This is not true: we can check it by only examining the segment vertices $\bar{g}(s,0)$ and $\bar{g}(s,2)$. In robust control theory [70, 71], it is known that Ω is stable if the following two conditions are satisfied:

(condition 1) $\bar{g}(s,0)$ and $\bar{g}(s,2)$ are stable;

(condition 2) $\phi(\omega) := \arg[\bar{g}(j\omega,0)] - \arg[\bar{g}(j\omega,2)] \neq \pm\pi$ for any $\omega \in [0,+\infty)$, where $j^2 = -1$.

Condition 1 provides stability for the segment vertices $\bar{g}(s,0)$ and $\bar{g}(s,2)$: all the roots of $\bar{g}(s,0) = 0$ and $\bar{g}(s,2) = 0$ are in the open left-half complex plane. These roots never cross the imaginary axis for any $\mu \in (0,1)$, since condition 2 implies that $(1-\mu)\bar{g}(j\omega,0) + \mu\bar{g}(j\omega,2) \neq 0$, as illustrated in Fig. 3.2(b), holds for any $\omega \in [0,+\infty)$. This is a rough explanation of these conditions: see Ref. [70] and Theorem 4.1.3 in Ref. [71] for a rigorous proof. The following lemmas and corollary provide k and T such that the above two conditions hold.

Lemma 2. *$\bar{g}(s,0)$ and $\bar{g}(s,2)$ are stable (i.e., condition 1 holds) if the connection delay $T > 0$ is set as*

$$T = \frac{1}{2}\tau, \tag{3.17}$$

and the coupling strength $k < 0$ is chosen from

$$k \in \left(4\beta - 2\sqrt{2\beta(\beta-\alpha)}, 4\beta + 2\sqrt{2\beta(\beta-\alpha)}\right). \tag{3.18}$$

Proof. This proof is divided into two steps: for step (i) $T = \tau = 0$; and for step (ii) $T = \tau/2 \geq 0$. Step (i) shall prove that all the roots of $\bar{g}(s,0) = 0$ and $\bar{g}(s,2) = 0$ for $T = \tau = 0$ are in the open left-half complex plane, and step (ii) shall show that these roots with $T = \tau/2 \geq 0$ never cross the imaginary axis for any $\tau \in [0, +\infty)$.

For step (i), $T = \tau = 0$ is substituted into $\bar{g}(s,0)$ and $\bar{g}(s,2)$:

$$\bar{g}(s,0) = s + \alpha - \beta, \;\; \bar{g}(s,2) = s + \alpha - 2k - \beta.$$

From assumption (3.14), we notice that all the roots of $\bar{g}(s,0) = 0$ and $\bar{g}(s,2) = 0$ with $T = \tau = 0$ are in the open left-half complex plane for any $k < 0$.

For step (ii), we consider $\bar{g}(j\omega,0) = \mathrm{Re}[\bar{g}(j\omega,0)] + j\mathrm{Im}[\bar{g}(j\omega,0)]$ and $\bar{g}(j\omega,2) = \mathrm{Re}[\bar{g}(j\omega,2)] + j\mathrm{Im}[\bar{g}(j\omega,2)]$. We see that $\bar{g}(j\omega,0) = 0$ is not satisfied for any $\omega \in \mathbb{R}$ (i.e., none of the roots of $\bar{g}(s,0) = 0$ ever cross the imaginary axis) if at least one of $\mathrm{Re}[\bar{g}(j\omega,0)] = 0$ and $\mathrm{Im}[\bar{g}(j\omega,0)] = 0$ does not hold for any $\omega \in \mathbb{R}$. The same holds true for $\bar{g}(j\omega,2) = 0$. Let us show that $\mathrm{Re}[\bar{g}(j\omega,0)] = 0$ and $\mathrm{Re}[\bar{g}(j\omega,2)] = 0$ with $T = \tau/2 \geq 0$ do not hold for any $\omega \in \mathbb{R}$. Here $\mathrm{Re}[\bar{g}(j\omega,0)]$ and $\mathrm{Re}[\bar{g}(j\omega,2)]$ are given by

$$\mathrm{Re}[\bar{g}(j\omega,0)] = \alpha - k + \beta + h_0(\omega\tau), \;\; \mathrm{Re}[\bar{g}(j\omega,2)] = \alpha - k + \beta + h_2(\omega\tau),$$

where

$$h_0(\omega\tau) := k\cos\frac{\omega\tau}{2} - 2\beta\cos^2\frac{\omega\tau}{2}, \;\; h_2(\omega\tau) := -k\cos\frac{\omega\tau}{2} - 2\beta\cos^2\frac{\omega\tau}{2}.$$

From a simple algebraic computation, we notice that these functions satisfy $h_{0,2}(\omega\tau) \geq k^2/(8\beta)$. As a result, we obtain $\mathrm{Re}[\bar{g}(j\omega,0)] \geq \underline{h}(k) > 0$ and $\mathrm{Re}[\bar{g}(j\omega,2)] \geq \underline{h}(k) > 0$ (see Fig. 3.2(b)), where

$$\underline{h}(k) := \alpha - k + \beta + \frac{k^2}{8\beta}. \tag{3.19}$$

These inequalities imply that $\mathrm{Re}[\bar{g}(j\omega,0)] = 0$ and $\mathrm{Re}[\bar{g}(j\omega,2)] = 0$ with $T = \tau/2 \geq 0$ do not hold for any $\omega \in \mathbb{R}$. Condition (3.18) presents the range for k that satisfies $\underline{h}(k) > 0$. □

This lemma is equivalent to a design procedure for a pair of oscillators (i.e., $N = 2$) [74], since $g(s) = \bar{g}(s,\rho_1)\bar{g}(s,\rho_2) = \bar{g}(s,0)\bar{g}(s,2)$.

Corollary 1. *$\phi(\omega) \neq \pm\pi$ for any $\omega \in [0, +\infty)$ holds (i.e., condition 2 holds), if the connection delay $T > 0$ and the coupling strength $k < 0$ are as designed in Lemma 2.*

Proof. $\phi(\omega) \neq \pm\pi$ suggests that the two vectors $\bar{g}(j\omega,0)$ and $\bar{g}(j\omega,2)$ on the complex plane (see Fig. 3.2(b)) never have opposite directions for any $\omega \in [0, +\infty)$. This is obviously true if the real parts of the two vectors are positive,

$$\mathrm{Re}[\bar{g}(j\omega,0)] > 0, \;\; \mathrm{Re}[\bar{g}(j\omega,2)] > 0, \;\; \forall\omega \in [0, +\infty). \tag{3.20}$$

Inequalities (3.20) were proved in Lemma 2. □

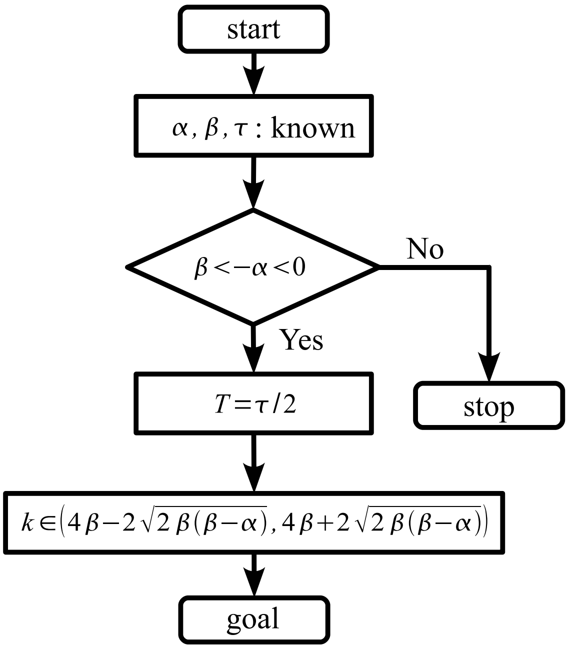

Figure 3.3: Flow chart of our systematic procedure for designing k and T. This procedure is based on a sufficient condition for the steady state to be stable.

Note that Eq. (3.17) and the range (3.18) are independent of each other. This independence implies that the designed k is valid for any $\tau > 0$. As a consequence, Lemmas 1 and 2 and Corollary 1, obtained above, lead to the following main result.

Theorem 1. *Assume that oscillators (3.1) satisfy inequality (3.14). A steady state (3.4) in the oscillators (3.1) coupled by connection (3.2) is stable for any network topology $\boldsymbol{C}$ and for any oscillator delay $\tau > 0$ if the connection delay $T > 0$ is set according to Eq. (3.17) and the coupling strength $k < 0$ is chosen from the range (3.18).*

Proof. Since it is obvious from Lemmas 1 and 2, and Corollary 2, the proof is omitted. □

This theorem provides a systematic procedure for designing the coupling strength k and the connection delay T (see Fig. 3.3): first, the oscillator parameters, α, β, and τ, are known; second, if assumption (3.14) is not satisfied, then we have to abandon this procedure for designing them; third, T is set according to Eq. (3.17), and $k < 0$ is chosen from the range (3.18). It must be emphasized that k and T designed in accordance with the flow chart illustrated in Fig. 3.3 are valid for any network topology $\boldsymbol{C}$ and for any $\tau \geq 0$. Note that it is possible to reach the goal by other design procedures, since this theorem is based on a sufficient condition for the steady state to be stable.

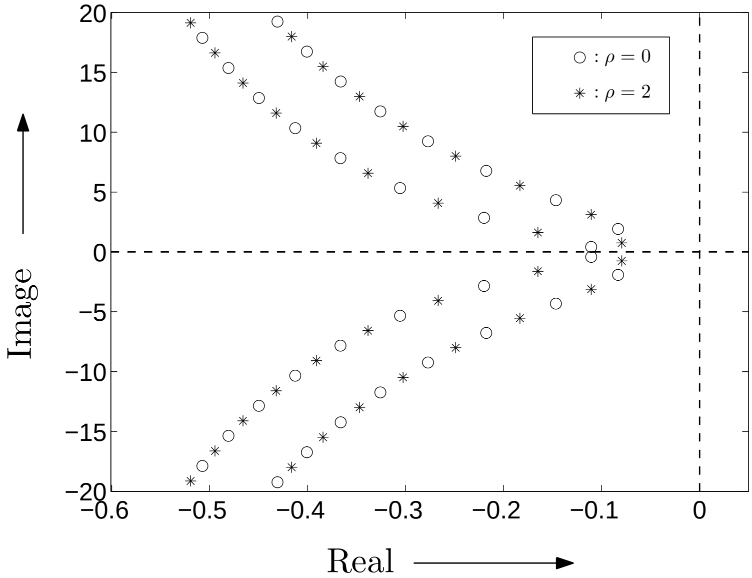

Figure 3.4: Roots of $\bar{g}(s, \rho) = 0$ $(\rho = 0, 2)$ $(\tau = 5, T = 2.5, k = -2)$.

3.5 Numerical examples

This section numerically confirms the analytical results provided in the preceding sections. Consider oscillators (3.1) with the parameter $\alpha = 1$ and the nonlinear function,

$$f(x) = \begin{cases} -2.0 & \text{if } x \leq -4.25 \\ 0.80x + 1.40 & \text{if } -4.25 < x \leq 1.85 \\ -1.80x + 6.21 & \text{if } 1.85 < x \leq 3.95 \\ -0.9 & \text{if } x > 3.95 \end{cases}. \tag{3.21}$$

Each oscillator can be implemented by real electronic circuits [37]. We follow the design procedure illustrated in Fig. 3.3: first, $\alpha = 1$, $\beta = -1.8$, and $\tau = 5$ are known; second, confirm they satisfy assumption (3.14), and go to the next step; third, $T = \tau/2 = 2.5$ and $k = -2 \in (-13.5498, -0.8502)$ are obtained.

Let us confirm that the designed parameters satisfy conditions 1 and 2 by performing numerical simulations. Figure 3.4 shows the roots of $\bar{g}(s, 0) = 0$ and $\bar{g}(s, 2) = 0$ with the designed parameters. There is no root in the right-half of the complex plane. Thus, we see that $\bar{g}(s, 0)$ and $\bar{g}(s, 2)$ are stable; that is, condition 1 is satisfied. Figures 3.5(a) and 3.5(b) illustrate the vector loci of $\bar{g}(j\omega, 0)$ and $\bar{g}(j\omega, 2)$, respectively, with the designed parameters. It can be seen that each locus is always located on the right side of $\underline{h}(-2) \simeq 0.92 > 0$, defined by Eq. (3.19). This result verifies that the two vectors $\bar{g}(j\omega, 0)$ and $\bar{g}(j\omega, 2)$ never have opposite directions; that is, condition 2 is satisfied.

Now, we numerically check that the designed parameters are valid for various networks. Note that since the parameters were designed on the basis of the sufficient

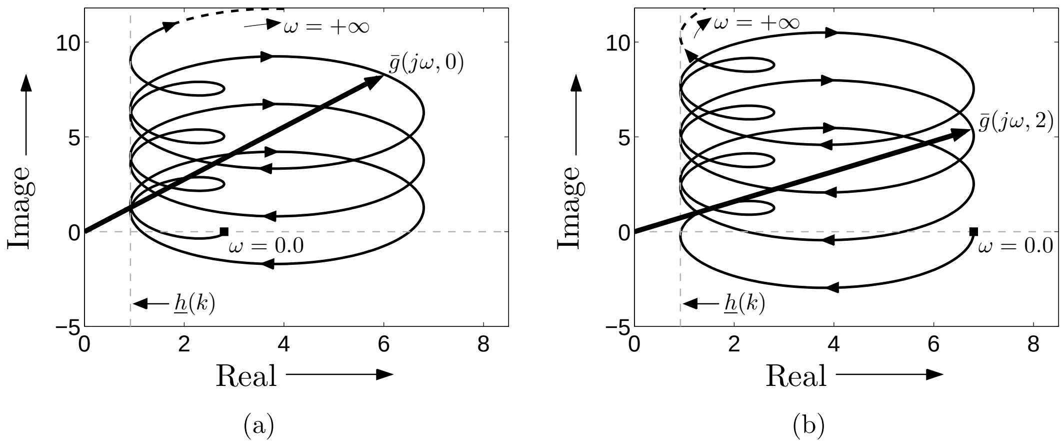

Figure 3.5: Vector loci of $\bar{g}(j\omega, 0)$ and $\bar{g}(j\omega, 2)$ ($\tau = 5, T = 2.5, k = -2$): (a) $\bar{g}(j\omega, 0)$, (b) $\bar{g}(j\omega, 2)$.

condition, they must be a subset of the stability region in (τ, T) space.This region consists of the parameter sets (τ, T) in which the steady state is stable. The marginal stability curves are obtained by solving $\bar{g}(j\omega, \rho) = 0$ for T and τ. The direction in which the roots of $\bar{g}(j\omega, \rho) = 0$ cross the imaginary axis depends on the sign of $\mathrm{Re}[\mathrm{d}s/\mathrm{d}T]_{s=j\omega}$ on the cur ves. The numerical procedure for estimating the curves and the direction is explained in Appendix 2. Note that if the network topology is known in advance, the region of stability can be estimated by the numerical procedure. However, the present chapter deals with the situation in which the topology is unknown, so this region cannot be obtained. In order to check that the designed parameters are valid for various networks, we employ the three typical networks: complete networks, ring networks, and small-world networks.

Consider a complete network (i.e., all-to-all connections) consisting of two hundred oscillators ($N = 200$). The eigenvalues of $\boldsymbol{H}$ are $\rho_1 = 0$ and $\rho_{2\text{-}200} = 200/199$. Figure 3.6(a) illustrates the region of stability and the marginal stability curves. The bold (thin) lines indicate the curves with negative (positive) signs of $\mathrm{Re}[\mathrm{d}s/\mathrm{d}T]_{s=j\omega}$. When T increases and crosses the bold (thin) line upward at a fixed value of τ, we subtract (add) 2 from (to) the number of unstable roots. Since $\bar{g}(s, \rho) = 0$ at the origin (i.e., $\tau = T = 0$) does not have unstable roots, there are no unstable roots in the region represented by Γ. Furthermore, it must be emphasized that Γ has a long strip that includes $T = \tau/2$, indicated by the dashed line (i.e., this line is a subset of the region Γ). This line never crosses the marginal curves. There is another long strip including $T = \tau$; however, this strip does not exist generally for other networks, as we shall show later. Figure 3.6(b) shows the time-series data of the first oscillator at point (A) in Fig. 3.6(a). Without coupling the state variable x_1 behaves chaotically until $t = 500$. At $t = 500$ the oscillators are coupled, and then x_1 and the coupling signal u_1 converge on x^* and zero, respectively. It can be seen that, according to our systematic design procedure, the stabilization remains

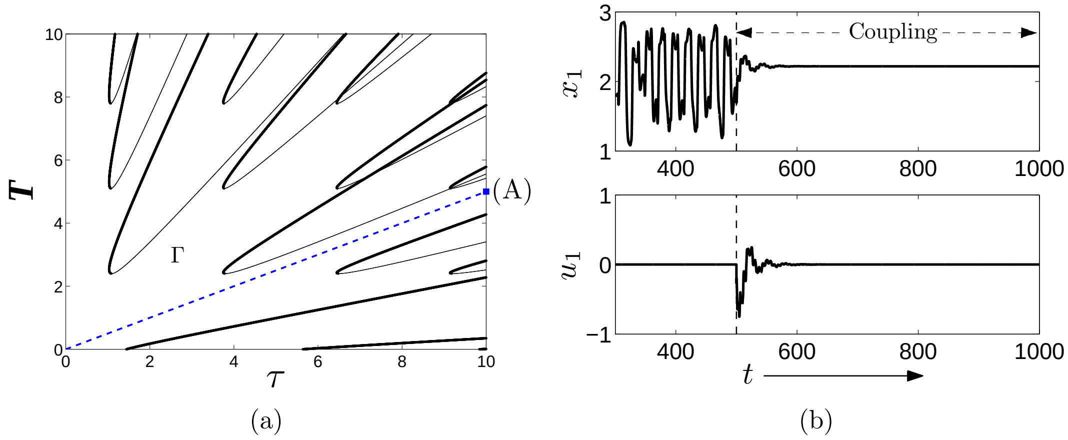

Figure 3.6: Marginal stability curves and time-series data of the complete network ($N = 200, k = -2$). (a) Marginal stability curves: bold (thin) lines indicate the curves with negative (positive) direction, from Eq. (3). The dashed line indicates $T = \tau/2$ where the sufficient condition for the steady state to be stable always holds. (b) Time-series data of the state variable x_1 and the coupling signal u_1 at point (A) ($\tau = 10, T = 5$) in (a).

even if the delay times τ and T are extended indefinitely.

Next, we consider networks on a ring topology and a small-world topology with N_C shortcuts [4]. Figures 3.7(a) and 3.7(b) illustrate the marginal stability curves for the ring topology ($N = 100, k = -4$) and the small-word topology ($N = 50, N_C = 20, k = -10$), respectively. The eigenvalues of $\boldsymbol{H}$ for the ring topology are $\rho_1 = 0$, $\rho_{2\text{-}99} \in [0.0020, 1.9980]$, and $\rho_{100} = 2$. For the small-world topology, we have $\rho_1 = 0$, $\rho_{2\text{-}50} \in [0.0807, 1.9522]$. The stability regions Γ in Figs. 3.7(a) and 3.7(b) contain the long strip that includes $T = \tau/2$ where the steady state is stable (i.e., this line is a subset of the region Γ). It must be noted that even though there are other long stability strips of (T, τ) in Fig. 3.6(a) and Fig. 3.7, these do not always appear for other topologies. Therefore, these strips cannot be used in our topology-free design.

Let us clarify the root distribution of $\bar{g}(s, \rho) = 0$ on the line $T = \tau/2$. Substituting $s = s_R + js_I$ into $\bar{g}(s, \rho) = 0$ with $T = \tau/2$, we obtain its real and imaginary parts as follows:

$$\begin{aligned} \mathrm{Re}\,[\bar{g}(s,\rho)] &= s_R + \alpha - k + k(1-\rho)e^{-s_R\tau/2}\cos s_I\tau/2 - \beta e^{-s_R\tau}\cos s_I\tau = 0, \\ \mathrm{Im}\,[\bar{g}(s,\rho)] &= s_I - k(1-\rho)e^{-s_R\tau/2}\sin s_I\tau/2 + \beta e^{-s_R\tau}\sin s_I\tau = 0. \end{aligned} \tag{3.22}$$

[4]For the small-world topology [75], every oscillator is coupled on a one-dimensional ring-type lattice with a periodic boundary and N_C shortcuts, the ends of which are randomly chosen, are added to the lattice. In particular, the elements c_{nm} are given by the following procedure: $c_{n(n+1)} = c_{(n+1)n} = 1, \forall n \in [1, N-1]$, and $c_{1N} = c_{N1} = 1$; choose N_C pairs of nodes $\{n, m\}$ randomly and connect them as $c_{nm} = c_{mn} = 1$; set the other elements to zero.

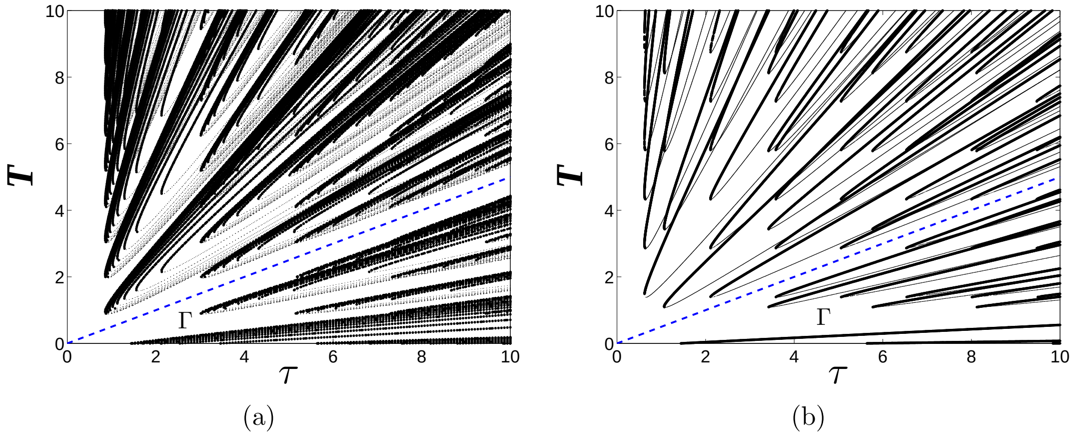

Figure 3.7: Marginal stability curves of the network system on (a) ring topology ($N = 100, k = -4$) and (b) small-world topology ($N = 50, N_C = 20, k = -10$). The dashed line $T = \tau/2$ indicates the sufficient condition for the steady state to be stable.

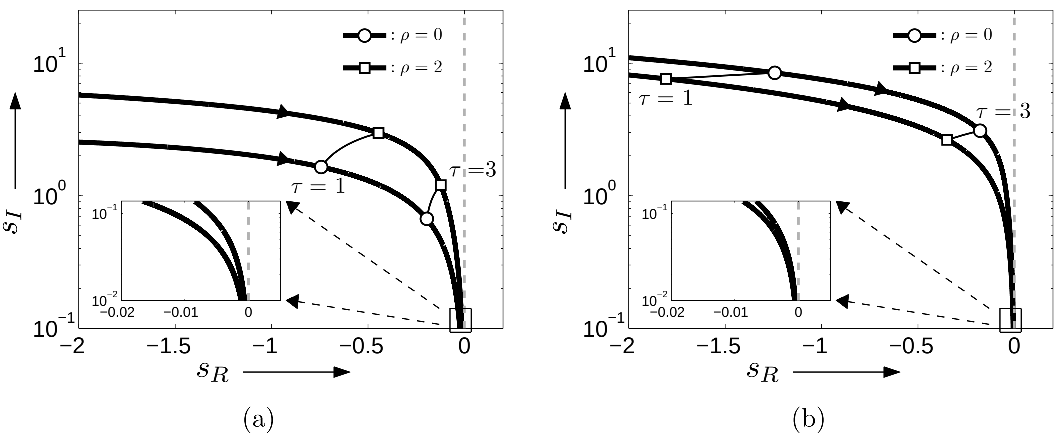

Figure 3.8: Root loci of $\bar{g}(s, \rho) = 0$ ($\rho = 0, 2$) for $k = -2$: (a) first right-most root loci, (b) second right-most root loci.

The roots of $\bar{g}(s, \rho) = 0$ are obtained by solving Eq. (3.22). Figures 3.8(a) and 3.8(b) illustrate the loci of the first and the second right-most roots for $k = -2$, respectively [5]. The bold curves with circles $\bigcirc$ (squares $\square$) indicate the root loci with $\rho = 0$ ($\rho = 2$) as τ varies from zero to infinity. The thin curves with $\bigcirc$ and $\square$ ends are the loci at $\tau = 1$ and $\tau = 3$ as ρ varies from zero to two. For any $\rho \in [0, 2]$, the root loci exist between the bold curves with $\rho = 0$ and $\rho = 2$. It can be seen from the insets of Fig. 3.8(a) and 3.8(b) that as τ increases, the roots asymptotically approach the imaginary axis $s_R = 0$, but they never cross the axis. These facts support the claim that there are no unstable roots on the line $T = \tau/2$.

3.6 Conclusion

This chapter showed that the stability of a steady state in a network with topology uncertainty is equivalent to the stability of a delayed linear system with parameter uncertainty. On the basis of the robust stability analysis of the linear system, we provided a simple systematic procedure for designing the connection parameters. This procedure has two advantages: the designed parameters can be used for any network topology, and the procedure is valid for long-delay oscillators. Our analytical results were numerically verified on complete, ring, and small-world networks.

[5] Since $\bar{g}(s, \rho) = 0$ has an infinite number of roots, an enormous number of loci can be obtained numerically. In order to make clear the loci characteristics, we focus on the first and the second right-most roots at $\tau = 1$. Figure 3.8 shows the loci starting from these roots as τ varies. We observed that the other loci have the similar characteristics.

Chapter 4

Stabilization of time-delay nonlinear oscillators controlled by multiple delay feedback

4.1 Introduction

Various methods for controlling chaos have been proposed and applied to real systems, such as electronic circuits, mechanical systems, and chemical reactions [76–80]. One such method, delayed feedback control (DFC), proposed by Pyragas [10], has created considerable interest in the field of nonlinear science [81] and the control theory [82]. The DFC method has been used to stabilize unstable periodic orbits (UPOs) and unstable fixed points (UFPs). Recently, the stabilization of UFPs has been investigated theoretically [9, 83–86], and applied to inverted pendulums [86, 87] and laser systems [88].

Multiple delay feedback control (MDFC), in which the controller has two or more time delays, was proposed by Ahlborn and Parlitz [11, 89, 90]. The UFPs are stabilized using the MDFC, with an appropriate combination of time delays. This method can achieve stabilization even for long delay times. Therefore, it is useful when controlling fast dynamic systems [11] or when either a computer with an analog-to-digital/digital-to-analog AD/DA converter [91] or a bucket brigade delay (BBD) device [92] (i.e., a series of sample-and-hold circuits) are used to implement the time delays. MDFC has been studied in detail from both physical [11] and theoretical [89, 93, 94] viewpoints.

The dynamics of time-delay nonlinear oscillators have gained increasing attention both from the theoretical viewpoint [20, 21] as well as for practical applications [7, 8, 95–101]. In particular, as time delays in engineering nonlinear systems such as the metal cutting process [7, 8] and the contact rotating systems [27] can induce undesirable oscillations, it would be important to investigate the stabilization of the time-delay induced oscillations. In order to avoid oscillations, the system parameters must be chosen on the basis of stability analysis. If this avoidance requires a major system change, it might have to be abandoned due to practical restrictions. An alternative method is to suppress the oscillations using feedback control. This is a practical method, since it does not require a major system change.

In 1995, Namajūnas *et al.* showed both theoretically and experimentally that the DFC method can stabilize UFPs in time-delay chaotic oscillators [34]. However, it is not easy to provide a procedure for designing the controller parameters, the feedback gain and the controller delay, since the characteristic equation includes the two delay terms (i.e., the oscillator delay and the controller delay). Furthermore, the controller delay must be chosen within several narrow stability intervals. Since these intervals are almost smaller than the oscillator delay, the controller delay should be set to around the oscillator delay or less than it. These features make it difficult to design the controller: for example, (a) numerical calculations for solving the characteristic equation including the two delay terms are needed to determine the controller parameters; (b) the controller delay must be set within the narrow stability intervals; (c) and the controller delay cannot be longer than around the oscillator delay.

In recent years, these problems of the DFC method have been partially solved. For problem (a), Guan *et al.* provided a systematic procedure for designing the delayed feedback controller on the basis of the Lyapunov–Krasovskii functional approach [102]. However, this procedure cannot be used for oscillators with long time delays. For problem (b), Gjurchinovski and Urumov proposed a type of feedback control with a time-varying delay [103]. Although the main advantage of this proposal is that the stability regions in the controller parameter space are greater than those for the original DFC, it is not easy to show a procedure for designing the controller and employing a control with a long delay. From problem (c), we notice that, for short time-delay oscillators, the controller delay of the DFC method has to be short. However, it is difficult to realize the short controller delay by the computer or the BBD device, since they have a finite speed operation.

The present study shows that the MDFC method provides answers to such unsolved problems for the stabilization of UFPs in time-delay nonlinear oscillators. The stability boundary curves in the control parameter space are derived using linear stability analysis. A simple procedure for designing the feedback gain and the controller delays, which is based on the observation of the root locus movement of the characteristic equation, is provided. The main advantages of this procedure are as follows: it is guaranteed that the UFPs can be stabilized by the designed controller for any oscillator delay if the oscillator parameters are within a large region in an oscillator parameter space; the controller delays, which retain a proportional relation with a certain bias, can be freely selected. These advantages are useful for the following practical situations: the UFPs in long time-delay oscillators can be stabilized by the designed controller; there is no need to numerically solve the characteristic equation in designing the controller; the controller delays can be arbitrarily chosen. This arbitrarily chosen indicates that the UFPs in short time-delay oscillators can be stabilized even by the slow computer or the slow BBD device. Furthermore, these analytical results are experimentally verified with electronic circuits.

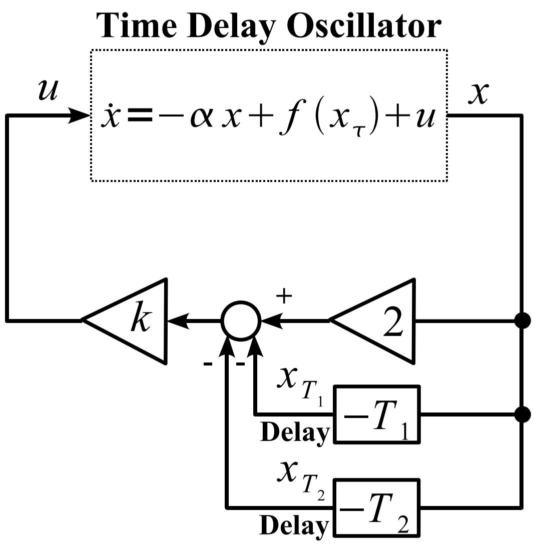

Figure 4.1: Block diagram of multiple delayed feedback control of time-delay oscillators.

4.2 Problem statement

Consider a first-order delay differential equation [20],

$$\dot{x} = -\alpha x + f(x_\tau) + u, \tag{4.1}$$

where $x \in \boldsymbol{R}$ is the state variable, $x_\tau := x(t-\tau)$ is the delayed variable, $\alpha > 0$ is the system parameter, and $f : \boldsymbol{R} \to \boldsymbol{R}$ is the nonlinear function. The fixed point is described by $x^* : 0 = -\alpha x^* + f(x^*)$. The MDFC signal $u \in \boldsymbol{R}$ is given by

$$u = k(2x - x_{T_1} - x_{T_2}), \tag{4.2}$$

where $x_{T_i} = x\,(t - T_i)\,,\ i = 1, 2$ are the delayed state variables and $k \in \boldsymbol{R}$ is the feedback gain (see Fig. 4.1). Note that controller (4.2) with $T_1 = T_2$ is identical to the original (i.e., single) delayed feedback controller. Oscillator (4.1) with controller (4.2) also has the fixed point x^*.

The control system linearized at $x = x^*$ is described by

$$\dot{z} = -\alpha z + \beta z_\tau + k\left\{2z - z_{T_1} - z_{T_2}\right\}, \tag{4.3}$$

where $z \in \boldsymbol{R}$ is the variation of state x around $x = x^*$, that is, $z := x - x^*$. Here β is the slope of $f(x)$ at x^*, that is, $\beta = \left\{\mathrm{d}f(x)/\mathrm{d}x\right\}_{x=x^*}$. The characteristic equation of linear system (4.3),

$$g(\lambda) := \lambda + \alpha - \beta e^{-\lambda\tau} - k\left(2 - e^{-\lambda T_1} - e^{-\lambda T_2}\right) = 0, \tag{4.4}$$

can be used to evaluate the stability of $x = x^*$; the fixed point x^* is stable if and only if all of the roots of Eq. (4.4) lie in the open left-half of the complex plane. It should be noted that the stability analysis is valid only in the vicinity of x^*; this fact implies that our stability analysis cannot guarantee the global stability of x^*.

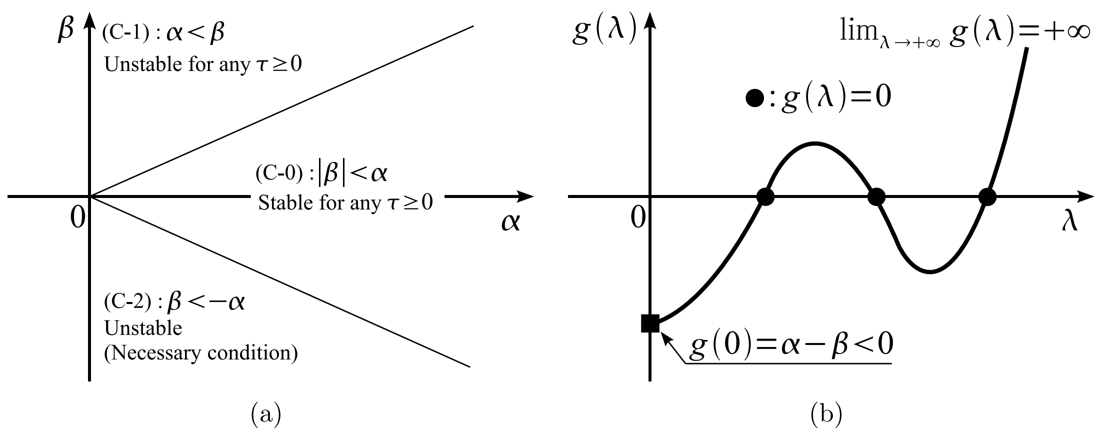

Figure 4.2: Sketches: (a) stability domain of x^* without control (i.e., $T_1 = T_2 = 0$) in the α-β plane; (b) function $g(\lambda)$ with the odd number property.

4.3 Stability analysis

The present study assumes that the oscillator (4.1) without control (i.e., $T_1 = T_2 = 0$) will oscillate; hence, the fixed point x^* is assumed to be unstable throughout this study. The stability of x^* is governed by the characteristic equation, $\lambda + \alpha - \beta e^{-\lambda\tau} = 0$. According to the well-known results of the first-order delay differential equation [73], in the oscillator parameter plane as sketched in Fig. 4.2(a), we know that there are three conditions: (C-0) $|\beta| < \alpha$; (C-1) $\alpha < \beta$; (C-2) $\beta < -\alpha$. Since x^* is stable for any $\tau \geq 0$ under condition (C-0), there is no need to stabilize x^*. Hence, we remove this condition from consideration. In contrast, x^* is unstable for any $\tau \geq 0$ under condition (C-1). Further, the stability of x^* depends on τ under condition (C-2); thus, $\beta < -\alpha$ is a necessary condition for x^* to be unstable. From these arguments, we have to focus only on the two conditions, (C-1) and (C-2).

For the oscillator (4.1) with control (i.e., $T_{1,2} > 0$), it is straightforward to derive a simple instability condition: if $\lim_{\lambda\to+\infty} g(\lambda) = +\infty$ and $g(0) = \alpha - \beta < 0$, then $g(\lambda)$ crosses the positive real axis $\lambda \in [0; +\infty)$ at least once as sketched in Fig. 4.2(b), that is, there exists at least one positive real root for $g(\lambda) = 0$. This fact yields that, if condition (C-1) is satisfied, the fixed point x^* in oscillator (4.1) cannot be stabilized by a control signal (4.2) for any $k \in \boldsymbol{R}$ and $T_{1,2} > 0$. Therefore, throughout this study, we focus only on the fixed points that satisfy condition (C-2). The instability condition (C-1) can be considered as the odd-number property for time-delay oscillators. It should be noted that the previous methods, such as the original DFC [34] and the time-varying DFC [103], never stabilize x^* under condition (C-1) due to their odd-number property. Section 4.6.3 mentions this property in detail.

Let us estimate the stability region in a control parameter space (T_1, T_2) on the basis of Eq. (4.4). The stability changes only when at least one root crosses the imaginary axis. To simplify the stability analysis, the roots on the axis are checked.

Substituting $\lambda = i\lambda_I$ into Eq. (4.4), its real and imaginary parts are obtained:

$$\begin{aligned} &-2k + \alpha - \beta \cos \lambda_I \tau + k(\cos \lambda_I T_1 + \cos \lambda_I T_2) = 0, \\ &\lambda_I + \beta \sin \lambda_I \tau - k(\sin \lambda_I T_1 + \sin \lambda_I T_2) = 0. \end{aligned} \tag{4.5}$$

The marginal stability curves are given by the roots $T_{1,2}$ of Eqs. (4.5). The procedure for obtaining the curves is as follows: set a value of T_1; solve Eqs. (4.5) numerically for T_2 and λ_I; plot (T_1, T_2); change the value of T_1; and then return to the first step. To investigate the direction in which the roots cross the imaginary axis, the sign of the real part of $\mathrm{d}\lambda/\mathrm{d}T_2$,

$$\mathrm{Re}\left[\frac{\mathrm{d}\lambda}{\mathrm{d}T_2}\right]_{\lambda=i\lambda_I} = \mathrm{Re}\left[\frac{i\lambda_I k e^{-i\lambda_I T_2}}{1 + \tau\beta e^{-i\lambda_I \tau} - k\left(T_1 e^{-i\lambda_I T_1} + T_2 e^{-i\lambda_I T_2}\right)}\right], \tag{4.6}$$

is checked, where T_2 and λ_I are the values estimated in the above procedure. With increasing T_2, a positive (negative) value of Eq. (4.6) corresponds to a root crossing the axis from left to right (right to left).

A numerical example illustrates the above procedure. The parameters are fixed at

$$\alpha = 1.0,\ \beta = -3.0,\ \tau = 5.0. \tag{4.7}$$

Let the feedback gain be fixed at $k \approx -6.4641$; the reason for setting this value will be explained in Sec. 4.5.2. Figure 4.3(a) shows the marginal stability curves estimated by this procedure. The bold (thin) lines express the curves with negative (positive) term (4.6). These curves separate the parameter space into several regions. We know that when T_2 increases and crosses the bold (thin) line upward, we subtract (add) 2 from (to) the number of unstable roots. Obviously, for $T_1 = T_2 = 0$, Eq. (4.4) is reduced to $g(\lambda) = \lambda + \alpha - \beta e^{-\lambda\tau}$. According to the stability analysis on scalar delayed systems [104], we notice that the number of unstable roots is 4. From these results, the numbers of unstable roots in the parameter space (T_1, T_2) are automatically obtained as shown in Fig. 4.3 (a). For example, in the regions labeled 2, there exist two unstable roots. Obviously, if (T_1, T_2) are within the region 0, the fixed point x^* is stable. Figure 4.3 (b) is a large-area display of Fig. 4.3 (a). It must be emphasized that the single delay feedback control method (i.e., $T_1 = T_2$) can stabilize x^* only for a small range (e.g., $T_1 = T_2 \lesssim 5.4$, as in Fig. 4.3(b)). Controller (4.2) with an appropriate combination of T_1 and T_2, however, can stabilize it over a wide parameter region (e.g., dotted line A-B).

4.4 Controller design

This section provides a simple procedure for designing controller (4.2), such that both delay times, T_1 and T_2, are as long as possible. From Fig. 4.3(b), it can be seen that there are two long stability strips, A-B and C-D[1]. On the strip A-B, T_1

[1]Although there are several narrow strips in Fig. 4.3(b), this study focuses only on the two typical strips A-B and C-D: diagonal strip and parallel strip to an axis.

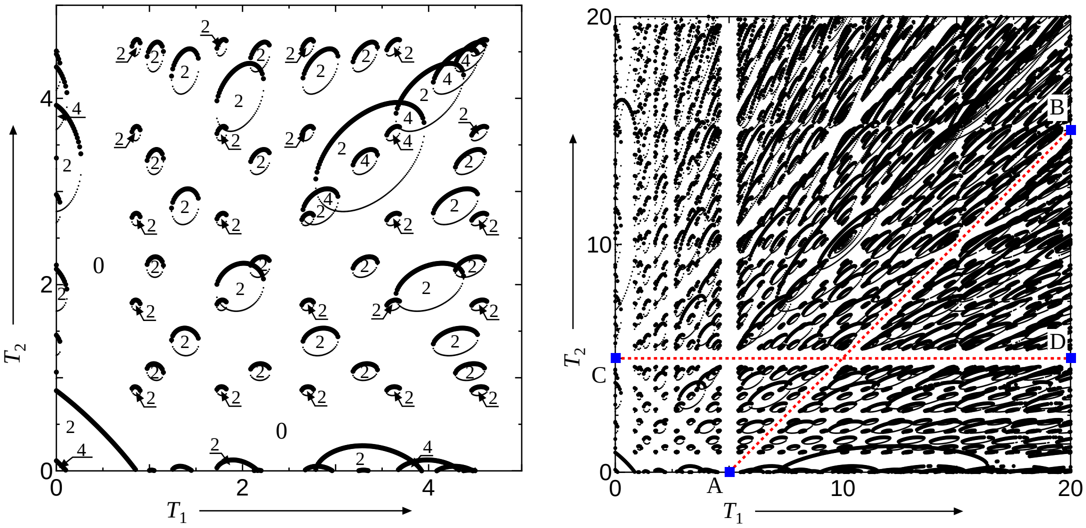

(a) (b)

Figure 4.3: Marginal stability curves of x^* ($\alpha = 1.0$, $\beta = -3.0$, $\tau = 5.0$, $k \approx -6.4641$): (a) $T_{1,2} \in [0, 5]$, (b) $T_{1,2} \in [0, 20]$

.

and T_2 can be set to arbitrary long; however, on the strip C-D, T_2 has to be fixed at a finite time $T_2 \approx \tau = 5$. Thus, the strip C-D is not suitable for designing the controller. Figure 4.3(b) suggests that if T_1 and T_2 keep the relation with τ,

$$T_2 = T_1 - \tau, \; (T_1 > \tau), \tag{4.8}$$

illustrated by the dotted line A-B, then the fixed point x^* remains stable. Now we provide an analytical design procedure, based on the assumption that T_1 and T_2 maintain the relationship (4.8). In order to derive this procedure, the stability analysis is divided into the following two cases: (i) $T_1 = \tau$ and $T_2 = 0$ (i.e., point A in Fig. 4.3(b)); and (ii) $T_2 = T_1 - \tau$ with $T_1 \geq \tau$ (i.e., dotted line A-B in Fig. 4.3(b)).

For case (i), substitution of $T_1 = \tau$ and $T_2 = 0$ into Eq. (4.4) leads to $\lambda + \alpha - k + (k - \beta)e^{-\lambda\tau} = 0$. From the well-known stability condition of the first-order delay differential equation [73], we obtain a sufficient condition for $g(\lambda)$ to be stable: $|k - \beta| < \alpha - k$. This condition can be rewritten as (C-3) $\beta < \alpha$ and (C-4) $k < (\alpha + \beta)/2$. Since $\alpha > 0$ and (C-2) $\beta < -\alpha \leftrightarrow \alpha + \beta < 0$ are assumed to be satisfied in the preceding section, we notice that (C-3) and (C-4) $k < (\alpha + \beta)/2 < 0$ always hold. This fact implies that if the gain is chosen as (C-4), then $g(\lambda)$ in case (i) is stable.

For case (ii), T_1 and T_2 are assumed to keep relation (4.8). Substituting this

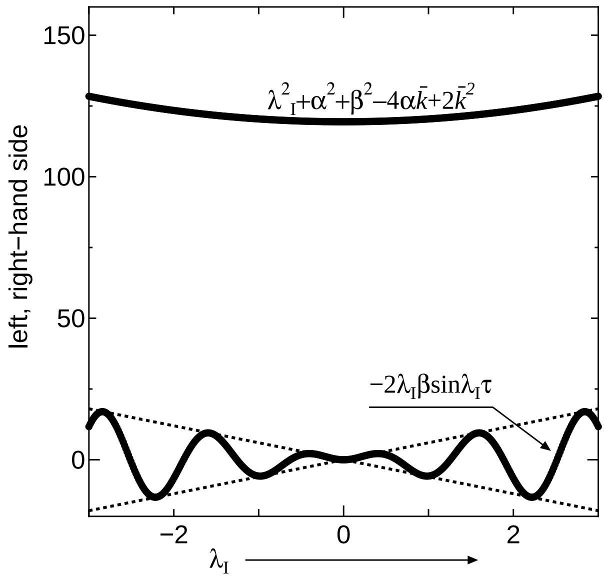

Figure 4.4: Sketch of the left and right-hand side of Eq. (4.13) ($\alpha = 1.0$, $\beta = -3.0$, $\tau = 5.0$, $k \approx -6.4641$).

relation and $\lambda = i\lambda_I$ into Eq. (4.4) yields

$$k(1+\cos\lambda_I\tau)\cos\lambda_I T_1 + k\sin\lambda_I\tau\sin\lambda_I T_1 = 2k - \alpha + \beta\cos\lambda_I\tau, \tag{4.9}$$

$$k(1+\cos\lambda_I\tau)\sin\lambda_I T_1 - k\sin\lambda_I\tau\cos\lambda_I T_1 = \lambda_I + \beta\sin\lambda_I\tau. \tag{4.10}$$

We know that the following two statements are equivalent: (a) the root of $g(\lambda) = 0$ with $T_2 = T_1 - \tau$, and $T_1 \geq \tau$ never crosses the imaginary axis; and (b) at least one equation of (4.10) does not hold. Now, we shall employ the second statement in order to design the controller. Both sides of Eqs. (4.10) are squared and added,

$$\lambda_I^2 + \alpha^2 + \beta^2 - 4\alpha k + 2k^2 = 2h(k)\cos\lambda_I\tau - 2\lambda_I\beta\sin\lambda_I\tau, \tag{4.11}$$

where $h(k) := k^2 - 2\beta k + \alpha\beta$. Here, the feedback gain is fixed at $k = \bar{k}$: $h(\bar{k}) = 0$. As $\alpha\beta < 0$ holds due to (C-2) $\beta < -\alpha$ and $\alpha > 0$, the equation $h(k) = 0$ has positive and negative roots. However, $k < 0$ must hold, due to the stability condition of case (i), and the feedback gain must be set to the negative root:

$$\bar{k} := \beta - \sqrt{\beta^2 - \alpha\beta} < 0. \tag{4.12}$$

The gain $\bar{k}$ simplifies Eq. (4.11) to

$$\lambda_I^2 + \alpha^2 + \beta^2 - 4\alpha\bar{k} + 2\bar{k}^2 = -2\lambda_I\beta\sin\lambda_I\tau. \tag{4.13}$$

If Eq. (4.13) does not hold, then at least one equation of (4.10) does not hold. Sketches of the left- and right-hand sides of Eq. (4.13) are shown in Figure 4.4: the parabolic bold curve is the left-hand side of the equation; and the sine wave represents the right-hand side; the dotted lines, $\pm 2|\beta|$, are the upper and lower limits of the sine wave. If the parabolic curve and the dotted lines do not cross, Eq. (4.13) does not hold. Thus, it is easy to derive the sufficient condition under which the curve and the lines do not cross,

$$\alpha^2 + 2\bar{k}(\bar{k} - 2\alpha) > 0. \tag{4.14}$$

From inequality (4.12) (i.e., $\bar{k} < 0$), condition (4.14) always holds. In addition, $\bar{k}$ denoted by Eq. (4.12) must satisfy (C-4):

$$\beta - \sqrt{\beta^2 - \alpha\beta} < (\alpha + \beta)/2 \iff \beta - \alpha - 2\sqrt{\beta(\beta - \alpha)} < 0.$$

We notice that the above inequality holds under $\alpha > 0$ and (C-2).

The above arguments are summarized as follows: *For $\beta < -\alpha < 0$, if controller (4.2) uses $k = \bar{k} := \beta - \sqrt{\beta^2 - \alpha\beta}$ and $T_2 = T_1 - \tau$, then the fixed point x^* of oscillator (4.1) is stabilized for any long $T_1 \in [\tau, \infty)$.*

The above summary allows us to design controller (4.2) by the following steps: (step 1) α, β, and τ are given; (step 2) if α and β satisfy $\beta < -\alpha < 0$, then go to the next step, otherwise we have to abandon to design it; (step 3) k is set to $\bar{k} := \beta - \sqrt{\beta^2 - \alpha\beta}$; (step 4) T_1 and T_2 are maintained to satisfy the relation $T_2 = T_1 - \tau$. Even for any long $T_1 \in [\tau, \infty)$, controller (4.2) designed by this procedure stabilizes the fixed point x^* of oscillator (4.1).

It must be emphasized that the previous methods never stabilize x^* under condition (C-1) due to their odd-number property and there is no guarantee that they reliably stabilize it under condition (C-2) [34] [103]. The MDFC method never stabilize it under condition (C-1); however, it is guaranteed that x^* is *stabilizable* by the designed controller for any oscillator delay $\tau > 0$ under condition (C-2).

The procedure requires the parameter values (i.e., α, β, and τ) to design k, T_1, and T_2; however, in practical situations, we may obtain the values with uncertainty such as the lower and upper limits of the values. Ishii *et al.* provided a procedure to design the single delayed feedback controller for one-dimensional discrete-time chaotic systems [105]. This procedure required only the lower and upper limits of the parameter values; the procedure is simple because the controlled systems do not include time delays and have discrete-time dynamics. On the other hand, it is not easy to provide a simple procedure for our problem, since the controlled system includes three time delays (i.e., τ, T_1, and T_2) and have continuous-time dynamics. The robust design which requires only the values with uncertainty for our problem still remains as an attractive future work.

4.5 Experimental verification

In this section, the theoretical results derived in previous sections are confirmed by electronic circuit experiments.

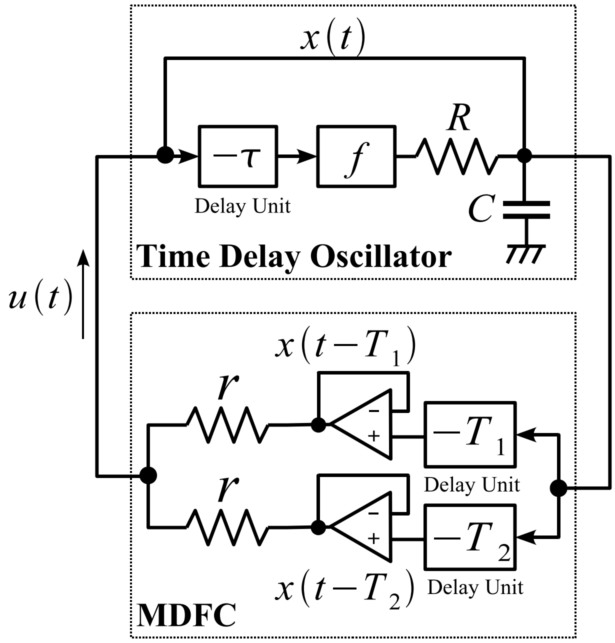

Figure 4.5: Schematic drawing of the time-delay nonlinear oscillator with MDFC.

4.5.1 Time-delay electronic oscillators

The circuit diagram of the time-delay nonlinear oscillator with MDFC is illustrated in Fig. 4.5. Here, $x(t)$ denotes the voltage of the oscillator. The boxes labeled $-\tau$, $-T_1$, and $-T_2$ are the time-delay units, and f is the nonlinear function unit. The time-delay units are almost the same as were used in previous studies [35, 95]. The circuit diagrams of the delay units and the nonlinear function unit are described in Appendix A. This oscillator is governed by the circuit equation,

$$C\frac{\mathrm{d}x(t)}{\mathrm{d}t} = \frac{1}{R}\left\{f\left(x(t-\tau)\right) - x(t)\right\} + u(t), \tag{4.15}$$

where R and C are a resistor and capacitor, respectively. The control signal $u(t)$ is the current from the MDFC circuit to the oscillator. The MDFC circuit exports the current $u(t)$,

$$u(t) = -\frac{1}{r}\left\{2x(t) - x(t-T_1) - x(t-T_2)\right\}. \tag{4.16}$$

In order to analyze the above circuits, we treat them as the dimensionless oscillator (4.1) with the following relations,

$$\begin{aligned}
&\tilde{t} := \frac{t}{RC},\ \tilde{\tau} := \frac{\tau}{RC},\ \tilde{T}_{1,2} := \frac{T_{1,2}}{RC},\ x := x(\tilde{t}),\\
&\dot{x} := \frac{\mathrm{d}x(\tilde{t})}{\mathrm{d}\tilde{t}},\ x_\tau := x(\tilde{t}-\tilde{\tau}),\ x_{T_{1,2}} := x(\tilde{t}-\tilde{T}_{1,2}),\\
&u := u(\tilde{t}),\ k := -R/r.
\end{aligned} \tag{4.17}$$

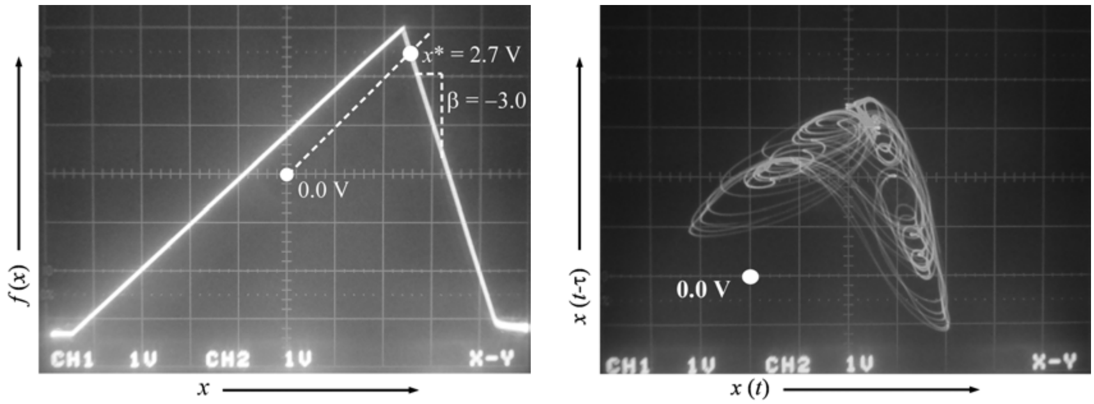

(a) (b)

Figure 4.6: Nonlinear function $f(x)$ and chaotic attractor: (a) x vs. $f(x)$ characteristic (horizontal axis: $x(t)$ (1V/div), vertical axis: $f(x(t))$ (1V/div)); (b) chaotic attractor for parameter set (4.18) (horizontal axis: $x(t-\tau)$ (1V/div), vertical axis: $x(t)$ (1V/div)).

These relations indicate that circuit equation (4.15) with MDFC is identical to oscillator (4.1) with controller (4.2) for $\alpha = 1$.

4.5.2 Experimental results

The input-output characteristic of the nonlinear function unit, which is similar to that of the well-known Mackey-Glass system [20, 34, 98], is shown in Fig. 4.6(a). From this figure, the fixed point x^* and the slope $\beta(x^*)$ are estimated as $x^* = 2.7$ V and $\beta(2.7) = -3.0$, respectively. Throughout this study, the circuit parameters for our experiments are as follows:

$$R = 1.0\ \mathrm{k}\Omega,\ C = 1.0\ \mu\mathrm{F},\ \tau = 5.0\ \mathrm{ms}, \tag{4.18}$$

where the oscillator exhibits chaotic behavior as shown in Fig. 4.6(b). The relations (4.17) indicate that the circuit parameters (4.18) are identical to the dimensionless parameters (4.7). Now let us design the controller according to the design procedure: (step 1) α, β, and τ are given; (step 2) $\alpha = 1$ and $\beta = -3$ satisfy $\beta < -\alpha < 0$, then go to the next step; (step 3) k is set to $\bar{k} := \beta - \sqrt{\beta^2 - \alpha\beta} \approx -6.4641$; (step 4) T_1 and T_2 are maintained to satisfy the relation $T_2 = T_1 - \tau$. The designed gain k is approximately implemented by setting $r = 154\ \Omega$. It is guaranteed that if T_1, T_2, and τ follow relation (4.8), then the controller delays T_1 and T_2 can be as long as required.

Figures 4.3 (a) and 4.3 (b) correspond to the stability curves for the parameter set (4.18) and the designed feedback resistor $r = 154\ \Omega$. The stability regions for the circuit experiments are shown in Fig. 4.7, where the symbol ◯ (×) denotes

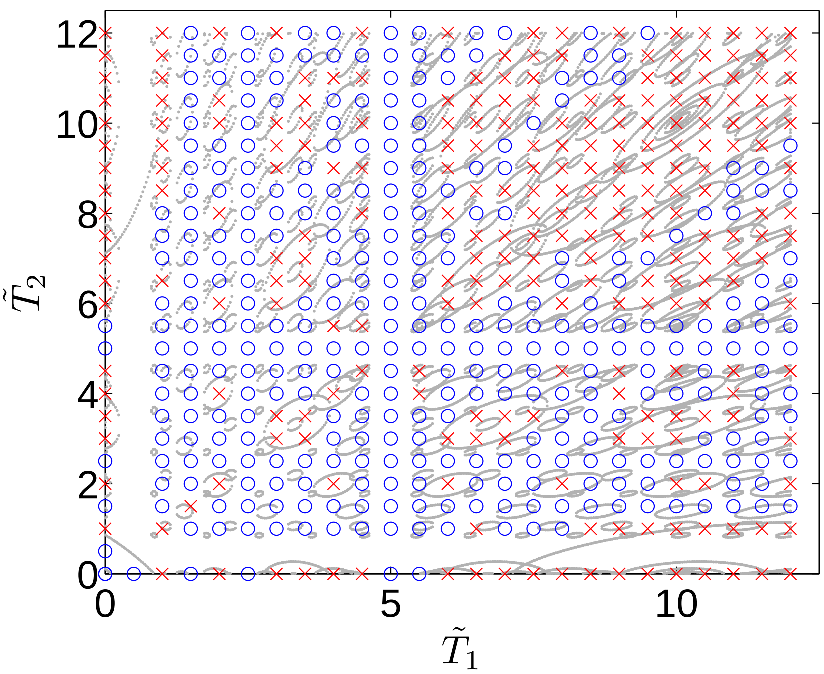

Figure 4.7: $\tilde{T}_1 - \tilde{T}_2$ parameter space for comparison of theoretical and experimental results: the symbol ◯ ($\times$) denotes the occurrence (non occurrence) of stabilization in the experiment; the gray lines are the theoretically estimated stability curves.

the occurrence (non occurrence) of stabilization in the experiment[2]. Stability was judged by the following steps: (i) oscillator (4.15) without control runs chaotically; (ii) control current (4.16) starts to flow into oscillator (4.15) at an arbitrary time; (iii) $x(t)$ converges on x^* within $x^* \pm 0.1$ V; (iv) steps (i)$\sim$(iii) are repeated several times; (v) if we observe the convergence of x^* (i.e., step (iii)) each time, then the symbol ◯ is filled in Fig. 4.7. Since the system dynamics, in principle, are not influenced by interchanging of T_1 and T_2, our experiment checked experimentally only the upper region of the diagonal line $T_2 = T_1$ in Fig. 4.7. The lower region is a copy of the upper one. From a comparison of theory with experimental results, it can be stated that the stability region estimated by the numerical procedure roughly agrees with that obtained by our circuit experiments.

The above steps guarantee that the stabilization occurs for several initial states embedded within the chaotic attractor. Therefore, we may say that our stability analysis for the vicinity of x^* is valid for most initial states on the chaotic attractor.

The time-series data of the electronic oscillator controlled by MDFC is shown in Fig. 4.8(a). The control signal corresponding to point A in Fig. 4.3 (b) ($T_1 = 5.0$ ms and $T_2 = 0.0$ ms) was applied to the oscillator. The oscillator without control

[2]Since it is difficult in an experiment to realize a very small delay (less than 1.0 ms), data for $T_1 = 0.5$ ms and $T_2 = 0.5$ ms could not be obtained.

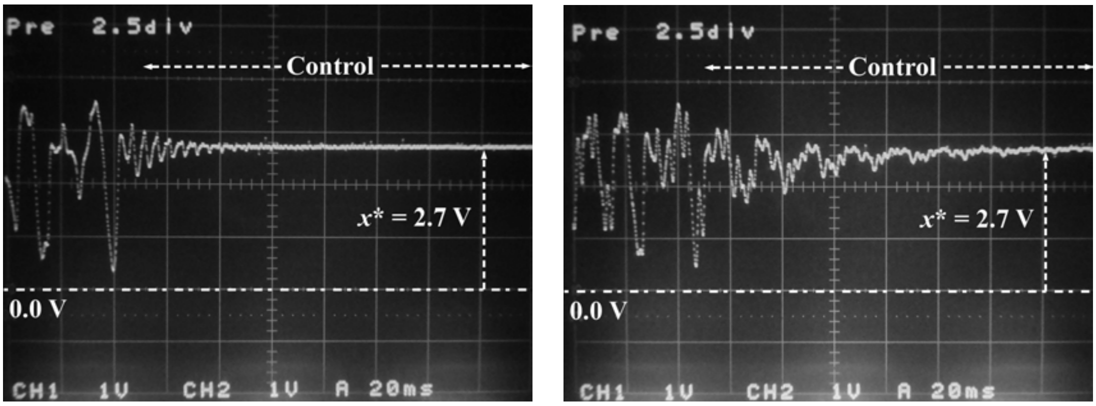

(a) (b)

Figure 4.8: Time series data of the circuit voltage $x(t)$ [V] just before and just after the control: (a) parameter set (A) ($T_1 = 5.0$ ms and $T_2 = 0.0$ ms); (b) parameter set (B) ($T_1 = 20.0$ ms and $T_2 = 15.0$ ms). Horizontal axis: t (20 ms/div); vertical axis: x (1 V/div).

behaved chaotically at first, and then $x(t)$ converged to x^*. Figure 4.8(b) shows the time-series data at point B in Fig. 4.3 (b) ($T_1 = 20.0$ ms and $T_2 = 15.0$ ms). This figure shows that stabilization occurs even with long delay times.

These experiments employ popular-priced circuit devices, which have an error of several percent. Thus, the designed controller inevitably has much more errors. However, as shown in Fig. 4.7, the controller works well on the circuit experiments. This fact experimentally verifies that the stabilization is robust to external noise and parameter uncertainty.

4.6 Discussion

4.6.1 Competition with other methods

Let us investigate the control performance of the MDFC method for stabilizing UFPs in time-delay oscillators. It is well known that a tracking filter and the original DFC [34] are the typical control methods for stabilizing time-delay oscillators. This subsection compares the MDFC method with these typical methods. The filter is described by

$$u = k(x - v),\ \frac{\mathrm{d}v}{\mathrm{d}t} = \omega_c(x - v),$$

where v is the additional variable, k is the feedback gain, and ω_c is the parameter. The original DFC is given by Eq. (4.2) with $T_1 = T_2$. Figure 4.9 (a) shows the largest real part of the roots $\mathrm{Re}[\lambda_{\max}]$ of the characteristic equation for the fixed point x^* controlled by the tracking filter. The parameter ω_c corresponds to the cutoff frequency. In order to stabilize x^*, the parameter should be within an interval

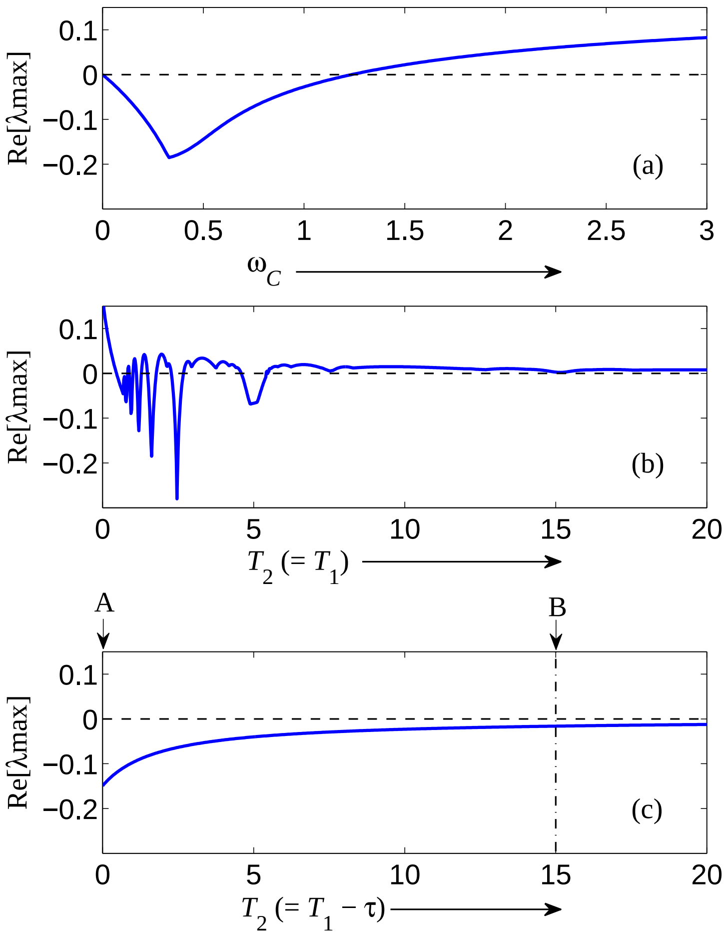

Figure 4.9: Largest real part of the roots $\mathrm{Re}[\lambda_{\max}]$ of the characteristic equation for the fixed point x^*: (a) the tracking filter; (b) the original DFC with $T_1 = T_2$; and (c) the MDFC with $T_2 = T_1 - \tau$. The parameters are the same as the numerical and experimental results in previous sections ($\alpha = 1.0$, $\beta = -3.0$, $\tau = 5.0$, $k \approx -6.4641$).

$\omega_c \in (0, 1.235)$. The largest real part for the original DFC with $T_1 = T_2$ is shown in Fig. 4.9 (b). The controller delay time $T_1 = T_2$ should be chosen from several narrow intervals for the stabilization. Figure 4.9 (c) illustrates the largest real part for the MDFC on the dotted line A-B in Fig. 4.3(b). It can be seen that the largest real part never exceeds zero for any $T_2 > 0$. Thus, if the two controller delays retain the proportional relation, $T_2 = T_1 - \tau$, then the controller delays can be arbitrarily chosen.

The convergence speed of the controlled orbit in the vicinity of x^* depends on $\mathrm{Re}[\lambda_{\max}]$. From a practical point of view, it is desirable to reduce $\mathrm{Re}[\lambda_{\max}]$ to improve the convergent performance. It is useful to design the optimal control parameters which get the best convergent performance; this optimal control problem is considered as an important future work.

4.6.2 Previous studies related to our results

Although, to the authors' knowledge, there have been few efforts to investigate the stabilization of UFPs in time-delay nonlinear oscillators using the MDFC method, there are a few previous methods for time-delay oscillators that are related to our results. With the exception of the three studies [34, 102, 103] mentioned in Section 4.1, they are reviewed below.

Blyuss *et al.* analyzed the stability of UFPs in time-delayed pendulum-mass-spring-damper systems controlled by the DFC method [106]. Xu *et al.* provided a delay-dependent condition, which is described by a linear matrix inequality, for the stabilization of UFPs in time-delay nonlinear oscillators controlled by the DFC method [107]. Rezaie *et al.* applied a dynamic DFC method to the problem of Hopf bifurcation control for time-delay nonlinear oscillators [108]. Vasegh and Sedigh analyzed the stability of UPOs in time-delay oscillators controlled by the DFC method [109,110]. Our previous study showed that UFPs in simple two-dimensional oscillators without time delay can be stabilized using diffusive connections with two long time delays [19]. If the two delay times retain a proportional relation with a certain bias, the stabilization occurs independent of the delay times or the network topology. Our present study considers the specific case of a single oscillator; however, a time-delay oscillator is used instead of a two-dimensional one.

4.6.3 Odd–number property

It is well known that the DFC method has a crucial disadvantage, in that it never stabilizes UPOs or UFPs which have the odd-number property [111–113]. This property for UPOs has been refuted recently [114–116], whereas that for UFPs is valid [85,86]. To overcome this property for UFPs, an observer-based controller [117] and a dynamic controller [118], both of which can be designed by a systematic procedure, have been proposed. Furthermore, an adaptive controller based on a conventional low-pass filter, which is the same as the tracking filter, also has the odd number property; however, an unstable filter was proposed to overcome this property [119, 120]. The multiple DFC method [80, 93] and the time-varying-delay method [121] also have this property [80, 93]. As in Sec. 4.3, the MDFC for time-delay oscillators also has this property. Although this disadvantage could be overcome using the above techniques, we do not discuss it in detail because it is a digression from our main topic.

4.7 Extension to amplitude death

The present section extends the MDFC method for a single time-delayed chaotic oscillator to amplitude death in a pair of time-delayed chaotic oscillators coupled by a multiple delay connection (see Fig. 4.10). A simple systematic procedure for designing the connection parameters, the coupling strength, and the connection delays, is provided. The stability analysis and the design procedure are verified by

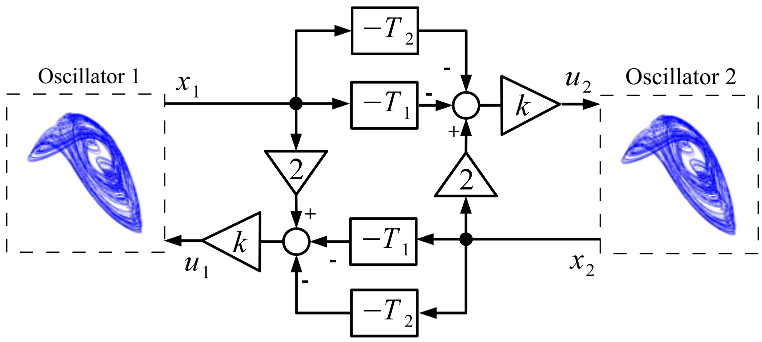

Figure 4.10: Block diagram of pair oscillators coupled by a multiple delay connection.

a numerical simulation.

4.7.1 Problem statement

Let us consider a pair of identical time-delayed chaotic oscillators (see Fig. 4.10) [35]:

$$\begin{cases} \dot{x}_1 = -\alpha x_1 + f(x_{1\tau}) + u_1 \\ \dot{x}_2 = -\alpha x_2 + f(x_{2\tau}) + u_2 \end{cases}, \tag{4.19}$$

where $x_{1,2} \in \mathbb{R}$ and $u_{1,2} \in \mathbb{R}$ are the system states and coupling signals, respectively, $x_{1,2\tau} := x_{1,2}(t-\tau)$ are the delayed states, $\tau \geq 0$ is the oscillator delay, $\alpha > 0$ is a parameter, and $f : \mathbb{R} \to \mathbb{R}$ denotes the nonlinear function. The symbol $\mathbb{R}$ denotes the set of real numbers. These oscillators are coupled by the multiple delay connection described as

$$\begin{aligned} u_1 &= k(2x_1 - x_{2T_1} - x_{2T_2}), \\ u_2 &= k(2x_2 - x_{1T_1} - x_{1T_2}), \end{aligned} \tag{4.20}$$

where $k \in \mathbb{R}$ represents the coupling strength, $x_{1,2T_{1,2}} := x_{1,2}(t-T_{1,2})$ are the delayed states, and $T_{1,2} \geq 0$ are the connection delays.

Each individual oscillator without coupling (i.e., $k = 0$) has a fixed point $x^* : 0 = f(x^*) - \alpha x^*$. Throughout this study, the fixed point is supposed to be unstable. It is noted that connection (4.20) changes the stability of x^*, but not its location. Oscillators (4.19) coupled by connection (4.20) have the steady state $[x^* \; x^*]^T$.

4.7.2 Stability analysis

The coupled oscillators linearized in the steady state are governed by

$$\begin{cases} \dot{z}_1 = -\alpha z_1 + \beta z_{1\tau} + k(2z_1 - z_{2T_1} - z_{2T_2}) \\ \dot{z}_2 = -\alpha z_2 + \beta z_{2\tau} + k(2z_2 - z_{1T_1} - z_{1T_2}) \end{cases}, \tag{4.21}$$

where $z_{1,2} := x_{1,2} - x^*$, $z_{1,2\tau} := x_{1,2\tau} - x^*$ and $z_{1,2T_{1,2}} := x_{1,2T_{1,2}} - x^*$ denote the variations of oscillators 1 and 2 around x^*. Here, $\beta := \{\mathrm{d}f(x)/\mathrm{d}x\}_{x=x^*}$ represents the slope of $f(x)$ at x^*. The stability of the linearized system (4.21) is governed by the characteristic equation,

$$g(\lambda) := g_1(\lambda)g_2(\lambda) = 0. \tag{4.22}$$

$g_1(\lambda)$ and $g_2(\lambda)$ are defined by

$$g_j(\lambda) := \gamma - k\{2 + (-1)^j\varepsilon\} = 0,\ j = 1,\ 2, \tag{4.23}$$

where

$$\gamma := \lambda + \alpha - \beta e^{-\lambda\tau},\ \varepsilon := e^{-\lambda T_1} + e^{-\lambda T_2}.$$

The necessary condition for x^* to be unstable without coupling is as follows: ① $\beta > \alpha > 0$ or ② $\beta < -\alpha < 0$ [73]. When the oscillators are coupled (i.e. $k \neq 0, T_{1,2} > 0$), it is easy to see that $\lim_{\lambda\to+\infty} g_{1,2}(\lambda) = +\infty$ and $g_1(0) = \alpha - \beta$ independently of $k, T_{1,2}, \tau$. Condition ① guarantees $g_1(0) < 0$, and so $g_1(\lambda) = 0$ has at least one positive real root. This fact implies that amplitude death never occurs under condition ①; hence, we focus attention only on condition ② below.

The steady state is stable if and only if all the roots λ of Eq. (4.22) lie in the open left-half complex plane. We shall investigate the roots of $g_1(\lambda) = 0$ and $g_2(\lambda) = 0$. The stability changes only when at least one root of these equations crosses the imaginary axis. To simplify the stability analysis, let us check the roots on the axis and estimate the stability region in (T_1, T_2) space. Substituting $\lambda = i\lambda_I$ into Eq. (4.23), we obtain its real and imaginary parts

$$\begin{aligned}\mathrm{Re}[g_j(i\lambda_I)] &= \alpha - \beta\cos(\lambda_I\tau) - k\{2 + (-1)^j C\} = 0,\\ \mathrm{Im}[g_j(i\lambda_I)] &= \lambda_I + \beta\sin(\lambda_I\tau) + (-1)^j kS = 0,\end{aligned} \tag{4.24}$$

where

$$\begin{aligned}C &:= \cos(\lambda_I T_1) + \cos(\lambda_I T_2),\\ S &:= \sin(\lambda_I T_1) + \sin(\lambda_I T_2).\end{aligned}$$

The boundary curves of the stability region are derived by using the roots $T_{1,2}$ of Eqs. (4.24). The sign of $\mathrm{Re}\,[\mathrm{d}\lambda/\mathrm{d}T_2]$ at $\lambda = i\lambda_I$, where

$$\frac{\mathrm{d}\lambda}{\mathrm{d}T_2} = \frac{-(-1)^j\lambda k e^{-\lambda T_2}}{1 + \tau\beta e^{-\lambda\tau} + (-1)^j k\left(T_1 e^{-\lambda T_1} + T_2 e^{-\lambda T_2}\right)},$$

can give us an insight into the cross-axis direction of the roots of Eq. (4.23). If the sign is positive (negative), then the roots cross the axis from left to right (right to left).

The above stability analysis is now illustrated with the following numerical example. The parameters of the oscillators are set to

$$\alpha = 1.0,\ \tau = 10.0,\ \beta = -1.8. \tag{4.25}$$

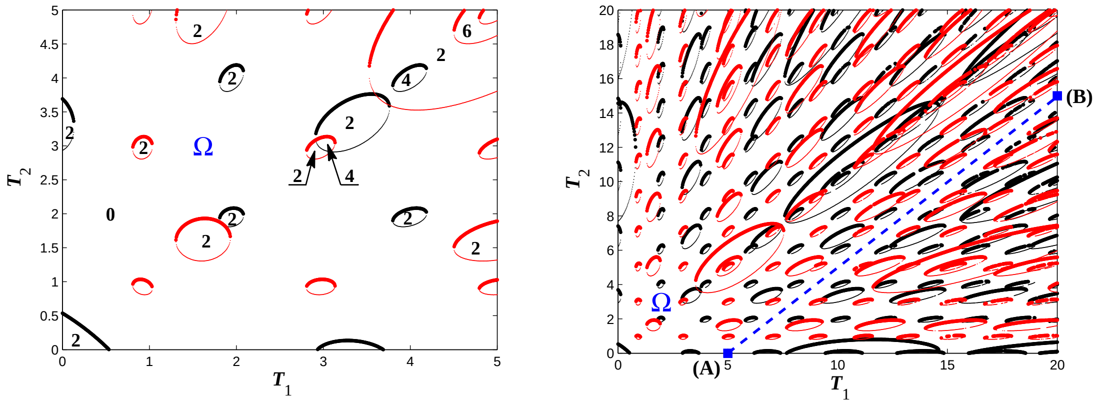

(a) (b)

Figure 4.11: Region of amplitude death Ω and boundary curves of the stability region ($\alpha = 1.0, \beta = -1.8, \tau = 5.0, k \approx -4.045$): (a) $T_{1,2} \in [0, 5]$, (b) $T_{1,2} \in [0, 20]$. Black and red (gray) curves correspond to $g_1(i\lambda_I) = 0$ and $g_2(i\lambda_I) = 0$, respectively.

Let the coupling strength be fixed at $k \approx -4.045$; the reason for choosing this value will be explained in the next section. Figure 4.11 shows the boundary curves consisting of the bold (thin) lines which depict the negative (positive) sign. Additionally, the black and red (gray) lines denote the curves for $g_1(i\lambda_I) = 0$ and $g_2(i\lambda_I) = 0$, respectively. The curves separate (T_1, T_2) space into several regions. At $T_1 = T_2 = 0$, Eq. (4.22) is reduced to

$$g(\lambda) = (\lambda + \alpha - \beta e^{-\lambda\tau})(\lambda + \alpha - \beta e^{-\lambda\tau} - 4k). \tag{4.26}$$

According to the stability analysis on scalar delayed systems [73], the number of unstable roots is 2; thus, the boundary curves including the point ($T_1 = T_2 = 0$) enclose an unstable region. This number turns out to be zero when T_2 increases and crosses the bold line in an upward direction. In other words, at a certain value of T_1, when T_2 crosses the bold (thin) line upwards (downwards), 2 is subtracted (added) from (to) the number of unstable roots. By this procedure, the numbers of unstable roots in the other regions are easily obtained as shown in Fig. 4.11(a). The region of amplitude death, where there are no unstable roots, is denoted by Ω. From Fig. 4.11(b), it should be pointed out that the single delay connection (i.e., $T_1 = T_2 = T$) [35] can induce death only for a small range $T \lesssim 7.5$; however, the multiple delay connection, with an appropriate combination of T_1 and T_2, can induce death in a wide parameter region Ω (e.g., dotted line A-B).

Note that $g_1(\lambda)$ is identical to the characteristic equation governing the dynamics around x^* in an isolated oscillator with the MDFC method. Thus, the black curves correspond to the isolated oscillator with the MDFC method. Further, note that the steady-state stabilization in the oscillators (4.19) coupled by connection (4.20) can be regarded as an extension of the fixed-point stabilization with the MDFC of our previous work.

4.7.3 Design of connection

This subsection provides a simple systematic procedure for designing a multiple delay connection (4.20), so that both connection delays, T_1 and T_2, can be as long as possible and still induce amplitude death. From the boundary curves shown in Fig. 4.11(b), we investigate the stability on the relation of (T_1, T_2, τ),

$$T_2 = T_1 - \tau, (T_1 \geq \tau). \tag{4.27}$$

For the case $(T_1 = \tau, T_2 = 0)$ corresponding to the point A in Fig. 4.11(b), substituting $T_1 = \tau$ and $T_2 = 0$ into Eq. (4.23) leads to

$$g_j(\lambda) = \lambda + \alpha - \{2 + (-1)^j\}k + \{(-1)^{j+1}k - \beta\}e^{-\lambda\tau} = 0.$$

From the stability analysis on scalar delayed systems [73], we derive the sufficient condition for $g(\lambda)$ to be stable: $|(-1)^{j+1}k - \beta| < \alpha - \{2+(-1)^j\}k$, for any $j = 1, 2$. This condition can be expressed by ③ $\beta < \alpha$, ④ $k < (\alpha-\beta)/4$, and ⑤ $k < (\alpha+\beta)/2$. Since the previous section assumes that condition ② is satisfied, condition ③ always holds. Moreover, if we choose the coupling strength as $k < (\alpha+\beta)/2 < 0$, conditions ④ and ⑤ always hold. Hence, according to these arguments, condition ③ has to be satisfied for the stability of $g(\lambda)$.

For the case of condition (4.27) corresponding to the dotted line in Fig. 4.11(b), substituting Eq. (4.27) into Eqs. (4.24), then squaring and adding both sides, leads to

$$\begin{aligned} &\lambda_I^2 + \alpha^2 + \beta^2 - 4\alpha k + 2k^2 \\ &= 2(k^2 - 2\beta k + \alpha\beta)\cos\lambda_I\tau - 2\lambda_I\beta\sin\lambda_I\tau. \end{aligned} \tag{4.28}$$

Conditions ② and ⑤ obtained above, require that k be set to

$$k = \tilde{k} := \beta - \sqrt{\beta^2 - \alpha\beta} < (\alpha + \beta)/2 < 0. \tag{4.29}$$

Equation (4.28) with $k = \tilde{k}$ is simplified as

$$\lambda_I^2 + \alpha^2 + \beta^2 - 4\alpha\tilde{k} + 2\tilde{k}^2 = -2\lambda_I\beta\sin\lambda_I\tau. \tag{4.30}$$

Since inequality (4.29) means that Eq. (4.30) does not hold, at least one of the equations (4.24) does not hold. Since $\lambda = i\lambda_I$ is not a root of characteristic equation (4.23), no root of $g(\lambda)$ crosses the imaginary axis. Hence, $g(\lambda)$ remains stable. Therefore, the unstable steady state is stabilized for $T_1 \geq \tau$ if $k = \tilde{k}$ and Eq. (4.27) are maintained.

It must be emphasized that relation (4.27) and coupling strength (4.29) are identical to those of Section 4.4; hence, the k, T_1, and T_2 for the isolated oscillator, that are designed with the MDFC method are valid for the coupled oscillators.

The above arguments can be reduced to a systematic design procedure, as follows: For $\beta < -\alpha < 0$, if connection (4.20) employs $k = \tilde{k}$ and $T_2 = T_1 - \tau$, then amplitude

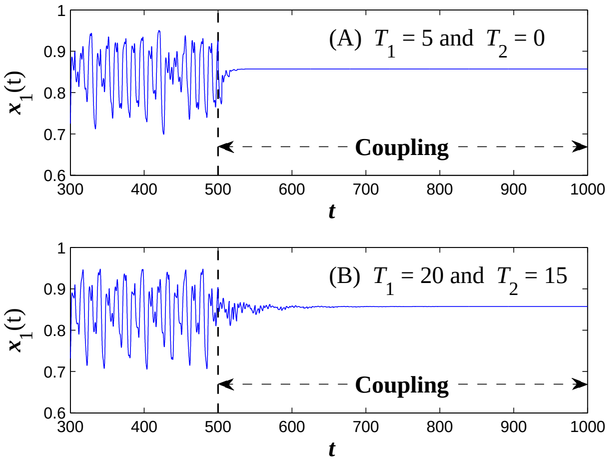

Figure 4.12: Time series data $x_1(t)$ of coupled oscillators ($\alpha = 1$, $\tau = 5$, $\beta = -1.8$, $k \approx -4.045$).

death is induced in the oscillators (4.19) coupled by connection (4.20), for any long $T_1 \in [\tau, +\infty)$. We shall verify the design procedure with numerical simulations. The following nonlinear function $f(x)$ will be used as a typical example [31]:

$$f(x) = \begin{cases} 0 & \text{if } x \leq -4/3 \\ -1.8x - 2.4 & \text{if } -4/3 < x \leq -0.8 \\ 1.2x & \text{if } -0.8 < x \leq 0.8 \\ -1.8x + 2.4 & \text{if } 0.8 < x \leq 4/3 \\ 0 & \text{if } x > 4/3 \end{cases}.$$

It has been reported that hyperchaos exists in Eq. (4.19) without coupling at $\alpha = 1$ and $\tau = 5$ [31]. The function $f(x)$ has three fixed points: $x^* = \pm 6/7$ and 0. When the slope of $f(x)$ at x^* is 0, and $\beta(0) = 1.2$, amplitude death never occurs for any k, T_1, T_2, due to condition ①. In contrast, amplitude death may occur at $x^* = \pm 6/7$, because the slope $\beta(\pm 6/7) = -1.8$ satisfies condition ②. The design procedure provides the coupling strength $\tilde{k} \approx -4.045$ from Eq. (4.29). T_1 and T_2 can be set to any length when Eq. (4.27) holds. Now we choose two parameter sets as typical examples: (A) $T_1 = 5$, $T_2 = 0$ and (B) $T_1 = 20$, $T_2 = 15$. The time-series data $x_1(t)$ of the coupled oscillators is shown in Fig. 4.12. The individual oscillator without coupling behaves chaotically until $t = 500$. At $t = 500$, multiple delay coupling is achieved. The oscillator ceases to oscillate after a transition, and it then converges to the steady state; amplitude death is induced at $x^* = +6/7$. Note that the numerical results for the two parameter sets, (A) and (B), are completely consistent with the two points (A) and (B) on the dotted line in Fig. 4.11(b).

4.8 Conclusion

This chapter demonstrated that the MDFC method can stabilize UFPs in time-delay nonlinear oscillators. A simple procedure was provided for designing the feedback gain and the controller delays. The main advantage of this procedure is that if T_1, T_2, and τ maintain the necessary relation, then the fixed point can be stabilized with long controller delays T_1 and T_2. The stability analysis and the design procedure were experimentally verified by electronic circuits. Furthermore, these results were extended to amplitude death in a pair of time-delayed chaotic oscillators coupled by a multiple delay connection.

Chapter 5

Stabilization of nonlinear oscillators coupled by a digital delay connection

5.1 Introduction

The dynamics of coupled oscillators have been actively investigated in nonlinear areas of science [50, 122, 123]. Recently, coupled oscillators have been used for engineering applications such as central pattern generators for robotic-legged locomotion [52], modular robots [53], sensor networks [54], and a car-following model [124]. Diffusive-coupling-induced stabilization of unstable steady states, one of the well-known phenomena in coupled oscillators, has been studied for almost a quarter of a century [16, 17]. This phenomenon, called amplitude death, has great industrial potential, but never occurs in coupled *identical* oscillators [17, 56]. Reddy *et al.* showed that a transmission delay in connections can induce this phenomenon even in coupled identical oscillators [18]. This time-delay-induced death has been widely investigated both experimentally [35, 66, 67] and analytically [56–64, 69, 125–128]. Furthermore, it was reported that amplitude death can be induced not only by using a simple time-delay connection [18] but also by leveraging various connections such as distributed-delay connections [125], dynamic connections [93, 129, 130], unsymmetrical time-delay connections [46,65], connections via conjugate variables [48,131], time-varying delay connections [43], two long-delay connections [19], and gradient time-delay connections [132]. These connections represent the *continuous-time* mutual influences of real oscillators for various situations.

In the field of control engineering, a networked control system whose subsystems (i.e., sensors, actuators, and controllers) communicate through a digital communication network (e.g., Ethernet), as shown in Fig. 5.1(a), has been extensively investigated. This is because this system has the following advantages: reduced system wiring, ease of system diagnosis and maintenance, and increased system agility [133]. The subsystems communicate with each other on the network by digital signals that are converted from continuous-time input–output signals of the

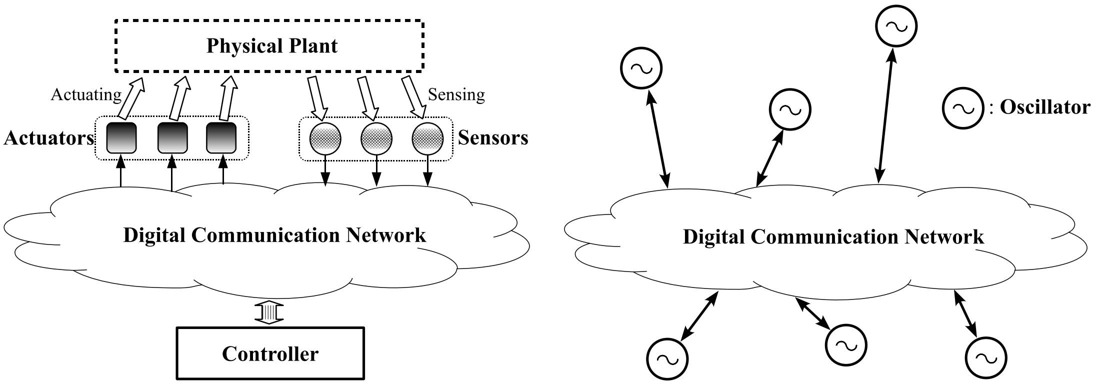

(a) (b)

Figure 5.1: Conceptual diagrams of networked systems: (a) networked control system; (b) networked oscillator system.

subsystems. Note that a communication delay, which may degrade the system performance, is inevitably caused by the transmission of the signal on the network. From the viewpoint of the engineering applications of coupled oscillators, it is important to investigate the dynamics of oscillators that are coupled through the digital communication network. We call such a configuration, as is illustrated in Fig. 5.1(b) a networked oscillator system. To the best of our knowledge, few studies have been conducted on networked oscillator systems in the field of nonlinear dynamics.

This chapter proposes a prototype model of a networked oscillator system that consists of oscillators coupled by a digital delayed connection. Figure 5.2 shows a sketch of the prototype model with two oscillators, where the digital delayed connection is implemented by first-in-first-out (FIFO) queues. The main purpose of this study is to investigate amplitude death induced by the digital delayed connection. The semi–discretization technique [134–137] allows us to derive a simple characteristic equation for steady-state stability. This equation can be expressed by real polynomials whose coefficients depend on the network topology. Stability analysis reveals that the digital delayed connection better facilitates the stabilization of the steady state than does the continuous-time delayed connection.

5.2 Problem statement

A network consisting of two-dimensional oscillators,

$$\dot{Z}_n(t) = \left\{\mu + i\omega - |Z_n(t)|^2\right\} Z_n(t) + \varepsilon u_n(t) \quad (n = 1, 2, \ldots, N), \tag{5.1}$$

is considered, where the complex number $Z_n(t) \in \boldsymbol{C}$ is the state variable of oscillator n. $N \geq 2$ denotes the total number of oscillators. The parameters $\mu > 0$ and $\omega > 0$ represent the degree of instability of the fixed point and the oscillator frequency, respectively. $\varepsilon \in \boldsymbol{R}$ is the coupling strength and $i = \sqrt{-1}$. For a normal delayed

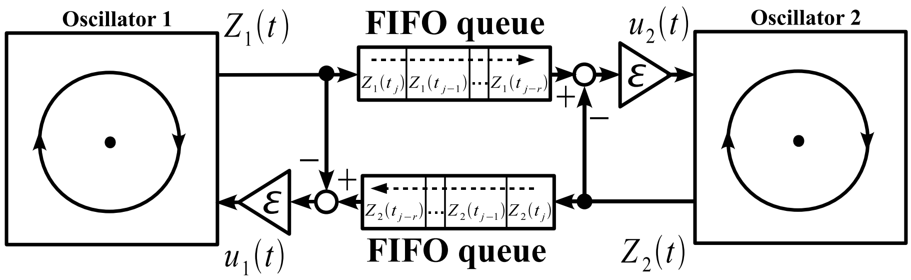

Figure 5.2: Block diagram of two oscillators coupled by a digital delayed connection (i.e., FIFO queues).

connection, the coupling signal $u_n(t) \in \boldsymbol{C}$ is given by

$$u_n(t) = \frac{1}{d_n}\left[\sum_{k=1}^{N} c_{nk} Z_k(t-\tau)\right] - Z_n(t), \tag{5.2}$$

where $\tau \geq 0$ is the delay time of the coupling signals. The network topology is governed by c_{nk} as follows: if oscillator n is connected to oscillator k, then $c_{nk} = c_{kn} = 1$, otherwise $c_{nk} = c_{kn} = 0$. The self-delayed signal $Z_n(t-\tau)$ is not allowed to be injected, that is, $c_{nn} = 0$. The number of oscillators that are connected to oscillator n (the degree of oscillator n) is written as $d_n := \sum_{k=1}^{N} c_{nk}$. Suppose that there is no isolated oscillator, that is, $d_n > 0$, $\forall n \in \{1, \ldots, N\}$.

Instead of a normal delayed connection (5.2), the present study employs the digital delayed connection

$$u_n(t) = \frac{1}{d_n}\left[\sum_{k=1}^{N} c_{nk} Z_k(t_{j-r})\right] - Z_n(t) \tag{5.3}$$

for $t \in [t_j, t_{j+1})$ $(j = 0, 1, \ldots)$. Figure 5.2 illustrates the two oscillators coupled by the digital delayed connection (5.3). As shown in Figs. 5.2 and 5.3, $Z_k(t)$ is periodically stored into the buffers on the FIFO queue with sampling period $h := t_{j+1} - t_j$, where j represents the sampling number. t_j denotes the time at the j-th sampling. $Z_k(t_{j-r}) := Z_k(t_j - rh)$ is the past state variable, which is maintained at a constant value during $t \in [t_j, t_{j+1})$. The integer $(r+1)$ is the number of buffers; thus, the time delay is given by $\tau = rh$.

It may be worth pointing out the following remarks about these connections. In the case of a single oscillator (i.e., $N = 1$, $c_{11} = 1$, and $d_1 = 1$), the oscillator (5.1) with normal delayed feedback (5.2) and the one with digital delayed feedback (5.3) are identical to the original delayed feedback control system [9] and the queue-based delayed feedback control system [12], respectively. The connection (5.3), with both a large number of buffers and a short sampling period (i.e., $1 \ll r$ and $h \ll 1$), is approximately identical to a normal delayed connection (5.2). In the field of nonlinear science, a delayed signal is often realized by a bucket-brigade delay (BBD)-line device in experimental situations [35, 66, 92, 138–140]. Such a device comprises

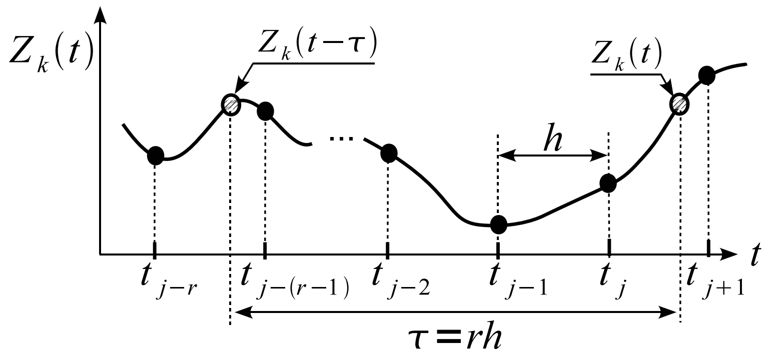

Figure 5.3: Sketch of the state variable $Z_k(t)$ for oscillator k.

a series of sample-and-hold circuits. The BBD-line device is also described by the FIFO queue; thus, the coupled oscillators in Fig. 5.2 are identical to oscillators coupled by a BBD line [66].

5.3 Stability analysis

Oscillators (5.1) with connection (5.3) have the homogeneous steady state $\boldsymbol{Z}^* := \begin{bmatrix} 0 & 0 & \cdots & 0 \end{bmatrix}^T \in \boldsymbol{C}^N$. The coupled oscillators are linearized around $\boldsymbol{Z}^*$:

$$\dot{z}_n(t) = (\mu + i\omega)\, z_n(t) + \varepsilon \left[\left\{ \frac{1}{d_n} \sum_{k=1}^{N} c_{nk} z_k(t_{j-r}) \right\} - z_n(t) \right] \tag{5.4}$$

for $t \in [t_j, t_{j+1})$ $(j = 0, 1, \ldots)$, where $z_n(t) \in \boldsymbol{C}$ is the variation in oscillator n around the fixed point $Z_n^* = 0$. System (5.4) can be written as

$$\dot{\boldsymbol{x}}(t) = \boldsymbol{A}\boldsymbol{x}(t) + \boldsymbol{B}\boldsymbol{x}(t_{j-r}), \;\; t \in [t_j, t_{j+1}) \;\; (j = 0, 1, \ldots), \tag{5.5}$$

where

$$\boldsymbol{x}(t) := \begin{bmatrix} \mathrm{Re}\{z_1(t)\} & \mathrm{Im}\{z_1(t)\} & \cdots & \mathrm{Re}\{z_N(t)\} & \mathrm{Im}\{z_N(t)\} \end{bmatrix}^T, \tag{5.6}$$

$$\boldsymbol{A} := \boldsymbol{I}_N \otimes \begin{bmatrix} \mu - \varepsilon & -\omega \\ \omega & \mu - \varepsilon \end{bmatrix}, \;\; \boldsymbol{B} := \varepsilon \boldsymbol{D} \otimes \boldsymbol{I}_2. \tag{5.7}$$

The elements of matrix $\boldsymbol{D} \in \boldsymbol{R}^{N \times N}$ are $\{\boldsymbol{D}\}_{nk} := c_{nk}/d_n$ for $n \neq k$ and $\{\boldsymbol{D}\}_{nn} := 0$. Here an N-dimensional identity matrix is represented by $\boldsymbol{I}_N$.

The semi-discretization technique [134–137] allows us to derive the mapping from the past state $\boldsymbol{x}(t_{j-r})$ and the current state $\boldsymbol{x}(t_j)$ to the future state $\boldsymbol{x}(t_{j+1})$,

$$\boldsymbol{x}(t_{j+1}) = \boldsymbol{L}_a \boldsymbol{x}(t_j) + \boldsymbol{L}_b \boldsymbol{x}(t_{j-r}),$$

where

$$\boldsymbol{L}_a := \exp\{\boldsymbol{A}h\},\ \boldsymbol{L}_b := \exp\{\boldsymbol{A}h\}\int_0^h \exp\{-\boldsymbol{A}s\}\mathrm{d}s\boldsymbol{B}. \tag{5.8}$$

This mapping implies that the dynamics of the linear system (5.5) can be reduced to that of a $2(r+1)N$-dimensional discrete-time system,

$$\boldsymbol{X}_{j+1} = \boldsymbol{\Phi}\boldsymbol{X}_j, \tag{5.9}$$

where

$$\boldsymbol{X}_j := \begin{bmatrix} \boldsymbol{x}(t_j) \\ \boldsymbol{x}(t_{j-1}) \\ \boldsymbol{x}(t_{j-2}) \\ \vdots \\ \boldsymbol{x}(t_{j-r}) \end{bmatrix},\ \boldsymbol{\Phi} := \begin{bmatrix} \boldsymbol{L}_a & \boldsymbol{0} & \cdots & \boldsymbol{0} & \boldsymbol{L}_b \\ \boldsymbol{I}_{2N} & \boldsymbol{0} & \cdots & \boldsymbol{0} & \boldsymbol{0} \\ \boldsymbol{0} & \boldsymbol{I}_{2N} & \cdots & \boldsymbol{0} & \boldsymbol{0} \\ \vdots & & \ddots & & \vdots \\ \boldsymbol{0} & \boldsymbol{0} & \cdots & \boldsymbol{I}_{2N} & \boldsymbol{0} \end{bmatrix}.$$

Note that $\boldsymbol{Z}^*$ is stable if and only if the transition matrix $\boldsymbol{\Phi}$ is a stable matrix (i.e., a Schur matrix).

The characteristic polynomial of the linear system (5.9) is described by

$$\begin{aligned} & g(\lambda) \\ & = \det\left(\lambda\boldsymbol{I}_{2(r+1)N} - \boldsymbol{\Phi}\right) \\ & = \det\left(\boldsymbol{H}\right) \\ & \cdot \det\left\{\lambda\boldsymbol{I}_{2N} - \boldsymbol{L}_a - \begin{bmatrix} \boldsymbol{0} & \boldsymbol{0} & \cdots & -\boldsymbol{L}_b \end{bmatrix} \boldsymbol{H}^{-1} \begin{bmatrix} -\boldsymbol{I}_{2N} \\ \boldsymbol{0} \\ \vdots \\ \boldsymbol{0} \end{bmatrix}\right\}, \end{aligned}$$

where $\boldsymbol{H} \in \boldsymbol{R}^{2rN\times 2rN}$ is given by

$$\boldsymbol{H} := \begin{bmatrix} \lambda\boldsymbol{I}_{2N} & \boldsymbol{0} & \cdots & \boldsymbol{0} & \boldsymbol{0} \\ -\boldsymbol{I}_{2N} & \lambda\boldsymbol{I}_{2N} & & \boldsymbol{0} & \boldsymbol{0} \\ \boldsymbol{0} & -\boldsymbol{I}_{2N} & & \boldsymbol{0} & \boldsymbol{0} \\ \vdots & & \ddots & \ddots & \vdots \\ \boldsymbol{0} & \boldsymbol{0} & \cdots & -\boldsymbol{I}_{2N} & \lambda\boldsymbol{I}_{2N} \end{bmatrix}.$$

Now $\boldsymbol{P} \in \boldsymbol{R}^{2N\times 2N}$ is denoted by

$$\boldsymbol{H}^{-1} = \begin{bmatrix} * & * \\ \boldsymbol{P} & * \end{bmatrix}. \tag{5.10}$$

As $\det(\boldsymbol{H}) = \lambda^{2rN}$ and $\boldsymbol{P} = \lambda^{-r}\boldsymbol{I}_{2N}$, polynomial $g(\lambda)$ can be further simplified to

$$g(\lambda) = \det\left\{\lambda^{r+1}\boldsymbol{I}_{2N} - \lambda^r\boldsymbol{L}_a - \boldsymbol{L}_b\right\}. \tag{5.11}$$

Let us calculate Eq. (5.11), as follow. Substituting $\boldsymbol{A}$ and $\boldsymbol{B}$ in Eq. (5.7) into $\boldsymbol{L}_a$ and $\boldsymbol{L}_b$ denoted in Eq. (5.8), we obtain

$$\boldsymbol{L}_a = \gamma\boldsymbol{I}_N \otimes \boldsymbol{\Theta}(h),\ \boldsymbol{L}_b = \eta\left(\boldsymbol{I}_N - \boldsymbol{M}\right) \otimes \boldsymbol{Q}\left(\gamma\boldsymbol{\Theta}(h) - \boldsymbol{I}_2\right),$$

where

$$\gamma := e^{(\mu-\varepsilon)h},\ \eta := \frac{\varepsilon}{\omega^2 + (\mu-\varepsilon)^2},\ \boldsymbol{M} := \boldsymbol{I}_N - \boldsymbol{D}, \tag{5.12}$$

$$\boldsymbol{\Theta}(h) := \begin{bmatrix} \cos\omega h & -\sin\omega h \\ \sin\omega h & \cos\omega h \end{bmatrix},\ \boldsymbol{Q} := \begin{bmatrix} \mu-\varepsilon & \omega \\ -\omega & \mu-\varepsilon \end{bmatrix}. \tag{5.13}$$

Since $\boldsymbol{M}$ is self-adjoint and positive semidefinite [58, 59], it can be diagonalized as $\boldsymbol{T}^{-1}\boldsymbol{M}\boldsymbol{T} = \mathrm{diag}(\rho_1, \rho_2, \ldots, \rho_N)$, where $\boldsymbol{T}$ is a diagonal transformation matrix and ρ_q $(q = 1, 2, \ldots, N)$ are the eigenvalues of $\boldsymbol{M}$. Therefore, we obtain

$$\begin{aligned} & g(\lambda) \\ & = \det\left\{\left(\boldsymbol{T}^{-1} \otimes \boldsymbol{I}_2\right)\left(\lambda^{r+1}\boldsymbol{I}_{2N} - \lambda^r\boldsymbol{L}_a - \boldsymbol{L}_b\right)\left(\boldsymbol{T} \otimes \boldsymbol{I}_2\right)\right\} \\ & = \det\left\{\lambda^{r+1}\boldsymbol{I}_{2N} - \lambda^r\gamma\boldsymbol{I}_N \otimes \boldsymbol{\Theta}(h) - \eta\left(\boldsymbol{T}^{-1} \otimes \boldsymbol{I}_2\right)\right. \\ & \qquad \left.\left(\boldsymbol{I}_N - \boldsymbol{M}\right) \otimes \boldsymbol{Q}\left(\gamma\boldsymbol{\Theta}(h) - \boldsymbol{I}_2\right)\left(\boldsymbol{T} \otimes \boldsymbol{I}_2\right)\right\} \\ & = \det\left\{\lambda^{r+1}\boldsymbol{I}_{2N} - \lambda^r\gamma\boldsymbol{I}_N \otimes \boldsymbol{\Theta}(h) - \eta\left(\boldsymbol{I}_N - \boldsymbol{T}^{-1}\boldsymbol{M}\boldsymbol{T}\right) \otimes \boldsymbol{Q}\left(\gamma\boldsymbol{\Theta}(h) - \boldsymbol{I}_2\right)\right\} \\ & = \det\left\{\lambda^{r+1}\boldsymbol{I}_{2N} - \lambda^r\gamma\boldsymbol{I}_N \otimes \boldsymbol{\Theta}(h)\right. \\ & \qquad \left. -\eta\left(\boldsymbol{I}_N - \mathrm{diag}(\rho_1, \rho_2, \ldots, \rho_N)\right) \otimes \boldsymbol{Q}\left(\gamma\boldsymbol{\Theta}(h) - \boldsymbol{I}_2\right)\right\}. \end{aligned} \tag{5.14}$$

As a result, $g(\lambda) = 0$ can be expressed as

$$g(\lambda) = \prod_{q=1}^{N} \bar{g}(\lambda, \rho_q) = 0, \tag{5.15}$$

$$\bar{g}(\lambda, \rho_q) = \det\left\{\lambda^{r+1}\boldsymbol{I}_2 - \lambda^r\gamma\boldsymbol{\Theta}(h) - \eta\left(1 - \rho_q\right)\boldsymbol{Q}\left(\gamma\boldsymbol{\Theta}(h) - \boldsymbol{I}_2\right)\right\}. \tag{5.16}$$

The function $\bar{g}(\lambda, \rho_q)$ can be described by the following $2(r+1)$-degree polynomial:

$$\bar{g}(\lambda, \rho_q) = \lambda^{2(r+1)} + \alpha_4\lambda^{2r+1} + \alpha_3\lambda^{2r} + \alpha_2(\rho_q)\lambda^{r+1} + \alpha_1(\rho_q)\lambda^r + \alpha_0(\rho_q), \tag{5.17}$$

where

$$\alpha_0(\rho_q) := (1-\rho_q)^2\varphi_0,\ \alpha_1(\rho_q) := (1-\rho_q)\varphi_1,$$

$$\alpha_2(\rho_q) := (1-\rho_q)\varphi_2,\ \alpha_3 := \gamma^2,\ \alpha_4 := -2\gamma\cos\omega h.$$

The parameters φ_0, φ_1, and φ_2 are defined by

$$\varphi_0 := \eta^2\left(\gamma^2 - 2\gamma\cos\omega h + 1\right)\left\{\omega^2 + (\mu-\varepsilon)^2\right\},$$

$$\varphi_1 := 2\eta\gamma\{(\mu-\varepsilon)(\gamma-\cos\omega h) + \omega\sin\omega h\},$$

$$\varphi_2 := -2\eta\{(\mu-\varepsilon)(\gamma\cos\omega h - 1) + \omega\gamma\sin\omega h\},$$

respectively. The homogeneous steady state $\boldsymbol{Z}^*$ of the coupled oscillators on network topology $\boldsymbol{D}$ is stable if and only if all the roots λ of $\bar{g}(\lambda,\rho_q) = 0$ $(q = 1, 2, \ldots, N)$ lie within the unit circle on the complex plane.

5.4 Numerical verification

This section investigates the stability regions in the connection parameter space $\varepsilon - \tau$ for the networked oscillator system on some typical network topologies. The marginal stability curves are estimated in order to obtain these regions. The following steps are used for the estimation: (i) number of oscillators, N, and network topology c_{nk} are given; (ii) eigenvalues ρ_q of matrix $\boldsymbol{M}$, as denoted in Eq. (5.12), are calculated; (iii) $\bar{g}(e^{i\theta},\rho_q) = g_R(\theta,\rho_q) + ig_I(\theta,\rho_q)$ is derived; (iv) marginal stability curves are estimated by solving $g_R(\theta,\rho_q) = 0$ and $g_I(\theta,\rho_q) = 0$ for $\theta \in [0,\pi]$.

5.4.1 A pair of oscillators ($N = 2$)

Let us now focus on the simplest case, a pair of oscillators (i.e., $N = 2$), as illustrated in Fig. 5.2. The eigenvalues of $\boldsymbol{M}$ are $\rho_1 = 0$ and $\rho_2 = 2$. The marginal stability curves are shown in Figs. 5.4 (a) – (d). Figure 5.4 (a) presents the curves with the normal delayed connection (5.2), which are estimated by solving

$$\bar{g}(i\lambda_I,\rho_q) := i\lambda_I - \mu + \varepsilon - i\omega - \varepsilon e^{-i\lambda_I\tau}(1-\rho_q) = 0,\ \lambda_I \in \boldsymbol{R}, \tag{5.18}$$

with $\rho_1 = 0$ and $\rho_2 = 2$ (for more details, see our previous paper [19]). There exists a thin stability region at around $\tau \approx 0.5$. The curves with the digital delayed connection (5.3) for $r = 1, 3, 10$ are shown in Figs. 5.4 (b) – (d), respectively. For small numbers of buffers, $r = 1$ and 3, the stability regions become much larger compared with those of the normal connection. On the other hand, for a large number $r = 10$, the curves closely resemble those of the normal connection. This result is exemplified by the fact that the digital connection (5.3) with $1 \ll r$ and $h \ll 1$ is approximately identical to the normal connection (5.2).

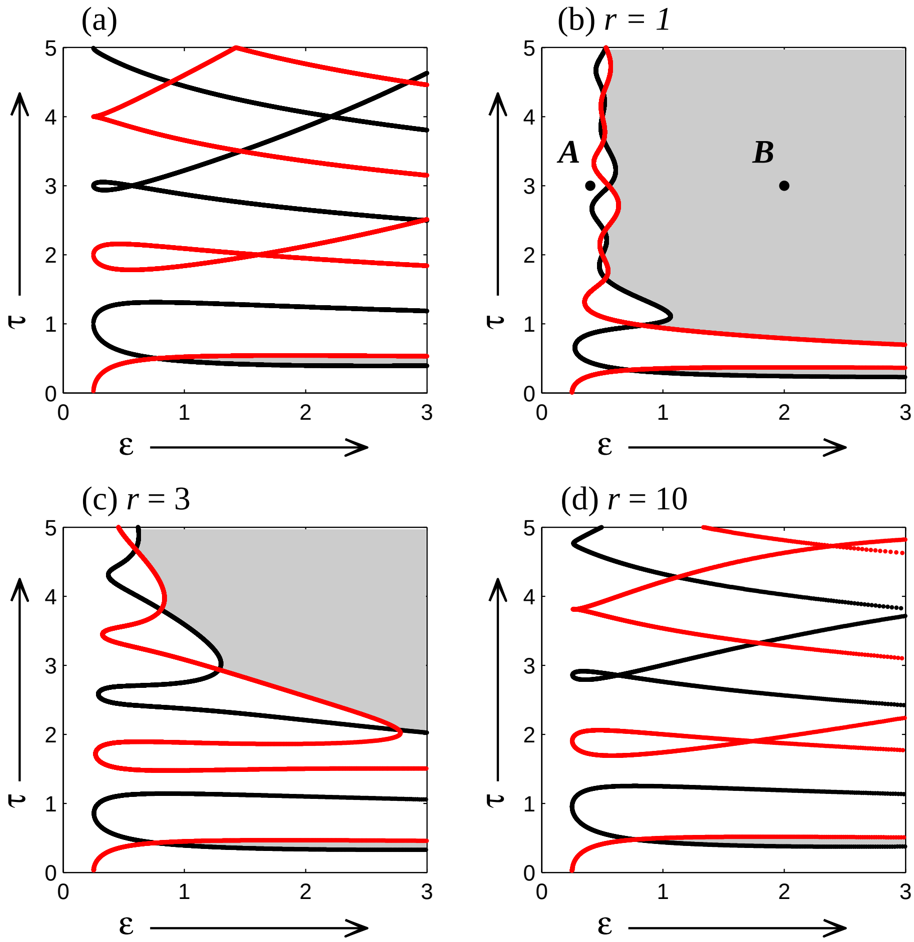

Figure 5.4: Marginal stability curves for a pair of oscillators ($N = 2, \mu = 0.5, \omega = \pi$): (a) normal delayed connection (5.2), (b) – (d) digital delayed connection (5.3) ($r = 1, 3, 10$). Black and red curves correspond to $\rho_1 = 0$ and $\rho_2 = 2$, respectively. The regions of stability are shaded.

Time-series data of real parts of Z_1 and u_1, i.e., Re$\{Z_1\}$ and Re$\{u_1\}$, with $r = 1$ and the parameter sets A and B in Fig. 5.4 (b) are plotted in Figs. 5.5(a) and 5.5(b), respectively. A pair of oscillators behave independently and are then coupled by the digital connection at $t = 20$. For the parameter set A, Re$\{Z_1\}$ and Re$\{u_1\}$ continue to oscillate even after coupling; that is, the connection fails to stabilize the steady state. In contrast, for the parameter set B, the connection succeeds in stabilizing it: Re$\{Z_1\}$ and Re$\{u_1\}$ converge to zero after coupling. These numerical results, which are agree with our analytical results depicted in Fig. 5.4.

5.4.2 Networked oscillators ($N = 5$)

Here we consider five oscillators on two typical network topologies, a complete network (i.e., all-to-all connections) and a ring network (i.e., chain connection with

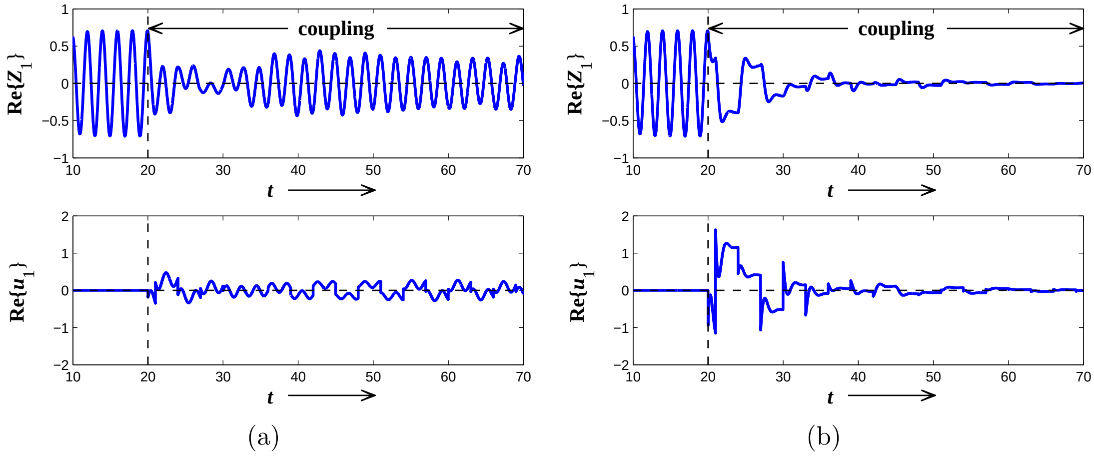

Figure 5.5: Time-series data, $\mathrm{Re}\{Z_1\}$ and $\mathrm{Re}\{u_1\}$, for a pair of oscillators coupled by digital delayed connection (5.3) ($N = 2, \mu = 0.5, \omega = \pi, r = 1$): (a) $\varepsilon = 0.3$ and $\tau = 3$ (i.e., A in Fig. 5.4 (b)), (b) $\varepsilon = 2.0$ and $\tau = 3$ (i.e., B in Fig. 5.4 (b)).

a periodic boundary). The eigenvalues of $\boldsymbol{M}$ for the complete network are $\rho_1 = 0$ and $\rho_{2,3,4,5} = 5/4$. The marginal stability curves for the normal connection (5.2), which are estimated by solving Eq. (5.18) with $\rho_{1\sim 5}$, are shown in Fig. 5.6 (a). The stability region exists at around $\tau \approx 1.0$. Figure 5.6 (b) illustrates the curves for the digital connection (5.3) with $r = 3$. It can be seen that there exists a large stability region with $\tau \gtrsim 2.0$: the stability regions become much larger than those of the normal connection.

For the ring network, the eigenvalues of $\boldsymbol{M}$ are $\rho_1 = 0$, $\rho_{2,3} = 0.691$, and $\rho_{4,5} = 1.809$. Figure 5.7 (a) shows the marginal stability curves for normal connection (5.2) on the ring network. We see a stability region for $0.5 \lesssim \tau \lesssim 1.3$. The curves for the digital connection (5.3) with $r = 3$ are shown in Fig. 5.7 (b). There exists a large stability region with $\tau \gtrsim 2.0$: the stability regions become much larger than those of the normal connection, as was the case with the complete network.

From these numerical results shown in Figs. 5.4, 5.6, and 5.7, it may be concluded that the digital delayed connection better facilitates stabilization than does the continuous-time delayed connection. Note that this conclusion is consistent with Ref. [137], which showed that digital delayed feedback signals facilitate stabilization better than does continuous-time delayed feedback.

5.5 Discussion

We now discuss the influence of network topology and the number of buffers on stability. According to the characteristic equation (5.15), the stability of the steady state $\boldsymbol{Z}^*$ depends on the eigenvalues ρ_q ($q = 1, \ldots, N$) of $\boldsymbol{M}$. This fact leads to

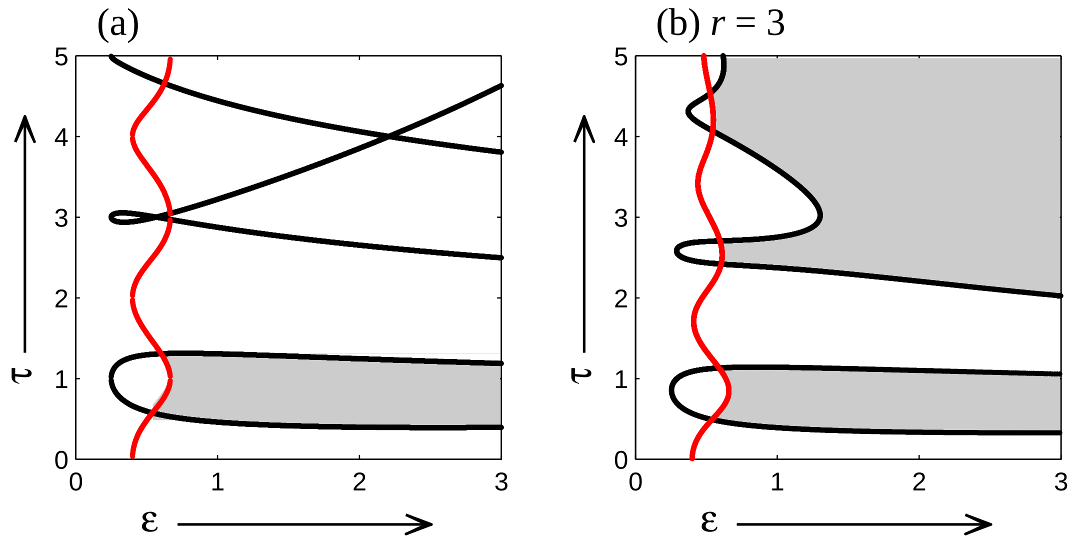

Figure 5.6: Marginal stability curves for a complete network ($N = 5, \mu = 0.5, \omega = \pi$): (a) normal delayed connection (5.2), (b) digital delayed connection (5.3) with $r = 3$. Black and red curves correspond to $\rho_1 = 0$ and $\rho_{2,3,4,5} = 5/4$, respectively. The regions of stability are shaded.

the conclusion that the network topology does not have a direct influence on the stability; for example, two different networks which have the same ρ_q have the same stability region. Although this is valid only for local stability, we think that the transient behavior far from the steady state might be influenced by not only ρ_q but also the network topology. The transient behavior needs further consideration.

From our numerical results shown in Fig. 5.4, it can be seen that the number of buffers, r, has a strong influence on the stability. In the numerical simulation, we observed that the stability region tends to be large for a small number of buffers. However, we were unable to obtain a theoretical relation between this number and the stability region, so this is still an open question.

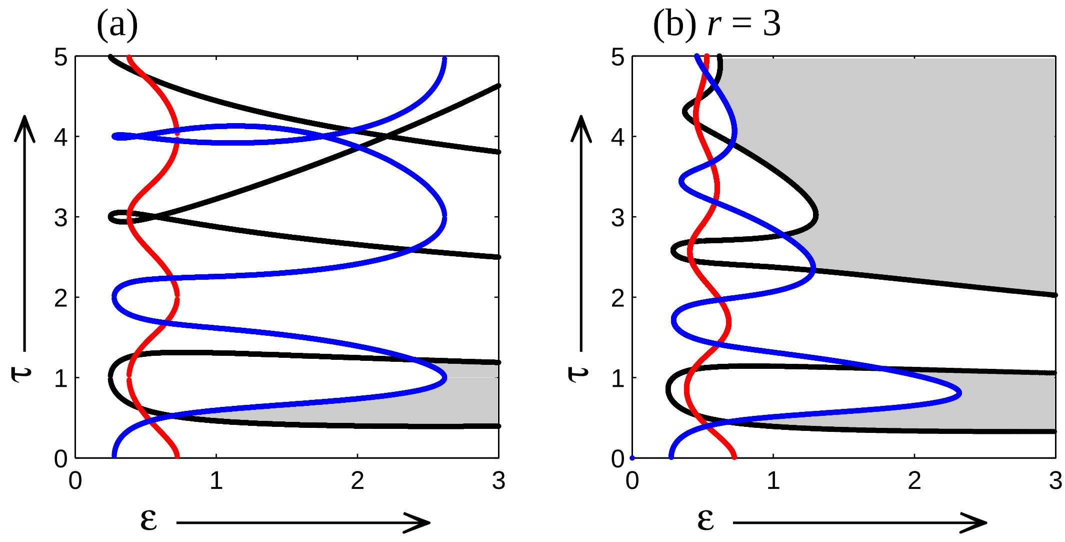

Figure 5.7: Marginal stability curves for a ring network ($N = 5, \mu = 0.5, \omega = \pi$): (a) normal delayed connection (5.2), (b) digital delayed connection (5.3) with $r = 3$. Black, red, and blue curves correspond to $\rho_1 = 0$, $\rho_{2,3} = 0.691$, and $\rho_{4,5} = 1.809$, respectively. The regions of stability are shaded.

5.6 Conclusion

The present chapter investigated the stability of the steady state in oscillators coupled by a digital delayed connection. Such a connection can be described by an FIFO queue. Using the semi-discretization technique, we derived a simple characteristic equation for steady-state stability, with real polynomials whose coefficients depend on the network topology. Our numerical results proved that the digital delayed connection better facilitates stabilization than does the well-known continuous-time delayed connection.

Chapter 6

Conclusions

This thesis considered with amplitude death, the stabilization of a steady state that is induced by diffusive-type connections, in coupled time-delay oscillators with uncertain topology and with static, delay, multiple delay, and digital delay connections. In particular, we have shown that amplitude death can be induced by long connection delays and the connection parameters can be designed by a systematic procedure. This chapter presents our conclusions.

In Chapter 2, we investigated amplitude death in the time-delay oscillators coupled by a static connection. It had been reported that static connections never induce amplitude death in a pair of coupled identical time-delay oscillators. However, we have shown that the static connection can induce death when the oscillators have different delay times. Its stability analysis was a difficult task, since the two different delays in its characteristic equation prevent a conventional stability analysis. We have shown that the cluster treatment of characteristic roots (CTCR) method can successfully perform this difficult task: the boundary curve of the region of amplitude deaths in the parameter space were determined. For three coupled time-delay oscillators, the three different delays in its characteristic equation prevent the use of the CTCR method. We have shown that the CTCR method with advanced clustering and frequency sweeping allows us to obtain the boundary curves.

In Chapter 3, we considered a network of time-delay oscillators coupled by a delay connection. It had been shown that the stability of a steady state with uncertain topology is equivalent to that of a linear delayed system with an uncertain parameter. A simple sufficient condition for the steady state to be stable has been derived on the basis of robust control theory. This condition provided us with a systematic procedure for designing the connection parameters. The procedure has two advantages: the designed parameters can be used for any network topology, and the design procedure is valid even for oscillators with long delays. We used numerical examples to verify the analytical results for complete, ring, and small-world networks.

In Chapter 4, we showed that the multiple delay feedback control (MDFC) method can stabilize an unstable steady state in time-delay oscillators. We provided a simple systematic procedure for designing the feedback gain and the two delays in the feedback loop. The advantage of this method is that arbitrarily long delay times can be used for the stabilization. An electronic circuit experiment was performed to verify the stability region and the systematic design procedure. Furthermore, we have shown that a multiple delay connection can induce amplitude death in two identical coupled time-delay oscillators. A systematic procedure for designing the coupling strength and the two delays in the delay connection was provided. The advantage of the multiple delay connection is the same as that of the MDFC method.

In Chapter 5, we studied steady-state stability in limit-cycle oscillators coupled by a digital delayed connection. The semi-discretization technique allowed us to derive a characteristic equation with real polynomials whose coefficients depend on the network topology. Our numerical results proved that the digital delayed connection better induces amplitude death than does the conventional delay connection.

Appendix

1 Electronic circuits

The delay unit circuit shown in Fig. 1 imports the voltage $x(t)$ and exports the delayed voltage $x(t-\tau)$. This circuit consists of four parts: delay, input, output, and low-pass filter. The delay employs the main device MN3011 (Panasonic) as a bucket-brigade delay-line device. This device exports the delayed voltage. The delay time (1.0–20.0 ms) depends on the function generator frequency (10–240 kHz). It should be noted that this device can delay the voltage only in the range 3.5–6.0 V. However, the voltage of the oscillator (4.15) is not within this range. To solve this problem, the input and output were added to the delay unit. The input transforms the voltage $x(t)$ into a value in the required range. Since the output has the opposing function, the output exports the delayed voltage to a value within the original range. As the delay device has a high-frequency switch operation, its output includes high-frequency noise. The low-pass filter removes the noise from the delayed voltage.

The nonlinear unit circuit is shown in Fig. 2. This circuit consists of the inverting amplifier, the half-wave rectifier, and the summing amplifier. The inverting amplifier inverts and amplifies the input voltage $x(t)$. The half-wave rectifier works as a piecewise linear function which has a break point. The summing amplifier adds up the voltages that are output from the inverting amplifier and the half-wave rectifier. As a result, a relation between the input $x(t)$ and the output $f(x(t))$ is obtained as shown in Fig. 4.6(a). The break point at the peak can be adjusted by R_1 and R_2. The nonlinear function can be shifted up and down by changing R_3.

2 Marginal stability curves

The marginal curves of a stability region are obtained by

$$\bar{g}(j\omega,\rho) = j\omega + \alpha - k\left\{1-(1-\rho)e^{-j\omega T}\right\} - \beta e^{-j\omega\tau} = 0. \tag{1}$$

The real and imaginary parts are described by

$$\begin{aligned} \mathrm{Re}\left[\bar{g}(j\omega,\rho)\right] &= \alpha - k + k(1-\rho)\cos\omega T - \beta\cos\omega\tau = 0, \\ \mathrm{Im}\left[\bar{g}(j\omega,\rho)\right] &= \omega - k(1-\rho)\sin\omega T + \beta\sin\omega\tau = 0. \end{aligned} \tag{2}$$

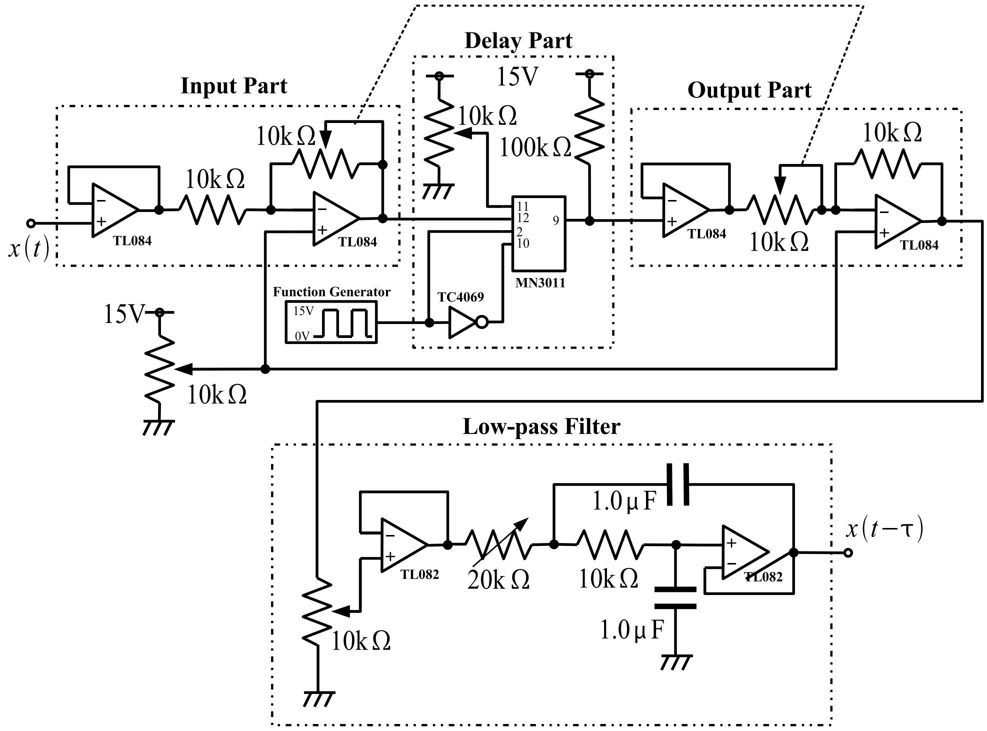

Figure 1: Delay unit circuit.

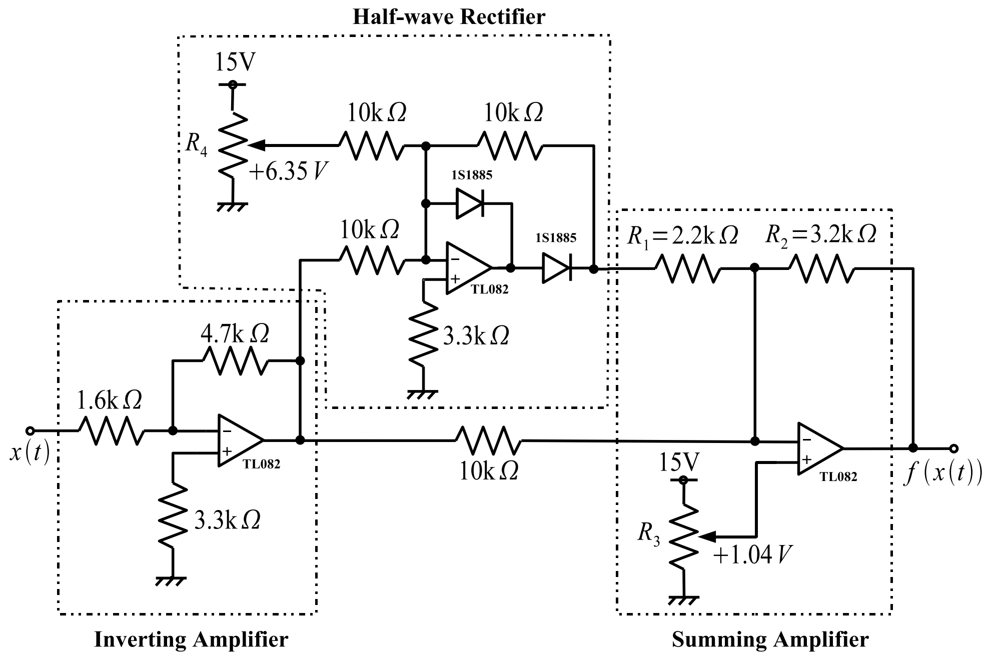

Figure 2: Nonlinear function circuit.

The marginal stability curves are sketched by using the roots T and τ of the above equations. The direction in which the roots cross the imaginary axis is given by the sign of the real part of $\mathrm{d}s/\mathrm{d}\tau$ at $s = j\omega$,

$$\mathrm{Re}\left[\frac{\mathrm{d}s}{\mathrm{d}T}\right]_{s=j\omega} = \mathrm{Re}\left[\frac{j\omega k(1-\rho)e^{-j\omega T}}{1 - kT(1-\rho)e^{-j\omega T} + \beta\tau e^{-j\omega\tau}}\right], \tag{3}$$

where T, τ, and ω satisfy Eq. (2). With increasing T, a positive (negative) value of Eq. (3) corresponds to a root crossing the axis from left to right (right to left). The marginal stability curves are estimated by using the following numerical procedure: set a value for τ; numerically solve $\bar{g}(j\omega, \rho) = 0$ for T and ω; check the sign of Eq. (3); plot (τ, T); change the value of τ; and return to the first step.

Acknowledgments

This thesis would not have been possible without the assistance and support of friends and colleagues at the Osaka Prefecture University and elsewhere. There are some people I particularly wish to thank for their help in completing my doctorate.

First of all, I would like to express my sincerest appreciation to my supervisor, Professor Keiji Konishi, for giving me the opportunity to pursue my doctor degree at Osaka Prefecture University, and for guidance and very valuable support throughout my five years as a master and then as a doctoral student in Japan. He was always patient, pushing, or constantly encouraging as the situation required. I am grateful for his outstanding efforts which always led me to the right research directions and have made this thesis possible. He is a model of how to supervise students, both current and prospective, and to work with colleagues. His insights were always inspiring.

Other advisors to whom I have the pleasure of offering special thanks are Professor Naoyuki Hara, Professor Shigeo Morimoto, and Professor Atsushi Ishigame for helping shape my thesis. Their academic guidances and encouragements were exceptional. Professor Hideki Kokame and Professor Yoshiharu Tsujikawa are also very important, and they gave me the chance to attain a master's degree in this university. Furthermore, I would like to thank my former undergraduate thesis supervisors Professor Dang Van Liet and Professor Chau Van Tao at the University of Sciences - Hochiminh City, Vietnam. Each of these professors has contributed in a substantial way to my progress.

Various other people have also influenced my life in a positive way over these five years and have made my graduate school experience go a bit smoother. Particularly, Professor Masahiro Terasako has helped widen my life experiences, and I thank him for his support, advice, encouragement and unfailing confidence in me and my abilities. Moreover, I owe a million thanks to Mrs. Keiko Mizobata for finding me scholarships for pursuing my post graduate degrees. On the nonacademic side, I also want to thank the student senior to me in the graduate program and the laboratory members who provided assistance to me. I would like to specially thank two junior members in my research team, Yuki Ueno and Yoshiki Sugitani, for their friendship and spiritual guidance, as well as for technical discussions, and fruitful comments.

And last but definitely not least, I wish to thank the organizations who have provided financial support: the Ichikawa International Scholarship Foundation for the first year of my studies, and the Rotary Yoneyama Scholarship Foundation for the next two years.

Bibliography

[1] A. Jenkins, "Self-oscillation," *Phys. Rep.*, vol. 525, no. 2, pp. 167–122, 2013.

[2] D. DiFrancesco, "Pacemaker mechanisms in cardiac tissue," *Annu. Rev. Physiol.*, vol. 55, pp. 455–472, 1993.

[3] D. DiFrancesco, "The role of the funny current in pacemaker activity," *Circ. Res.*, vol. 106, no. 3, pp. 434–446, 2010.

[4] J. Glover, A.C. Lazer, and P.J. McKenna, "Existence and stability of large scale nonlinear oscillations in suspension bridges," *ZAMP Zeitschrift fur angewandte Mathematik und Physik*, vol. 40, no. 2, pp. 172–200, 1989.

[5] F. Gazzola, "Nonlinearity in oscillating bridges," *Electron. J. Differ. Equ.*, vol. 2013, no. 211, pp. 1–47, 2013.

[6] S.R. Huddy and J.D. Skufca, "Amplitude death solutions for stabilization of dc microgrids with instantaneous constant-power loads," *IEEE Trans. Power Electron.*, vol. 28, no. 1, pp. 247–253, 2013.

[7] F.C. Moon, *Dynamics and Chaos in Manufacturing Processes*, John Wiley and Sons, 1998.

[8] G. Radons and R. Neugebauer, *Nonlinear Dynamics of Production Systems*, John Wiley and Sons, 2004.

[9] P. Hövel and E. Schöll, "Control of unstable steady states by time-delayed feedback methods," *Phys. Rev. E*, vol. 72, no. 4, p. 046203, 2005.

[10] K. Pyragas, "Continuous control of chaos by self-controlling feedback," *Phys. Lett. A*, vol. 170, no. 6, pp. 421–428, 1992.

[11] A. Ahlborn and U. Parlitz, "Stabilizing unstable steady states using multiple delay feedback control," *Phys. Rev. Lett.*, vol. 93, no. 26, p. 264101, 2004.

[12] K. Konishi and N. Hara, "Stabilization of unstable fixed points with queue-based delayed feedback control," *Dynam. Cont. Dis. Ser. B*, vol. 18, no. 5, pp. 679–693, 2011.

[13] S.H. Strogatz and I. Stewart, "Coupled oscillators and biological synchronization," *Sci. Am.*, vol. 269, no. 6, pp. 102–109, 1993.

[14] H.M. Smith, "Synchronous flashing of fireflies," *Science*, vol. 82, no. 2120, pp. 151–152, 1935.

[15] T.J. Walker, "Acoustic synchrony: Two mechanisms in the snowy tree cricket," *Science*, vol. 166, no. 3907, pp. 891–894, 1969.

[16] Y. Yamaguchi and H. Shimizu, "Theory of self-synchronization in the presence of native frequency distribution and external noises," *Physica D*, vol. 11, no. 1–2, pp. 212–226, 1984.

[17] D. Aronson, G. Ermentout, and N. Kopell, "Amplitude response of coupled oscillators," *Physica D*, vol. 41, no. 3, pp. 403–449, 1990.

[18] D. Reddy, A. Sen, and G. Johnston, "Time delay induced death in coupled limit cycle oscillators," *Phys. Rev. Lett.*, vol. 80, no. 23, pp. 5109–5112, 1998.

[19] K. Konishi, H. Kokame, and N. Hara, "Stabilization of a steady state in network oscillators by using diffusive connections with two long time delays," *Phys. Rev. E*, vol. 81, no. 1, p. 016201, 2010.

[20] J.D. Farmer, "Chaotic attractors of an infinite-dimensional dynamical system," *Physica D*, vol. 4, no. 3, pp. 366–393, 1982.

[21] N. MacDonald, *Biological Delay Systems: Linear Stability Theory*, Cambridge University Press, 2008.

[22] H. Smith, *An Introduction to Delay Differential Equations with Applications to the Life Sciences*, Springer, 2011.

[23] R.E. Plant, "Bifurcation and resonance in a model for bursting nerve cells," *J. Math. Biol.*, vol. 11, no. 1, pp. 15–32, 1981.

[24] S.-I. Niculescu, P. Kim, K. Gu, P.P. Lee and D. Levy, "Stability crossing boundaries of delay systems modeling immune dynamics in leukemia," *Discrete Contin. Dyn. Syst. Ser. B.*, vol. 13, no. 1, pp. 129–156, 2010.

[25] R. Sipahi, S.-I. Niculescu, C. Abdallah, W. Michiels, and K. Gu, "Stability and stabilization of systems with time delay," *IEEE Control Syst. Mag.*, vol. 31, no. 1, pp. 38–65, 2011.

[26] R. Sipahi and I.I. Delice, "Stability of inventory dynamics in supply chains with three delays," *Int. J. Prod. Econ.*, vol. 123, no. 1, pp. 107–117, 2010.

[27] N. Sowa, T. Kondou, H. Mori, and M.-S. Choi, "Method of preventing unstable vibration caused by time delays in contact rotating systems," *JSME Int. J., Ser. C*, vol. 49, no. 4, pp. 973–982, 2006.

[28] E.M. Navarro-Lopez and D. Cortes, "Avoiding harmful oscillations in a drill-string through dynamical analysis," *J. Sound Vib.*, vol. 307, no. 1–2, pp. 152–171, 2007.

[29] J. Loiseau, W. Michiels, S.-I. Niculescu, and R. Sipahi, *Topics in Time Delay Systems*, Springer, 2009.

[30] P. Hövel, *Control of Complex Nonlinear Systems with Delay*, Springer, 2010.

[31] M. Lakshmanan and D. Senthilkumar, *Dynamics of Nonlinear Time-Delay Systems*, Springer, 2011.

[32] L.B. Le, K. Konishi, H. Kokame, and N. Hara, "Amplitude death in a pair of time-delayed chaotic oscillators coupled by a static connection," *Proc. of International Symposium on Nonlinear Theory and its Applications*, pp. 631–634, 2010.

[33] L.B. Le, K. Konishi, and N. Hara, "Stability analysis of a steady state in three time-delayed nonlinear oscillators coupled by a static connection," *Proc. of IUTAM Symposium on 50 Years of Chaos*, pp. 279–282, 2011.

[34] A. Namajūnas, K. Pyragas, and A. Tamaševičius, "Stabilization of an unstable steady state in a Mackey-Glass system," *Phys. Lett. A*, vol. 204, no. 3–4, pp. 255–262, 1995.

[35] K. Konishi, K. Senda, and H. Kokame, "Amplitude death in time-delay chaotic oscillators coupled by diffusive connections," *Phys. Rev. E*, vol. 78, no. 5, p. 056216, 2008.

[36] L.B. Le, K. Konishi, and N. Hara, "Topology-free design for amplitude death in time-delayed oscillators coupled by a delayed connection," *Phys. Rev. E*, vol. 87, no. 4, p. 042908, 2013.

[37] L.B. Le, K. Konishi, and N. Hara, "Design and experimental verification of multiple delay feedback control for time-delay nonlinear oscillators," *Nonlinear Dyn.*, vol. 67, no. 2, pp. 1407–1418, 2012.

[38] L.B. Le, K. Konishi, and N. Hara, "Design of amplitude death in a pair of time-delayed chaotic oscillators coupled by a multiple delay connection," *Proc. of Conference on Nonlinear Dynamics of Electronic Systems*, pp. 257–260, 2012.

[39] K. Konishi, L.B. Le, and N. Hara, "Stabilization of a steady state in oscillators coupled by a digital delayed connection," *Eur. Phys. J. B*, vol. 85, no. 5, p. 166, 2012.

[40] S. Strogatz, "Death by delay," *Nature*, vol. 394, no. 6691, pp. 316–317, 1998.

[41] F. Atay, "Distributed delays facilitate amplitude death of coupled oscillators," *Phys. Rev. Lett.*, vol. 91, no. 9, p. 094101, 2003.

[42] K. Konishi, "A tuning strategy to avoid blocking and starving in a buffered production line," *Eur. J. Oper. Res.*, vol. 200, no. 2, pp. 616–620, 2010.

[43] K. Konishi, H. Kokame, and N. Hara, "Stability analysis and design of amplitude death induced by a time-varying delay connection," *Phys. Lett. A*, vol. 374, no. 5, pp. 733–738, 2010.

[44] R. Sipahi and N. Olgac, "A unique methodology for the stability robustness of multiple time delay systems," *Syst. Control Lett.*, vol. 55, no. 10, pp. 819–825, 2006.

[45] D.V. Senthilkumar and M. Lakshmanan, "Transition from anticipatory to lag synchronization via complete synchronization in time-delay systems," *Phys. Rev. E*, vol. 71, no. 1, p. 016211, 2005.

[46] W. Zou and M. Zhan, "Partial time-delay coupling enlarges death island of coupled oscillators," *Phys. Rev. E*, vol. 80, no. 6, p. 065204, 2009.

[47] K. Konishi, "Limitation of amplitude death in two identical systems coupled with a time delay," *Proc. of the 11th International IEEE Workshop on Nonlinear Dynamics of Electronic Systems*, pp. 137–140, 2003.

[48] R. Karnatak, R. Ramaswamy, and A. Prasad, "Amplitude death in the absence of time delays in identical coupled oscillators," *Phys. Rev. E*, vol. 76, p. 035201, 2007.

[49] I.I. Delice and R. Sipahi, "Delay-independent stability test for systems with multiple time-delays," *IEEE Trans. Automat. Contr.*, vol. 57, no. 4, pp. 963–972, 2012.

[50] A. Pikovsky, M. Rosenblum, and J. Kurths, *Synchronization*, Cambridge University Press, 2001.

[51] S. Boccaletti, V. Latora, Y. Moreno, M. Chavez, and D.-U. Hwang, "Complex networks: Structure and dynamics," *Phys. Rep.*, vol. 424, no. 4–5, pp. 175–308, 2006.

[52] P. Holmes, R.J. Full, D. Koditschek, and J. Guckenheimer, "The dynamics of legged locomotion: Models, analyses, and challenges," *SIAM Review*, vol. 48, no. 2, pp. 207–304, 2006.

[53] A. Ishiguro, M. Shimizu, and T. Kawakatsu, "A modular robot that exhibits amoebic locomotion," *Rob. Auton. Syst.*, vol. 54, no. 8, pp. 641–650, 2006.

[54] Y.-W. Hong and A. Scaglione, "A scalable synchronization protocol for large scale sensor networks and its applications," *IEEE J. Sel. Areas Comm.*, vol. 23, no. 5, pp. 1085–1099, 2005.

[55] T. Okuda, K. Konishi, and N. Hara, "Experimental verification of synchronization in pulse-coupled oscillators with a refractory period and frequency distribution," *Chaos*, vol. 21, no. 2, p. 023105, 2011.

[56] K. Konishi, "Limitation of time-delay induced amplitude death," *Phys. Lett. A*, vol. 341, no. 5–6, pp. 401–409, 2005.

[57] D. Reddy, A. Sen, and G. Johnston, "Time delay effects on coupled limit cycle oscillators at Hopf bifurcation," *Physica D*, vol. 129, no. 1–2, pp. 15–34, 1999.

[58] F.M. Atay, "Oscillator death in coupled functional differential equations near Hopf bifurcation," *J. Differ. Equ.*, vol. 221, no. 1, pp. 190–209, 2006.

[59] F.M. Atay and O. Karabacak, "Stability of coupled map networks with delays," *SIAM J. Appl. Dyn. Syst.*, vol. 5, no. 3, pp. 508–527, 2006.

[60] C.-Y. Cheng, "Induction of Hopf bifurcation and oscillation death by delays in coupled networks," *Phys. Lett. A*, vol. 374, no. 2, pp. 178–185, 2009.

[61] J. Yang, "Transitions to amplitude death in a regular array of nonlinear oscillators," *Phys. Rev. E*, vol. 76, no. 1, p. 016204, 2007.

[62] K. Konishi, "Time-delay-induced stabilization of coupled discrete-time systems," *Phys. Rev. E*, vol. 67, no. 1, p. 017201, 2003.

[63] R. Dodla, A. Sen, and G. Johnston, "Phase-locked patterns and amplitude death in a ring of delay-coupled limit cycle oscillators," *Phys. Rev. E*, vol. 69, no. 5, p. 056217, 2004.

[64] M. Mehta and A. Sen, "Death island boundaries for delay-coupled oscillator chains," *Phys. Lett. A*, vol. 355, no. 3, pp. 202–206, 2006.

[65] Y. Song, J. Wei, and Y. Yuan, "Stability switches and Hopf bifurcations in a pair of delay-coupled oscillators," *J. Nonlinear Sci.*, vol. 17, no. 2, pp. 145–166, 2007.

[66] D. Reddy, A. Sen, and G. Johnston, "Experimental evidence of time-delay induced death in coupled limit-cycle oscillators," *Phys. Rev. Lett.*, vol. 85, no. 16, pp. 3381–3384, 2000.

[67] R. Herrero, M. Figueras, J. Rius, F. Pi, and G. Orriols, "Experimental observation of the amplitude death effect in two coupled nonlinear oscillators," *Phys. Rev. Lett.*, vol. 84, no. 23, pp. 5312–5315, 2000.

[68] K. Makita, R.E. Christenson, K. Seto, and T. Watanabe, "Optimal design strategy of connected control method for two dynamically similar structures," *J. Eng. Mech.*, vol. 133, no. 12, pp. 1247–1257, 2007.

[69] J.M. Höfener, G.C. Sethia, and T. Gross, "Stability of networks of delay-coupled delay oscillators," *Europhys. Lett.*, vol. 95, no. 4, p. 40002, 2011.

[70] V.L. Kharitonov and A.P. Zhabko, "Robust stability of time-delay systems," *IEEE Trans. Autom. Control*, vol. 39, no. 12, pp. 2388–2397, 1994.

[71] H.Y. Hu and Z.H. Wang, *Dynamics of Controlled Mechanical Systems with Delayed Feedback*, Springer, 2002.

[72] F.R.K. Chung, *Spectral Graph Theory*, American Mathematical Society, 1997.

[73] J.K. Hale and S.M.V. Lunel, *Introduction to Functional Differential Equations*, Springer, 1993.

[74] L.B. Le, K. Konishi, and N. Hara, "Design of amplitude death in time-delay oscillators coupled by a delayed connection," *Proc. of International Scientific Conference on Physics and Control*, CS1-3, CD-ROM, total 4 pages, 2011.

[75] C. Moore and M.E.J. Newman, "Epidemics and percolation in small-world networks," *Phys. Rev. E*, vol. 61, no. 5, pp. 5678–5682, 2000.

[76] G. Chen and X. Dong, *From Chaos to Order*, World Scientific, 1998.

[77] H. Schuster, *Handbook of Chaos Control*, Wiley, 1999.

[78] B. Andrievskii and A. Fradkov, "Control of chaos: Methods and applications -I. Methods," *Autom. Remote Control*, vol. 64, no. 5, pp. 673–713, 2003.

[79] B. Andrievskii and A. Fradkov, "Control of chaos: Methods and applications -II. Applications," *Autom. Remote Control*, vol. 65, no. 4, pp. 503–533, 2004.

[80] E. Schöll and H. Schuster, *Handbook of Chaos Control*, Wiley, 2008.

[81] K. Pyragas, "Delayed feedback control of chaos," *Philos. Trans. R. Soc. Lond. A*, vol. 364, no. 1846, pp. 2309–2334, 2006.

[82] K. Gu, V.L. Kharitonov, L. Vladimir, and J. Chen, *Stability of time-delay systems*, Springer, 2003.

[83] A. Chang, J.C. Bienfang, G.M. Hall, J. R. Gardner, and D.J. Gauthier, "Stabilizing unstable steady states using extended time-delay autosynchronization," *Chaos*, vol. 8, no. 4, pp. 782–790, 1998.

[84] T. Dahms, P. Hövel, and E. Scholl, "Control of unstable steady states by extended time-delayed feedback," *Phys. Rev. E*, vol. 76, no. 5, p. 056201, 2007.

[85] H. Kokame, K. Hirata, K. Konishi, and T. Mori, "State difference feedback for stabilizing uncertain steady states of non-linear systems," *Int. J. Control*, vol. 74, no. 6, pp. 537–546, 2001.

[86] H. Kokame, K. Hirata, K. Konishi, and T. Mori, "Difference feedback can stabilize uncertain steady states," *IEEE Trans. Autom. Control*, vol. 46, no. 12, pp. 1908–1913, 2001.

[87] K. Hirata, H. Kokame, K. Konishi, and H. Fujita, "Observer-based delayed-feedback control of continuous-time systems," *Proc. of American Control Conference*, pp. 25–27, 2001.

[88] V.Z. Tronciu, H. Wunsche, M. Wolfrum, and M. Radziunas, "Semiconductor laser under resonant feedback from a Fabry-Perot resonator: Stability of continuous-wave operation," *Phys. Rev. E*, vol. 73, no. 4, p. 046205, 2006.

[89] A. Ahlborn and U. Parlitz, "Controlling dynamical systems using multiple delay feedback control," *Phys. Rev. E*, vol. 72, no. 1, p. 016206, 2005.

[90] A. Ahlborn and U. Parlitz, "Laser stabilization with multiple-delay feedback control," *Opt. Lett.*, vol. 31, no. 4, pp. 465–467, 2006.

[91] T. Hikihara and T. Kawagoshi, "An experimental study on stabilization of unstable periodic motion in magneto-elastic chaos," *Phys. Lett. A*, vol. 211, no. 1, pp. 29–36, 1996.

[92] A. Kittel, J. Parisi, K. Pyragas, and R. Richter, "Delayed feedback control of chaos in an electronic double-scroll oscillator," *Z. Naturforsch*, vol. 49a, pp. 843–846, 1994.

[93] K. Konishi and H. Kokame, "Odd number property of multiple delayed feedback control," *Proc. of the 15th International IEEE Workshop on Nonlinear Dynamics of Electronic Systems*, pp. 249–252, 2007.

[94] J. Lu, Z. Ma, and L. Li, "Double delayed feedback control for the stabilization of unstable steady states in chaotic systems," *Commun. Nonlinear Sci. Numer. Simul.*, vol. 14, no. 7, pp. 3037–3045, 2009.

[95] H.U. Voss, "Anticipating chaotic synchronization," *Phys. Rev. E*, vol. 61, no. 5, pp. 5115–5119, 2000.

[96] M. Bunner and W. Just, "Synchronization of time-delay systems. *Phys. Rev. E*, vol. 58, pp. 4072–4075, 1998.

[97] E.M. Shahverdiev and K.A. Shore, "Generalized synchronization in time-delayed systems," *Phys. Rev. E*, vol. 71, p. 016201, 2005.

[98] S. Sano, A. Uchida, S. Yoshimori, and R. Roy, "Dual synchronization of chaos in Mackey-Glass electronic circuits with time-delayed feedback," *Phys. Rev. E*, vol. 75, no. 1, p. 016207, 2007.

[99] W.H. Kye, M. Choi and C.M. Kim, "Encryption with synchronized time-delayed systems," *Phys. Rev. E*, vol. 71, p. 045202, 2005.

[100] M. Suzuki and N. Sakamoto, "Controlling ideal turbulence in time-delayed Chua ' s circuit: Stabilization and synchronization," *Int. J. Bifur. Chaos*, vol. 20, pp. 1351–1363, 2010.

[101] C.F. Feng, "Projective synchronization between two different time-delayed chaotic systems using active control approach," *Nonlinear Dyn.*, vol. 62, pp. 453–459, 2010.

[102] X. Guan, G. Feng, C. Chen, and G. Chen, "A full delayed feedback controller design method for time-delay chaotic systems," *Physica D*, vol. 227, no. 1, pp. 36–42, 2007.

[103] A. Gjurchinovski and V. Urumov, "Variable-delay feedback control of unstable steady states in retarded time-delayed systems," *Phys. Rev. E*, vol. 81, no. 1, p. 016209, 2010.

[104] W. Michiels and S.-I. Niculescu, *Stability and Stabilization of Time-Delay Systems: an Eigenvalue-Based Approach*, SIAM, 2007.

[105] M. Ishii, K. Konishi, and H. Kokame, "Robust stability of extended delayed-feedback control in one-dimensional chaotic systems," *Phys. Lett. A*, vol. 235, pp. 603 – 609, 1997.

[106] K.B. Blyuss, Y.N. Kyrychko, P. Hovel, and E. Schöll, "Control of unstable steady states in neutral time-delayed systems," *Eur. Phys. J. B*, vol. 65, no. 4, pp. 571–576, 2008.

[107] S. Xu, J. Lam, and Y. Zou, "Delay-dependent approach to stabilization of time-delay chaotic systems via standard and delayed feedback controllers," *Int. J. Bifur. Chaos*, vol. 15, no. 4, pp. 1455–1465, 2005.

[108] B. Rezaie, M.R.J. Motlagh, M. Analoui, and S. Khorsandi, "Stabilizing fixed points of time-delay systems close to the Hopf bifurcation using a dynamic delayed feedback control method," *J. Phys. A*, vol. 42, no. 39, p. 395102, 2009.

[109] N. Vasegh and A.K. Sedigh, "Delayed feedback control of time-delayed chaotic systems: Analytical approach at Hopf bifurcation," *Phys. Lett. A*, vol. 372, no. 31, pp. 5110–5114, 2008.

[110] N. Vasegh and A.K. Sedigh, "Chaos control via TDFC in time-delayed systems: The harmonic balance approach," *Phys. Lett. A*, vol. 373, no. 3, pp. 354–358, 2009.

[111] T. Ushio, "Limitation of delayed feedback control in nonlinear discrete-time systems," *IEEE Trans. Circuits Syst. I*, vol. 43, no. 9, pp. 815–816, 1996.

[112] H. Nakajima, "On analytical properties of delayed feedback control of chaos," *Phys. Lett. A*, vol. 232, no. 3-4, pp. 207–210, 1997.

[113] W. Just, E. Reibold, H. Benner, K. Kacperski, P. Fronczak, and J. Holyst, "Limits of time-delayed feedback control," *Phys. Lett. A*, vol. 254, no. 3–4, pp. 158–164, 1999.

[114] B. Fiedler, V. Flunkert, M. Georgi, P. Hövel, and E. Schöll, "Refuting the odd-number limitation of time-delayed feedback control," *Phys. Rev. Let.*, vol. 98, no. 11, p. 114101, 2007.

[115] W. Just, B. Fiedler, M. Georgi, V. Flunkert, P. Hövel, and E. Schöll, "Beyond the odd number limitation: A bifurcation analysis of time-delayed feedback control," *Phys. Rev. E*, vol. 76, no. 2, p. 026210, 2007.

[116] C.M. Postlethwaite and M. Silber, "Stabilizing unstable periodic orbits in the Lorenz equations using time-delayed feedback control," *Phys. Rev. E*, vol. 76, no. 5, p. 056214, 2007.

[117] K. Konishi, M. Hirai, and H. Kokame, "Decentralized delayed-feedback control of a coupled map model for open flow," *Phys. Rev. E*, vol. 58, no. 3, pp. 3055 – 3059, 1998.

[118] S. Yamamoto, T. Hino, and T. Ushio, "Dynamic delayed feedback controllers for chaotic discrete-time systems," *IEEE Trans. Circuits Syst. I*, vol. 48, no. 6, pp. 785–789, 2001.

[119] K. Pyragas, V. Pyragas, I.Z. Kiss, and J.L. Hudson, "Stabilizing and tracking unknown steady states of dynamical systems," *Phys. Rev. Lett.*, vol. 89, no. 24, p. 244103, 2002.

[120] K. Pyragas, V. Pyragas, I.Z. Kiss, and J.L. Hudson, "Adaptive control of unknown unstable steady states of dynamical systems," *Phys. Rev. E*, vol. 70, no. 2, p. 026215, 2004.

[121] A. Gjurchinovski and V. Urumov, "Stabilization of unstable steady states by variable-delay feedback control," *Europhys. Lett.*, vol. 84, no. 4, p. 40013, 2008.

[122] T. Endo and S. Mori, "Mode analysis of a multimode ladder oscillator," *IEEE Trans. Circuits Syst.*, vol. 23, no. 2, pp. 100–113, 1976.

[123] Y. Nishio and A. Ushida, "Spatio-temporal chaos in simple coupled chaotic circuits," *IEEE Trans. Circuits Syst. I*, vol. 42, no. 10, pp. 678–686, 1995.

[124] G. Orosz and G. Stepan, "Subcritical Hopf bifurcations in a car-following model with reaction-time delay," *Proc. R. Soc. A*, vol. 462, no. 2073, pp. 2643–2670, 2006.

[125] F. Atay, "Total and partial amplitude death in networks of diffusively coupled oscillators," *Physica D*, vol. 183, no. 1–2, pp. 1–18, 2003.

[126] K. Konishi, "Amplitude death in oscillators coupled by a one-way ring time-delay connection," *Phys. Rev. E*, vol. 70, no. 5, p. 066201, 2004.

[127] W. Michiels and H. Nijmeijer, "Synchronization of delay-coupled nonlinear oscillators: An approach based on the stability analysis of synchronized equilibria," *Chaos*, vol. 19, no. 3, p. 033110, 2009.

[128] R. Karnatak, N. Punetha, A. Prasad, and R. Ramaswamy, "Nature of the phase-flip transition in the synchronized approach to amplitude death," *Phys. Rev. E*, vol. 82, no. 4, p. 046219, 2010.

[129] K. Konishi, "Amplitude death induced by dynamic coupling," *Phys. Rev. E*, vol. 68, no. 6, p. 067202, 2003.

[130] K. Konishi and N. Hara, "Topology-free stability of a steady state in network systems with dynamic connections," *Phys. Rev. E*, vol. 83, no. 3, p. 036204, 2011.

[131] T. Singla, N. Pawar, and P. Parmananda, "Exploring the dynamics of conjugate coupled Chua circuits: Simulations and experiments," *Phys. Rev. E*, vol. 83, no. 2, p. 026210, 2011.

[132] W. Zou, C. Yao, and M. Zhan, "Eliminating delay-induced oscillation death by gradient coupling," *Phys. Rev. E*, vol. 82, no. 5, p. 056203, 2010.

[133] W. Zhang, M.S. Branicky, and S.M. Phillips, "Stability of networked control systems," *IEEE Control Syst. Mag.*, vol. 21, no. 1, pp. 84–97, 2001.

[134] T. Insperger and G. Stepan, "Semi-discretization method for delayed systems," *Int. J. Numer. Meth. Eng.*, vol. 55, no. 5, pp. 503–518, 2002.

[135] F. Hartung, T. Insperger, G. Stepan, and J. Turi, "Approximate stability charts for milling processes using semi-discretization," *Appl. Math. Comput.*, vol. 174, no. 1, pp. 51–73, 2006.

[136] T. Insperger, G. Stepan, and J. Turi, "On the higher-order semi-discretizations for periodic delayed systems," *J. Sound Vib.*, vol. 313, no. 1–2, pp. 334–341, 2008.

[137] T. Insperger, G. Stepan, and J. Turi, "Delayed feedback of sampled higher derivatives," *Phil. Trans. R. Soc. A*, vol. 368, no. 1911, pp. 469–482, 2010.

[138] P. Celka, "Experimental verification of Pyragas's chaos control method applied to Chua's circuit," *Int. J. Bifur. Chaos*, vol. 4, no. 6, p. 1703, 1994.

[139] T. Imai, K. Konishi, H. Kokame, and K. Hirata, "Experimental evidence for spatiotemporal stability and control of a one-way open CML," *Int. J. Bifur. Chaos*, vol. 12, no. 12, pp. 2937–2944, 2002.

[140] H.U. Voss, "Real-time anticipation of chaotic states of an electronic circuit," *Int. J. Bifur. Chaos*, vol. 12, no. 7, pp. 1619–1625, 2002.

Publications

The contents of this thesis have been published or submitted in journals or conference proceedings. The links between these publications and each chapter of the thesis are listed below.

- Chapter 2: B.(1), B.(2)
- Chapter 3: A.(2), B.(3)
- Chapter 4: A.(1), B.(4)
- Chapter 5: A.(3)

A. Journal papers

(1) Luan Ba Le, Keiji Konishi and Naoyuki Hara, "Design and experimental verification of multiple delay feedback control for time-delay nonlinear oscillators," Nonlinear Dynamics, vol. 67, no. 2, pp. 1407–1416 (2012).

(2) Luan Ba Le, Keiji Konishi and Naoyuki Hara, "Topology-free design for amplitude death in time-delayed oscillators coupled by a delayed connection," Physical Review E, vol. 87, no. 4, pp. 042908-1–042908-7 (2013).

(3) Keiji Konishi, Luan Ba Le and Naoyuki Hara, "Stabilization of a steady state in oscillators coupled by a digital delayed connection," European Physical Journal B, vol. 85, no. 5, pp. 166-1–166-6 (2012).

B. Refereed international conference papers

(1) Luan Ba Le, Keiji Konishi, Hideki Kokame and Naoyuki Hara, "Amplitude death in a pair of time-delayed chaotic oscillators coupled by a static connection," Proc. of International Symposium on Nonlinear Theory and its Applications, pp. 631–634, Krakow, Poland September, 2010.

(2) Luan Ba Le, Keiji Konishi and Naoyuki Hara, "Stability analysis of a steady state in three time-delayed nonlinear oscillators coupled by a static connection," Proc. of IUTAM Symposium on 50 Years of Chaos: Applied and Theoretical, P12, pp. 279–282, Kyoto, Japan, 2011.

(3) Luan Ba Le, Keiji Konishi and Naoyuki Hara, "Design of amplitude death in time-delay oscillators coupled by a delayed connection," the 5th International Scientific Conference on Physics and Control, CSI-3, CD-ROM Total 4 pages, Leon, Spain, 2011.

(4) Luan Ba Le, Keiji Konishi and Naoyuki Hara, "Design of amplitude death in a pair of time-delayed chaotic oscillators coupled by a multiple delay connection," Proc. of Conference on Nonlinear Dynamics of Electronic Systems, pp. 257–260, Wolfenbuttel, Germany, 2012.